

General Disclaimer

One or more of the Following Statements may affect this Document

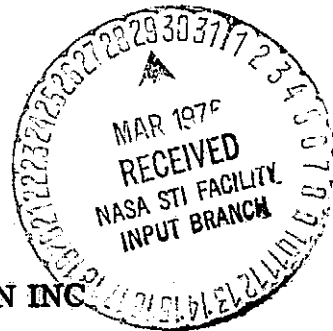
- This document has been reproduced from the best copy furnished by the organizational source. It is being released in the interest of making available as much information as possible.
- This document may contain data, which exceeds the sheet parameters. It was furnished in this condition by the organizational source and is the best copy available.
- This document may contain tone-on-tone or color graphs, charts and/or pictures, which have been reproduced in black and white.
- This document is paginated as submitted by the original source.
- Portions of this document are not fully legible due to the historical nature of some of the material. However, it is the best reproduction available from the original submission.

NASA CR-134966

PERFORMANCE ANALYSIS OF A LASER PROPELLED INTERORBITAL TRANSFER VEHICLE

by M A Minovitch

(NASA-CR-134966) PERFORMANCE ANALYSIS OF A
LASER PROPELLED INTERCRBITAL TRANSFER VEHICLE
Final Report, 24 Jun. 1974 - 31 May 1975
(Phaser Telepropulsion, Inc., Los Angeles)
143 p HC \$6.00



PHASER TELEPROPULSION INC

Prepared for

NATIONAL AERONAUTICS AND SPACE ADMINISTRATION

NASA Lewis Research Center
Contract NAS3-18536

1. Report No. NASA CR-134966	2. Government Accession No.	3. Recipient's Catalog No.
4. Title and Subtitle PERFORMANCE ANALYSIS OF A LASER PROPELLED INTERORBITAL TRANSFER VEHICLE		5. Report Date February 1976
7. Author(s) M. A. Minovitch		6. Performing Organization Code 2M833
9. Performing Organization Name and Address Phaser Telepropulsion Inc. 1888 Century Park East, Suite 1606 Los Angeles, CA 90067		8. Performing Organization Report No.
12. Sponsoring Agency Name and Address National Aeronautics & Space Administration Lewis Research Center Cleveland, OH 44135		10. Work Unit No.
15. Supplementary Notes Project Manager: Stephen M. Cohen, Laser and Energy Systems Branch, NASA Lewis Research Center, Cleveland, Ohio		11. Contract or Grant No. NAS 3-18536
16. Abstract Performance capabilities of a laser-propelled interorbital transfer vehicle receiving propulsive power from one ground-based transmitter is investigated. The laser transmits propulsive energy to the vehicle during successive station fly-overs. By applying a series of these propulsive maneuvers, large payloads can be economically transferred between low earth orbits and synchronous orbits. Operations involving the injection of large payloads onto escape trajectories with $C_3 = 120 \text{ km}^2/\text{sec}^2$ are also studied. Payloads to be boosted to the higher energy orbits are assumed to be brought up from the earth's surface by other vehicles such as the Shuttle. Since the propulsion periods of a laser propelled vehicle are constrained to periods of time when it is moving above the local horizon of the laser station, the duration of each successive engine burn must be carefully timed so that the vehicle will reappear over the laser station to receive additional propulsive power within the shortest possible time. The analytical solution for determining these time intervals is presented, as is a solution to the problem of determining maximum injection payloads. Extensive parametric computer analysis based on these optimization studies is presented. The results show that relatively low beam powers, on the order of 50 MW to 60 MW, will result in significant performance capabilities.		13. Type of Report and Period Covered Final Report 6/24/74 - 5/31/75
		14. Sponsoring Agency Code 5331 500-318
17. Key Words (Suggested by Author(s)) Laser Propulsion Mission Analysis Space Shuttle Tug Vehicle		18. Distribution Statement Unlimited
19. Security Classif. (of this report) Unclassified	20. Security Classif. (of this page) Unclassified	21. No. of Pages 138
22. Price*		

ORIGINAL PAGE IS
OF POOR QUALITY

* For sale by the National Technical Information Service, Springfield, Virginia 22161

PERFORMANCE ANALYSIS OF A LASER PROPELLED INTERORBITAL TRANSFER VEHICLE

ABSTRACT

Performance capabilities of a laser-propelled interorbital transfer vehicle receiving propulsive power from one ground-based transmitter is investigated. The laser transmits propulsive energy to the vehicle during successive station flyovers. By applying a series of these propulsive maneuvers, large payloads can be economically transferred between low earth orbits and synchronous orbits. Operations involving the injection of large payloads onto escape trajectories with $C_3 = 120 \text{ km}^2/\text{sec}^2$ are also studied. Payloads to be boosted to the higher energy orbits are assumed to be brought up from the earth's surface by other vehicles such as the shuttle. Since the propulsion periods of a laser propelled vehicle are constrained to periods of time when it is moving above the local horizon of the laser station, the duration of each successive engine burn must be carefully timed so that the vehicle will reappear over the laser station to receive additional propulsive power within the shortest possible time. The analytical solution for determining these time intervals is presented, as is a solution to the problem of determining maximum injection payloads. Extensive parametric computer analysis based on these optimization studies is presented. The results show that relatively low beam powers, on the order of 50 MW to 60 MW, will result in significant performance capabilities.

TABLE OF CONTENTS

	Page
SUMMARY	1
INTRODUCTION	3
INTERORBITAL TRANSFER VEHICLES FOR MISSIONS TO SYNCHRONOUS ORBITS	8
LASER PROPULSION SYSTEM	
CONFIGURATION	13
PROPULSION MANEUVERS FOR LASER PROPELLED TRANSFER VEHICLES	19
A. Duration of Available Propulsion Periods during Station Flyovers	21
B. Propulsion Maneuvers for Transfer between Low Initial Orbits and Synchronous Orbits	25
1. Analysis based on spherical potential function	27
2. Analysis based on "pear-shaped" potential function	45
3. Numerical comparison of trajectories to synchronous orbit using spherical and pear-shaped potential functions	58
C. Laser Propelled Injection Maneuvers	63
1. The determination of optimum pre-injection orbits for laser propelled injection maneuvers	66
2. The determination of optimum injection maneuvers which will maximize injection mass for prescribed values of I_{SP} and propulsive power	73

	Page
D. Optimum Specific Impulses of Laser Propelled Vehicles for Achieving Maximum ΔV s during One Burn Maneuvers	75
1. The determination of optimum I_{SP} that will generate a given ΔV in least time	76
2. The determination of optimum I_{SP} that maximizes ΔV	79
3. The determination of optimum I_{SP} that maximizes final mass	81
RESULTS AND DISCUSSION	84
A. Parametric Analysis of Missions to Synchronous Orbits	85
B. Parametric Analysis of $C_3 = 120 \text{ km}^2/\text{sec}^2$ Injection Maneuvers	107
CONCLUSIONS	124
SYMBOLS	131
REFERENCES	134

PERFORMANCE ANALYSIS OF A LASER PROPELLED
INTERORBITAL TRANSFER VEHICLE

by

Michael A. Minovitch
Phaser Telepropulsion, Inc.

SUMMARY

Performance capabilities of a laser propelled interorbital transfer vehicle receiving propulsive power from one ground based transmitter is investigated. The laser transmitter is assumed to be located on a high mountain in southern Arizona at latitude 31.8° and transmits propulsive energy to the vehicle during successive station flyovers. Since the propulsive energy of the vehicle is not the result of chemical combustion of propellants, the resulting engine I_{SP} and thrust are not bounded by the conventional limitations of chemical rocket propulsion. Moreover, since the energy-generating mechanism is removed from the vehicle, a considerable reduction in vehicle inertial mass is possible, which can result in very high vehicle thrust to weight ratios.

By using a series of propulsive maneuvers during successive station flyovers, large payloads can be economically transferred between low initial orbits and synchronous orbits. The propulsive strategy, therefore, closely resembles that of a synchrotron machine used in accelerating atomic particles - only in this case the particles are replaced by a space vehicle, and the

confining magnetic field is replaced by the gravitational field of the earth.

Since the propulsive periods of a laser-propelled vehicle are constrained to periods of time when it is moving above the local horizon of the laser station, the duration of each successive engine burn must be carefully timed, so that the vehicle will reappear over the laser station to receive additional propulsive power within the shortest possible time. The analytical solution for determining this interval, using a high accuracy earth gravitational potential function, is presented. The analytical solution for determining maximum injection payloads is also presented. Extensive parametric computer analysis based on these optimization studies is presented. This parametric analysis covered a span of specific impulses that ranged from 500 seconds to 2,000 seconds and propulsive powers that ranged from 2 MW to 65 MW. The results show that a laser-propelled vehicle having an I_{SP} and propulsive power in the neighborhood of 1,500 seconds and 50 MW respectfully, will be capable of transferring payloads on the order of 30,000 kg from low initial orbits to synchronous orbits. The vehicle will also be capable of injecting large payloads onto escape trajectories with $C_3 = 120 \text{ km}^2/\text{sec}^2$. In this case, all propulsive maneuvers are performed within 50,000 km of the laser transmitter.

The laser-propelled vehicle studied here is designed to operate with the ground-to-orbit chemical shuttle already under development to give a complete low cost reusable shuttle system for a wide range of orbital missions and/or injections.

INTRODUCTION

Beamed power for rocket propulsion has its origin in the concept of wireless power transmission, which was initially proposed by Nikola Tesla near the end of the 19th century (ref. 1,2). Tesla not only invented wireless radio communication (Marconi's original radio patent was ruled invalid because of Tesla's early work), but there is strong evidence that he also performed the first original work on masers and lasers (ref. 3). Tesla carried out large scale experimental research in wireless power transmission in Denver, Colorado, during the years 1899-1900. He later advanced his work in this area by building a large wireless power transmitting station on Long Island, utilizing the phenomenon of standing waves. This effort was financed by J. P. Morgan. Unfortunately, Tesla was so far ahead of his time, his scientific contemporaries had great difficulty in understanding his papers and tended to call them unscientific - even at times, mystical. J. P. Morgan soon withdrew his support and Tesla's Long Island laboratory was closed. Later, in 1933, Tesla described how beamed power transmission could be used to propel aircraft (ref. 4). The beams he used in this application were probably lasers, but of course he did not call them that.

The first actual application of wireless power transmission began with the development of efficient microwave generators. This capability began to emerge with the microwave generators developed for radar during World War II and later for microwave communications.

The event which led eventually to the use of microwaves for power transmission was the development of very high power microwave tubes by the Department of Defense in the early 1960s (ref. 5,6). Mr. William C. Brown of the Raytheon Company subsequently utilized these results to formulate, in a practical way, the transmission of power by a microwave beam (ref. 7). Brown became the leading exponent of wireless power transmission using microwaves and was the principal force behind the development of a small 50-pound microwave powered helicopter (ref. 8). The concept was soon extended to rocket booster vehicles by Schad and Moriarty (ref. 9).

The reason that lasers may be ideal as carriers of beamed power is their capability for long range transmission. In theory, a parallel beam of coherent electromagnetic radiation diverges by an angle α given by $\alpha = 2.44 \lambda/D$ where λ and D refer to the wavelength and aperture diameter respectively. Hence, at a distance R , the beam will have a diameter (i.e., spot size) s given by $s = \frac{2.44\lambda R}{D}$ (circular aperture). By employing a focused aperture, the spot size can be reduced to $s = \lambda R/D$, where R is within the aperture's near-field range defined by D^2/λ (ref. 10). For example, if the microwave transmitter has $D = 10\text{m}$ and $\lambda = 3\text{ cm}$, the near field range is only 3.33 km. On the other hand, if the radiation were laser instead of microwave, λ would be much smaller, and it will be possible to attain much greater transmission distances. For example, if $\lambda = 10.6\mu$ (CO_2 laser), the near field distance of a 10m diameter aperture would be 9,434 km. Thus, in order to obtain efficient long range wireless power transmission via microwaves, the transmitting and receiving antennas have to be very large. This is not the case when lasers are used.

Dr. Abraham Hertzberg was one of the early researchers to identify and work out a practical system for long-range wireless power transmission using laser beams (ref. 11). The suggested use of laser power transmission to achieve high thrust rocket propulsion was made by Kantrowitz (ref. 12,13) and the author (14,15).

Kantrowitz's method, which was advanced by Rom and Putre at the Lewis Research Center (ref. 16) and by Pirri and Weiss at the Avco Everett Research Laboratory (ref. 17) involved shining a high intensity laser beam on a specially treated material located in the throat of a rocket nozzle. The interaction caused the formation of a plasma, which produced a shock wave that transferred momentum to the rocket vehicle for propulsion. In theory, the resulting specific impulse can be very high. In addition, the resulting vehicle thrust-to-weight ratios can also be very high, which results in high vehicle accelerations. The original operational application of this method of laser propulsion was to accelerate a vehicle from rest to orbital velocities before it passed out of the range and/or line of sight of the laser transmitter. Since the Kantrowitz application required enormous beam powers (1 GW per metric ton payload according to Kantrowitz, ref. 13), his method appeared to be impractical because of the multiplying effects of the various energy conversion inefficiencies. For example, it would require a beam power of at least 30 GW to match the 30 metric ton payload capability of the chemical ground to orbit shuttle vehicle. Based on a 20% electrical-to-laser conversion efficiency, the required input power would have to be at least 150 GW, which is a significant fraction of the total electric generating capacity of the United States. But this seemingly impossible task of concentrating 150 GW of electric power could in fact be accomplished with relative ease. The solution is to charge a

superconducting magnetic energy storage system (10 GW-hr to 30 GW-hr capacity) over a relatively long time interval (i.e., many hours) and discharge it into the laser generator over a relatively short time interval (i.e., a few minutes). Such a system could in fact generate 100 GW to 300 GW of input electric power over a time interval sufficient to propel a vehicle to orbit. Large superconducting magnetic energy storage systems are described in references 18 and 19.

The laser propulsion scheme studied in this report involves transmitting power over much greater distances but at much lower power levels to vehicles already in orbit. The vehicle intercepts the laser beam and uses it to heat a convenient working fluid to high temperatures. The hot gas is expelled through a rocket nozzle as in conventional propulsion to generate vehicle thrust. The laser transmitter is located at a fixed position on the earth's surface, preferably on a high mountain to reduce beam attenuation by the atmosphere. It is energized by a nearby superconducting magnetic energy storage system which is continually being charged by a relatively low power transmission line (on the order of 20 MW).

Power is transmitted to the vehicle as it makes successive passes over the laser station. Since the station is assumed to be off the equator, successive fly-overs will occur only once every sidereal day or multiples of a sidereal day depending on vehicle acceleration. Thus, by applying a series of these propulsion maneuvers, the vehicle can boost payloads from low orbits to synchronous orbits or beyond with very high specific impulse, without burdening itself with the large dead inertial mass usually associated with high specific impulse, high thrust rocket engines. The vehicle is designed to operate as an

interorbital transfer vehicle (ferry) that takes payloads deposited in low orbits by the chemical shuttle and delivers them to high orbits (e.g., synchronous orbits) or injects them onto escape trajectories.

There are other significant benefits that a laser propelled transfer vehicle can offer. For example, the most expensive item in the system will be the laser transmitting station, and this system will remain on the ground where it can be serviced by routine maintenance. It can never be lost by vehicle malfunction. The vehicle's propulsion system is essentially an optical device for receiving the laser beam and concentrating it on the working fluid. Control will be relatively easy. One laser transmitting station will be capable of powering a fleet of perhaps 10 or 20 such vehicles where each vehicle receives propulsion power at different times.

The aim of this report is to analyze the performance capabilities of a laser propelled vehicle over a wide range of system parameters in order to evaluate its potential. Although a prior study (ref. 20) did show striking performance possibilities, it was based on rather high propulsive power (460 MW) and specific impulse (2,000 seconds) and lacked a comprehensive parametric study. This report will cover a much lower range of propulsive powers and specific impulses. The analysis will be based on a high accuracy "pear-shaped" gravitational potential function which was missing in the previous work. It will be shown that the "pear-shaped" potential function will significantly reduce the transfer times to synchronous orbit with high mass payloads that would ordinarily be required using a spherical potential function.

INTERORBITAL TRANSFER VEHICLES FOR MISSIONS TO SYNCHRONOUS ORBITS

Current mission studies involving large communication satellites, astronomical telescopes (manned and unmanned), and manned space stations, suggest that future traffic to geosynchronous orbits is likely to be very heavy. Indeed, it has already been estimated that 50% to 60% of all payloads brought up from the earth's surface by the reusable ground-to-orbit shuttle will require insertion into synchronous orbits (ref. 21).

Unfortunately, missions to synchronous orbits are not easy to achieve. The minimum total ΔV required for a round trip stop-over mission to synchronous orbit, starting from a 100 nautical mile circular parking orbit with inclination 28.6° , is 8.602 km/sec. This is achieved by four burns. The first burn $\Delta V = 2.461$ km/sec, raises the apoapsis altitude to 35,793 km (synchronous orbit altitude). The second burn, $\Delta V = 1.840$ km/sec, is carried out when the vehicle passes through its apoapsis just as it crosses through one of its nodes. This maneuver is a combined plane change and circularization maneuver. Hence, the total round trip $\Delta V = 2x(2.461 \text{ km/sec} + 1.840 \text{ km/sec}) = 8.602 \text{ km/sec}$. This ΔV is approximately equal to that developed by the ground-to-orbit shuttle vehicle. It is interesting to compare this minimum ΔV with the average minimum ΔV required for a round trip stop-over interplanetary mission to Mars. Omitting the calculations, it can be shown that the average minimum transfer velocity for an interplanetary transfer from a 100 nautical mile high circular parking orbit about the earth to a 100

nautical mile high circular parking orbit about Mars and return to the initial parking orbit at earth is 11.818 km/sec. Hence, a round trip stop-over interplanetary mission to Mars requires a total transfer velocity of only 3.216 km/sec more than the minimum total transfer velocity required for a round trip mission to synchronous orbit. Thus, only 1/3 more ΔV is required for a round trip transfer between a low earth orbit and a low Mars orbit than is required for a round-trip transfer between a low earth orbit and synchronous earth orbit. Consequently, as far as ΔV is concerned, every round trip mission to synchronous orbit can almost be regarded as a round trip, stop-over mission to the planet Mars. If we assume identical propulsion systems, the fuel requirement for both missions will be of the same order of magnitude.

The purpose for these calculations is to focus attention on the fact that round trip missions to synchronous orbits are difficult to achieve - much more difficult than is generally realized. The ground-to-orbit shuttle vehicle currently under development falls short of having the capability to deliver payloads directly to synchronous orbit by a wide margin. Figure 1 describes the payload capability of this shuttle as a function of orbital altitude and inclination. It is clear that no significant approach to synchronous orbit can be made with this vehicle. Although future ground-to-orbit reusable shuttle vehicles will inevitably be developed that will have the capability to deliver payloads directly to synchronous orbits, it appears unlikely that these shuttles could be operational before the end of the century. Thus, one is forced to conclude that, at least for the foreseeable future, any complete shuttle system will have to be composed of two different vehicles: a ground-to-orbit shuttle

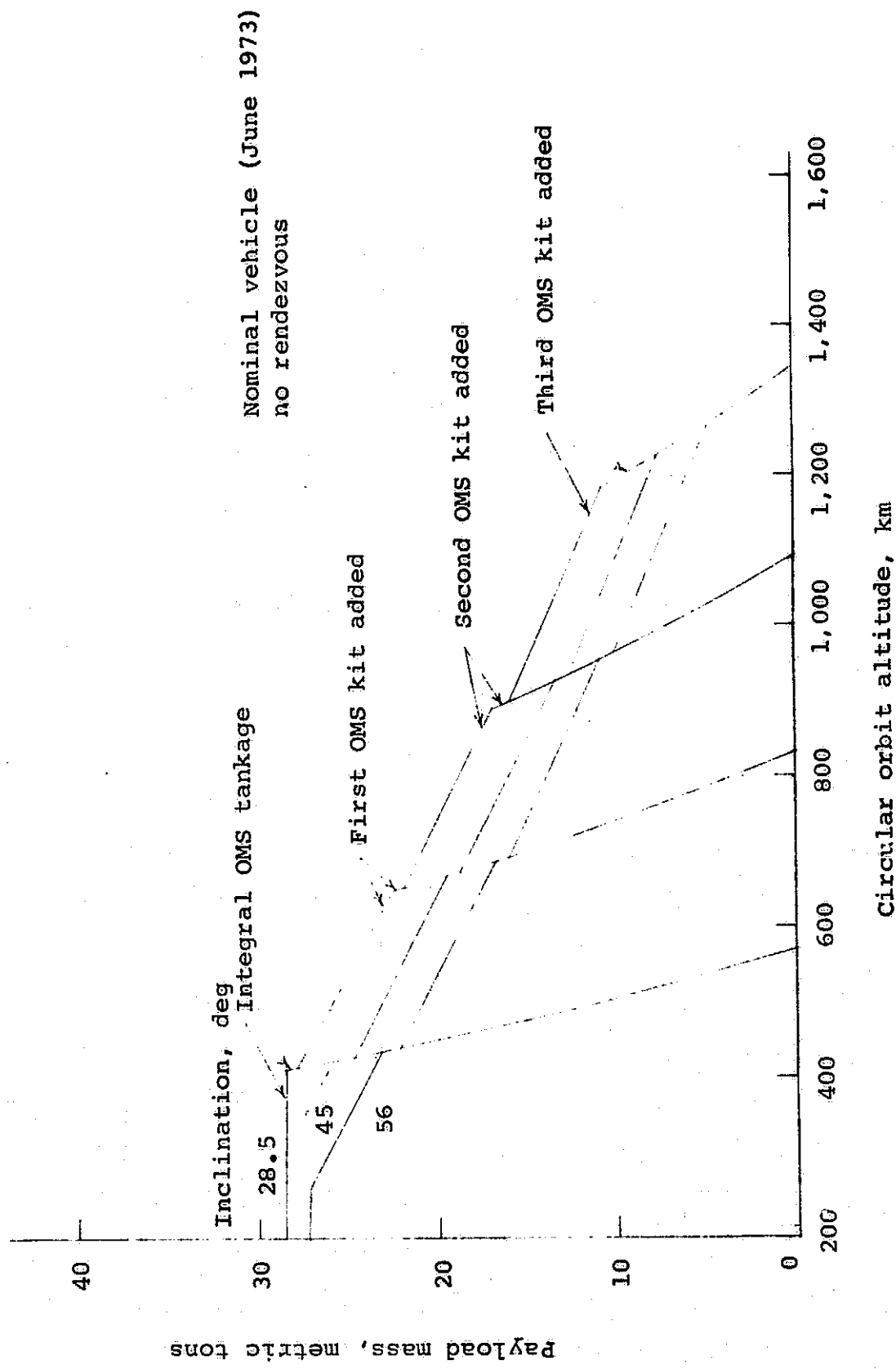


Figure 1. - Shuttle payload weight vs. circular orbit altitude for ETR launch and delivery only.

vehicle to bring up payloads from the earth's surface and deliver them to low orbits and another vehicle that will transfer payloads between these low initial orbits and synchronous (or other high energy) orbits. These interorbital transfer vehicles are often referred to as tugs. We shall refer to them as interorbital transfer vehicles. In view of the above analysis, it appears that for all practical purposes these vehicles will have to be almost as powerful as an interplanetary shuttle that transfers payloads directly between low earth orbits and low Mars orbits.

Several tug configurations are under active study. The vehicles that appear least costly to develop into tugs are the Centaur and the Agena. Similar vehicles have been designed by ELDO (European Launcher Development Organization). All of them are chemical and would be carried to orbit for each mission inside the cargo bay of the ground-to-orbit shuttle and attached to the final payload. Assuming that a round trip mission is possible, this vehicle would be returned by the shuttle to the earth's surface where it would be refurbished, refueled, and prepared for the next mission. These vehicles will be referred to as chemical tugs.

In view of the high ΔV requirements for transfers between low earth orbits and synchronous orbits, transfer vehicles with higher specific impulse propulsion systems have been proposed. These are the solar electric propulsion orbiters, nuclear electric propulsion orbiters, and the nuclear rocket propulsion orbiters. A description of all of these vehicles can be found in references 22-26.

TABLE 1. - PERFORMANCE CAPABILITIES OF ADVANCED REUSABLE TRANSFER VEHICLES
ON MISSIONS TO SYNCHRONOUS ORBIT

	CHEMICAL TUG (Ref. 22)	SOLAR ELECTRIC (Ref. 24)	NUCLEAR ELECTRIC (Ref. 25)	CHEMICAL ELECTRIC (Ref. 23)	NUCLEAR TUG (colloid core) (Ref. 26)
<u>Launch Vehicle</u>	Shuttle	Thor Δ	Thor Δ	Shuttle	Shuttle
<u>Payload (Kg) (delivered to synchronous orbit)</u>					
Tug expended	8,182	680	680	9,000	15,000
Tug returned empty	3,636	300	300	4,000	8,400
Round trip	1,364	200	200	2,300	3,100
<u>Mass (Kg)</u>					
Dry mass	2,727	1,000	1,000	674	3,000
Fuel mass	24,546	500	500	1,180	12,700
Initial (excluding payload)	27,273	1,500	1,500	1,854	15,700
Total initial mass	29,540	2,180	2,180	29,540	29,540
Propellant fraction	.83	.23	.23	-	.43
<u>Engine</u>					
Isp	460	3,000	3,000	444/3500	1,100
Thrust (lbs.)	10,000-15,000	.184	.184	-	20,000
Propulsive power (MW)	100-150	.020	.020	-	480
<u>Mission Duration (days)</u>					
One-way	0.5	370	370	45	0.5
Round trip	1.0	600	600	90	1.0

Table 1 summarizes typical performance characteristics of these transfer vehicles. They are given here so that they can be compared with one another and with the performance capabilities of a laser propelled transfer vehicle.

LASER PROPELLED TRANSFER VEHICLE SYSTEM CONFIGURATION

The laser transmitting station will be the most important system associated with a laser propelled inter-orbital transfer vehicle concept. In order to minimize beam attenuation by the earth's atmosphere, the station will be located on the summit of a high mountain with exceptionally clear visibility and little cloud cover. A previous study (ref. 20) has identified several mountain tops in southern Arizona that are promising for the station. Figure 2 shows the laser station equipped with a very large optical phased array transmitting aperture for electronic beam steering (ref. 27) and a large superconducting magnetic energy storage system for load leveling.

One possible configuration for the laser propelled transfer vehicle is shown in figures 3A and 3B (ref. 28). The advantage of this particular design over others previously given (ref. 20) is that the main reflector is circular and in most situations, will be much larger in diameter than the incident laser beam. All of the rays of the beam will be reflected onto a secondary mirror, located on the focal axis of the main reflecting disc and reflected onto a beam splitting mirror and along opposite directions inside a tubular beam which serves as a rotation axis for the reflector. The laser radiation is fed into two laser rocket engines mounted on each end of the tube. The main reflector is shown in figure 3C.

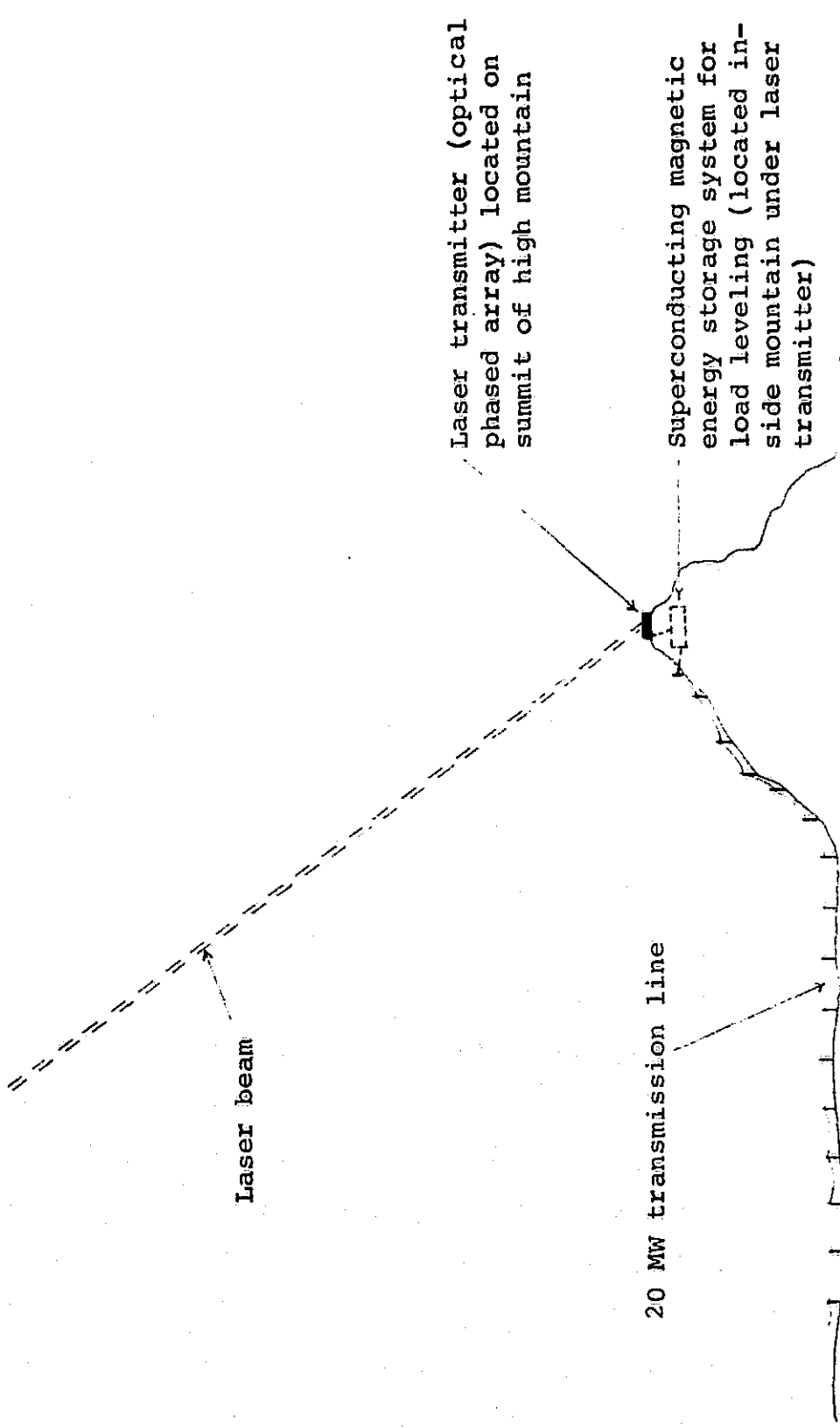


Figure 2. - System configuration for laser transmitting station.

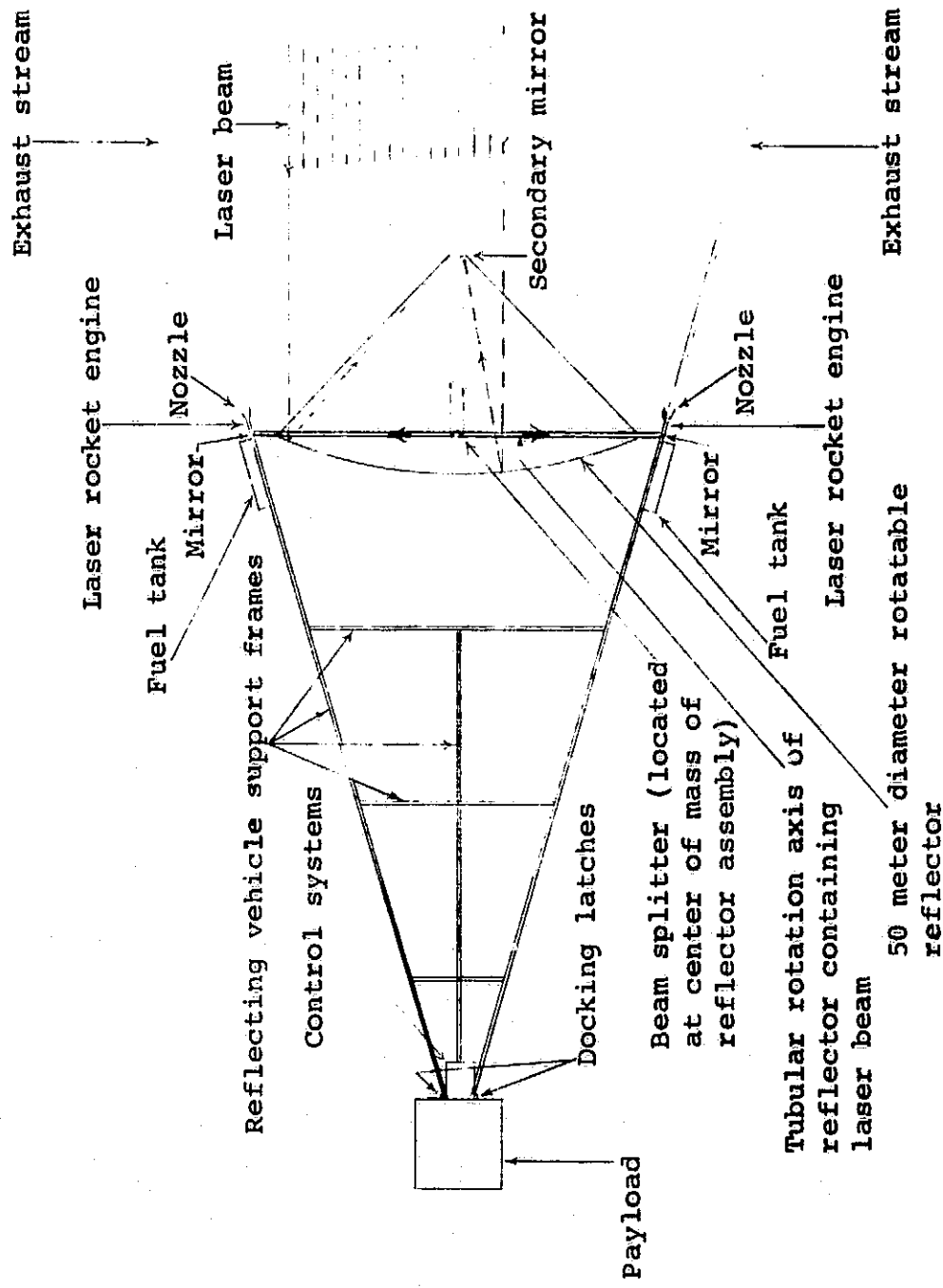


Figure 3A. - Laser propelled transfer vehicle (reflector perpendicular to plane of paper).

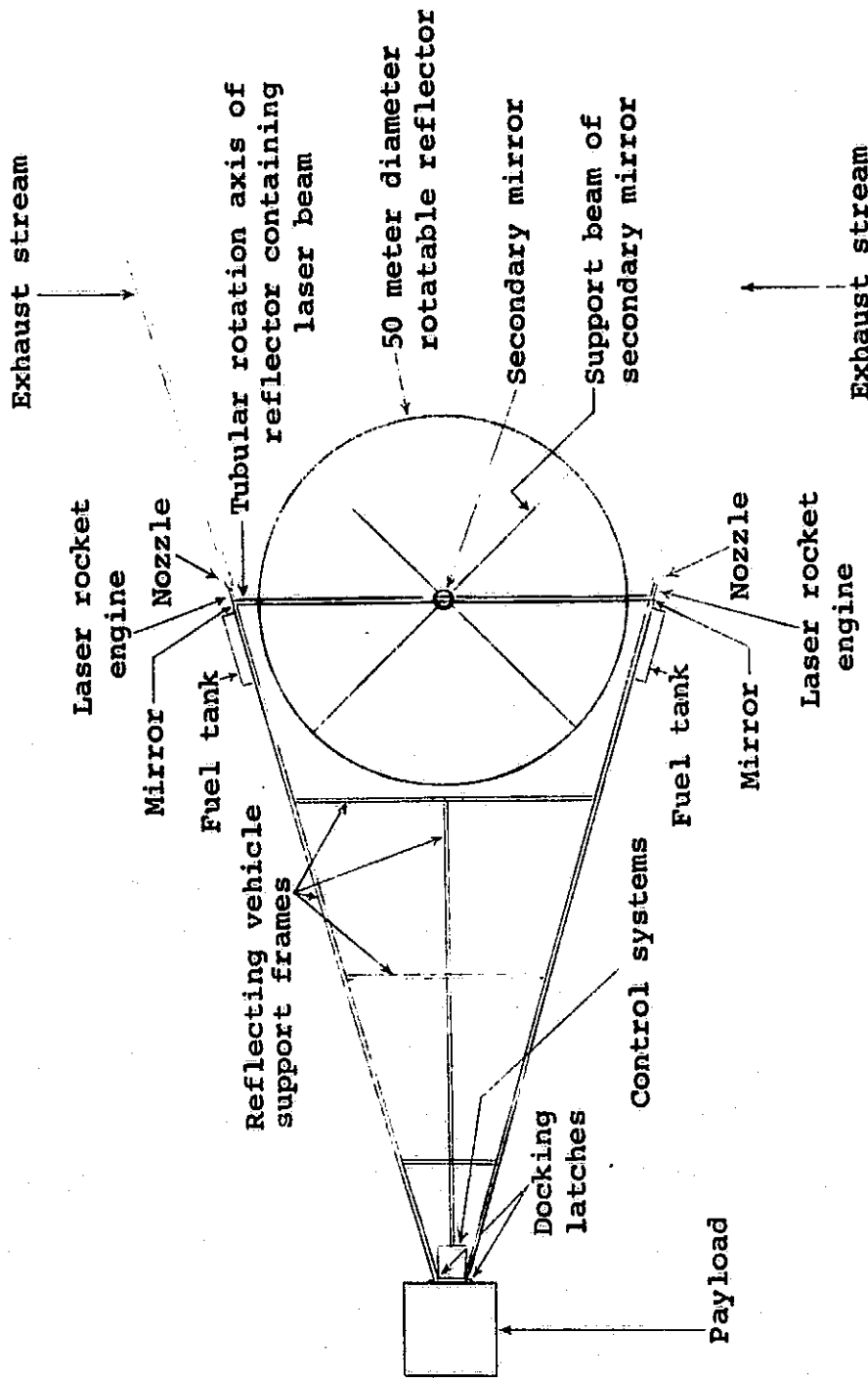


Figure 3B. - Laser propelled transfer vehicle (reflector in plane of paper).

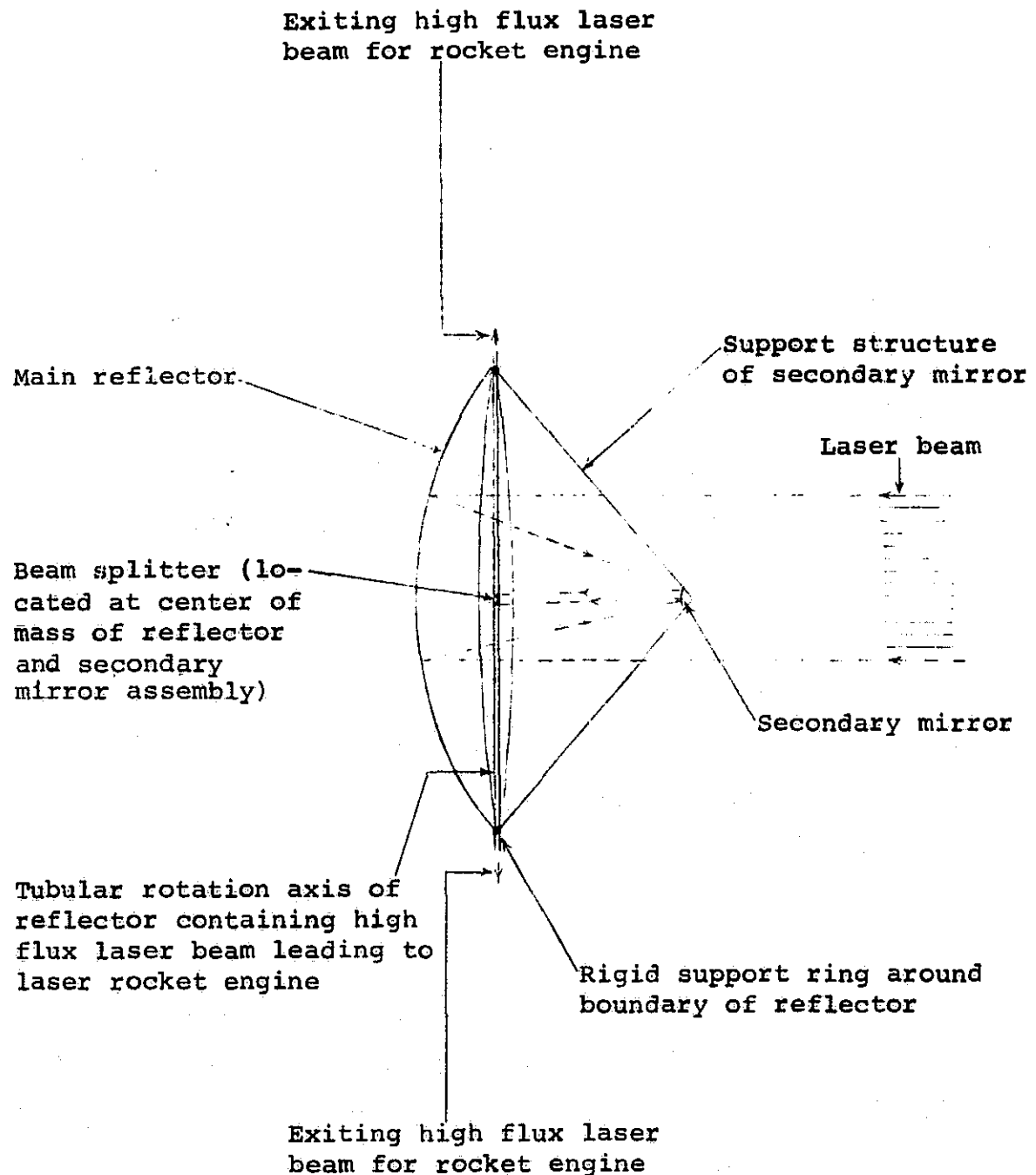


Figure 3C. - Possible, large diameter, low mass, inflatable paraboloid mirror for collecting and concentrating laser beams over great distances.

Thus, the incident beam could wander around the entire disc in any random manner without causing any reduction in propulsion power. Of course, sensors on various parts of the disc will feed back information to the electronic beam steering system on the ground so as to keep the center of the beam as close to the center of the disc as possible. The diameter of the array on the ground and the diameter of the disc on the vehicle will determine the full power operational range of the system. We shall assume that this full power operational range is 50,000 km.

The vehicle and propulsion system is also designed to operate as a solar powered vehicle if laser propulsion is unavailable. This could be used during the final placement of satellites in specific synchronous orbits. This capability will be very important because only about 1/4 of all synchronous orbits would be within the laser transmission cone of any fixed laser transmitting station. Solar propulsion would be accomplished by moving the disc to an attitude perpendicular to the incident solar radiation. This would illuminate the entire disc, and all of the intercepted radiation would be fed into the absorption chamber of the rocket engine. If the disc radius is 25 meters, for example, this radiation would represent approximately 2.6 MW. If LH_2 is used as the working fluid, a specific impulse of 600 to 700 seconds could be generated (ref. 29). Assuming a propulsive power conversion efficiency of 75%, this power level would provide a thrust of about 663 N to 568 N (149 lbs. to 128 lbs. respectively).

PROPELLION MANEUVERS FOR LASER PROPELLED
INTERORBITAL TRANSFER VEHICLES

A laser propelled interorbital vehicle will transfer payloads between low earth orbits and synchronous orbits by a series of discrete engine burns that will occur every time the vehicle flies over the transmitting station (providing the local weather conditions are favorable). If the laser transmitting station is located on the equator and if the vehicle's orbit has zero inclination, the vehicle will pass over the transmitting station on each and every orbit revolution no matter what its orbital period, because the motion of the station (due to the rotation of the earth) will always remain in the orbital plane of the vehicle. Therefore, power could be transmitted as soon as the vehicle rises sufficiently high above the station's local horizon and continued until it passes below a minimum allowed beam elevation angle. Unfortunately, this situation is radically changed if the transmitting station is located off the equator, because then the motion of the station will no longer be in the orbital plane of the vehicle. In fact, since this plane does not pass through the earth's center, no orbital plane exists that can be co-planer with it. Thus, in order for an orbiting space vehicle to be able to make repeated passes over a non-equatorial laser station, the inclination of its orbit will have to be equal to or greater than the latitude of the station and its orbital period will have to be in resonance with the rotation period of the station (i.e., the earth's period of rotation). Consequently, the propulsion periods for a non-equatorial laser transfer vehicle will have to be carefully timed, so that each successive burn is terminated only when the vehicle's

orbital period reaches a certain resonant value with the station's rotation. This will enable the vehicle to reappear over the laser station to receive the next power transmission. Each propulsion maneuver is designed to propel the vehicle from one resonant orbit to another resonant orbit. The intervals between these successive station passes is one sidereal day or an integral multiple of a sidereal day. The shortest possible interval is one sidereal day. Thus, the burns are timed to enable the vehicle to reach the targeted orbit (e.g., synchronous orbit) in the minimum overall time.

Since each intermediate orbit is in resonance with the station, it is not absolutely essential to beam power during each and every station flyover. For example, if the local weather conditions above the transmitting station are unfavorable for power transmission during a particular flyover, the transmission can be postponed to the next flyover without any serious effect on the total flight time.

The determination of the precise duration of each successive engine burn that will place the vehicle into higher energy resonant orbits is an important part of this study. We shall solve this problem using a simple spherical gravitational potential function and a high accuracy "pear-shaped" gravitational potential function. In the first case, each coasting orbit remains fixed in inertial space, and the analysis is relatively simple. In the second case, the coasting orbits do not remain fixed in inertial space. There is a drift in the line of apsides and the orbital plane that will result in a very complicated ground track. This must be considered when determining the duration of each engine burn.

A. Duration of Available Propulsion Periods during Station Flyovers

It is important to have some general understanding of the total power transmission time that will be available when a laser propelled interorbital transfer vehicle passes directly over the laser transmitting station for various altitudes h , orbit eccentricities e and minimum beam elevation angles α . These times have been calculated on the assumption that the vehicle passes through its perigee when it is directly over the station. The available thrusting time is defined as that time interval ΔT during which the vehicle is α degrees or higher in the sky above the station's local horizon, where α represents the minimum beam elevation angle (see figure 4). Consequently, these times are in fact lower bounds and are given in table 2 along with other important parameters - such as periapsis altitude q_h , apoapsis altitude Q_h , eccentricity e , and semi-major axis a . The orbital period is given in hours.

It is apparent that a laser propelled transfer vehicle system will operate on a principle similar to that of a large synchrotron machine used to accelerate atomic particles. Each time the vehicle appears over the laser transmitting station it will receive a relatively small ΔV .

A series of resonant orbits with increasing energy is shown in figure 5. The duration of each burn is carefully timed so that each new orbit is in resonance with the moving transmitting station that traces out a circle about the earth's rotation axis. Consequently, by applying a series of these burns, the vehicle can be accelerated to very high terminal velocities, exceeding, for example, the earth's escape velocity. Or the vehicle could be placed in a synchronous orbit above the local horizon of the laser station.

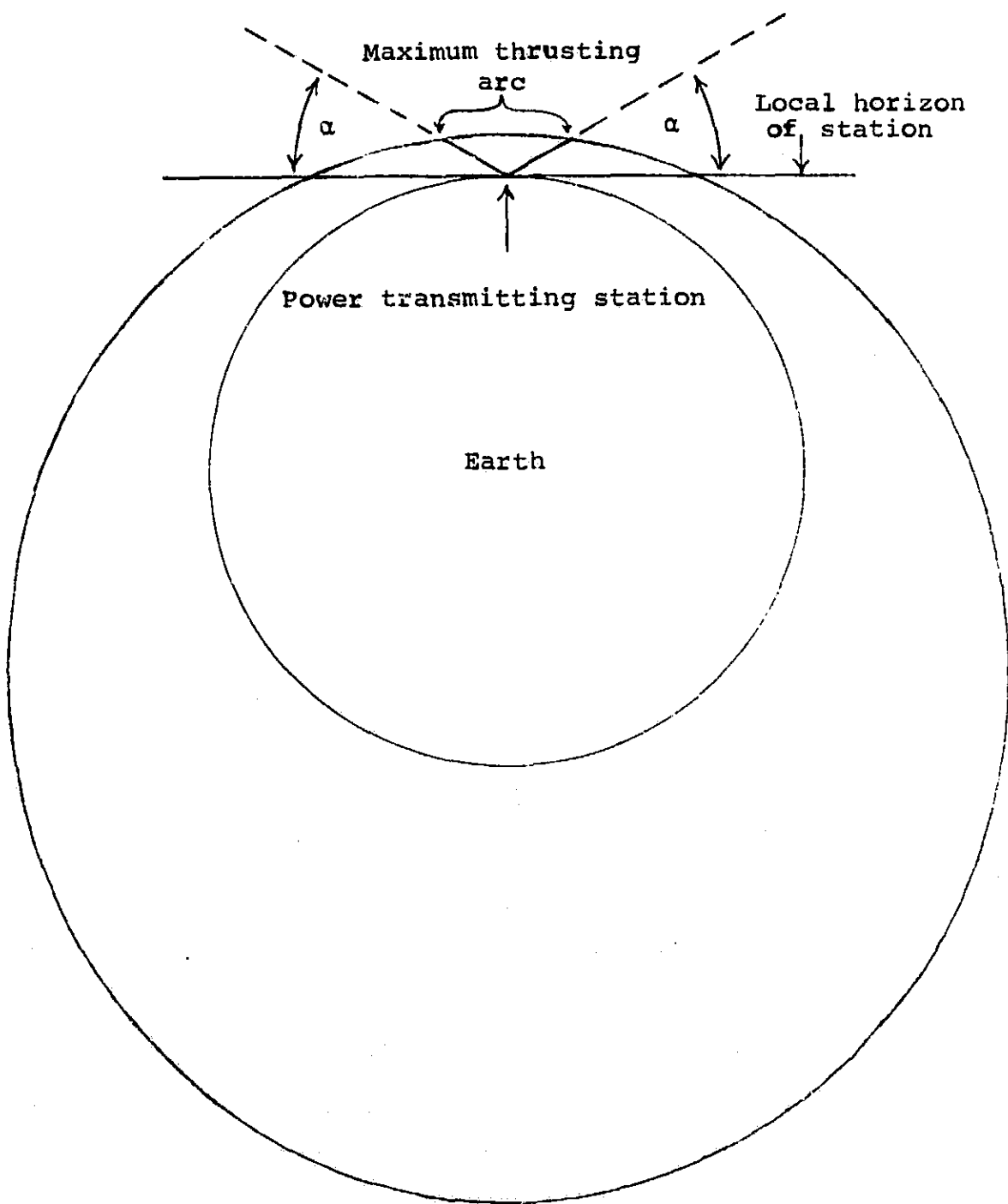


Figure 4. - Maximum thrusting arc for laser propelled transfer vehicles.

Table 2
 Maximum Periapsis Burn Times for Various Orbits
 and for Various Minimum Beam Elevation Angles

q_h (km)	Q_h (km)	e	a (km)	Period (hours)	Δt ($\alpha=20$) (sec)	Δt ($\alpha=30$) (sec)	Δt ($\alpha=40$) (sec)
200	200	.0000	6,578.16	1.4749	128	85	60
200	500	.0223	6,728.16	1.5256	126	84	59
200	1,000	.0573	6,978.16	1.6115	124	83	58
200	5,000	.2673	8,978.16	2.3517	114	76	53
200	10,000	.4269	11,478.16	3.3995	107	71	50
200	20,000	.6008	16,478.16	5.8475	101	67	47
200	30,000	.6937	21,478.16	8.7017	98	66	46
200	40,000	.7516	26,478.16	11.9103	97	64	45
400	400	.0000	6,778.16	1.5427	242	167	120
400	500	.0073	6,828.16	1.5598	241	166	119
400	1,000	.0424	7,078.16	1.6462	237	164	117
400	5,000	.2533	9,078.16	2.3911	216	150	107
400	10,000	.4146	11,578.16	3.4440	204	141	101
400	20,000	.5911	16,578.16	5.9008	192	133	95
400	30,000	.6859	21,578.16	8.7625	187	129	92
400	40,000	.7450	26,578.16	11.9783	183	127	90
600	600	.0000	6,978.16	1.6115	348	247	179
600	1,000	.0279	7,178.16	1.6812	336	239	173
600	5,000	.2397	9,178.16	2.4508	313	222	161
600	10,000	.4025	11,678.16	3.4888	295	209	151
600	20,000	.5816	16,678.16	5.9543	278	197	143
600	30,000	.6781	21,678.16	8.8235	270	191	138
600	40,000	.7384	26,678.16	12.0460	266	188	136
1,000	1,000	.0000	7,378.16	1.7520	549	404	299
1,000	5,000	.2133	9,378.16	2.5106	501	368	272
1,000	10,000	.3788	11,878.16	3.5788	471	345	255
1,000	20,000	.5629	16,878.16	6.0617	443	325	240
1,000	30,000	.6628	21,878.16	8.9459	430	315	232
1,000	40,000	.7255	26,878.16	12.1817	423	309	228

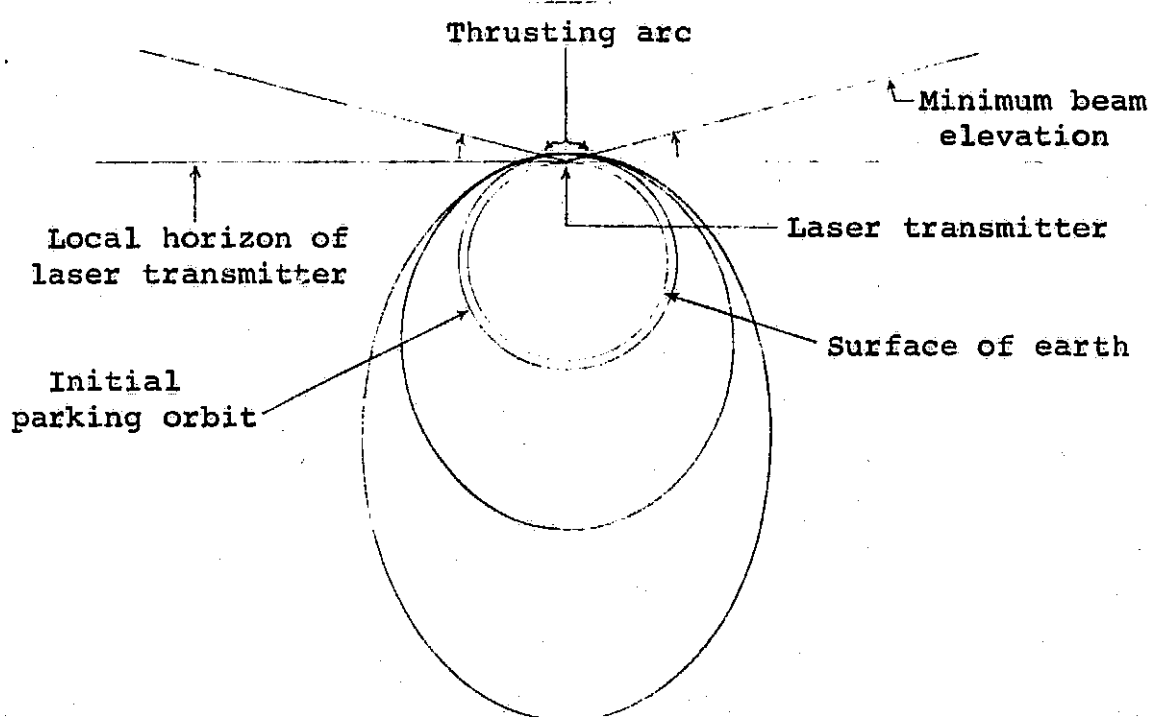


Figure 5. - Higher energy resonant orbits during primary boosting maneuvers based on spherical potential function resulting in essentially constant thrusting arcs.

B. Propulsive Maneuvers for Transfer
between Low Initial Orbits and
Synchronous Orbits

We shall now develop a propulsive strategy for laser propelled transfer vehicles which receive propulsive power from one non-equatorial laser transmitting station. This strategy will allow economical transfer between low initial orbits with inclination $i \neq 0^\circ$ and high synchronous orbits with inclination 0° . The transfer will be accomplished by a series of intermittent propulsive maneuvers that will boost the vehicle to higher and higher energy levels that are in resonance with the power transmitting station. The fact that laser propulsion can occur only when the vehicle is above the local horizon of the laser transmitter imposes unusual constraints on the burns - in fact, constraints that are not found in any other rocket propulsion concept. This will force the total ΔV required to reach synchronous orbit above the minimum values associated with more conventional rockets. However, we shall see that the possible benefits of laser transfer vehicles will more than compensate for this slight decrease in efficiency.

Let ϕ_l and ϕ_t denote the latitudes of the launch site (e.g., Cape Canaveral) and the laser transmitter, respectively. If i denotes the inclination of the laser transfer vehicle then in order for the vehicle to fly directly over the laser station it is clear that $i \geq \phi_t$. Hence, if $\phi_t > \phi_l$, than in order to minimize the total ΔV required to reach synchronous orbit, it is clear that the vehicle's inclination should be equal to the latitude of laser transmitter (i.e., $i = \phi_t$). The geometry is shown in figure 6.

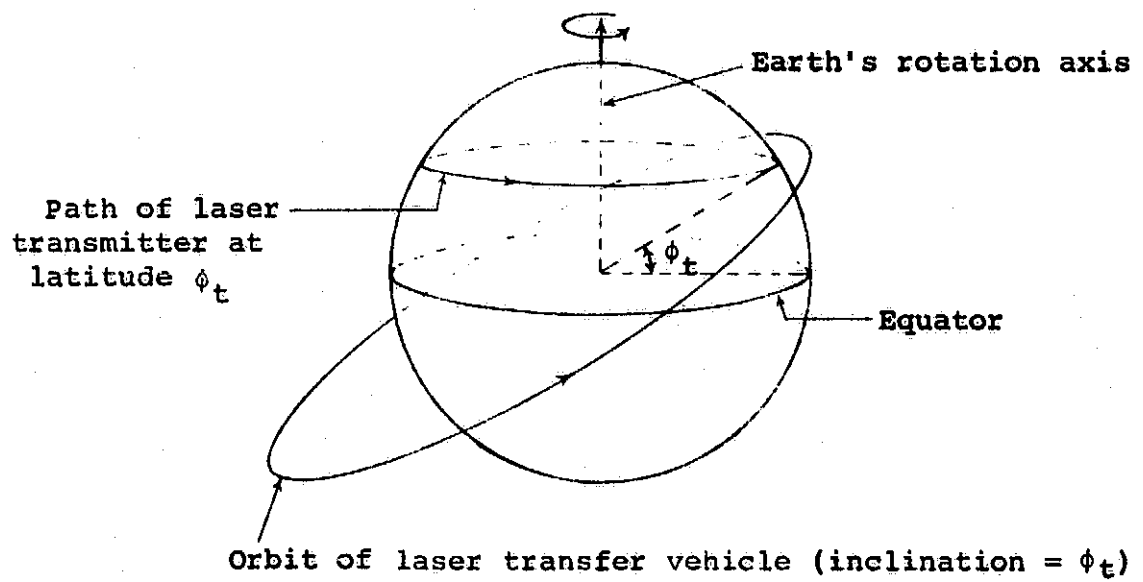


Figure 6. - Orbit of laser propelled transfer vehicle relative to path of laser transmitter.

The process of delivering a payload to synchronous orbit from the earth's surface, retrieving another payload in synchronous orbit and bringing it down to the earth's surface by a laser-propelled transfer vehicle is described in Table 3 as a sequence of 11 major steps.

This study will concern itself only with steps 2, 3, 4, 8, 9, and 10, which are the steps carried out by laser propulsion. These steps will determine the performance capabilities of laser-propelled transfer vehicles. We shall determine this performance parametrically by numerically simulating the flight profiles corresponding to these steps by a digital computer using detailed numerical integrations. The analysis will be performed using a simple spherical gravitational potential function and a high accuracy "pear-shaped" gravitational potential function.

1. Analysis based on spherical potential function

Let U denote the gravitational potential function of the earth. If \vec{r} is the position vector for any point in space, a spherical potential is simply $U = \mu/r$

where $\mu = GM$ (universal gravitational constant \times mass of earth) = $398600.7 \text{ km}^3/\text{sec}^2$ (ref. 30). The equation of motion of a free-fall vehicle moving in the field is

$$\frac{d^2 \vec{r}}{dt^2} = -\nabla U \quad (1)$$

and the solution is a conic section. We assume $\{\}$ is a right-handed Cartesian coordinate system fixed in inertial space (i.e., relative to the fixed stars). The conic orbit is fixed in space relative to $\{\}$. We shall assume that the conic orbit is either circular or elliptical. If its semi-major axis is given by a ,

TABLE 3. - OPERATIONS FOR THE DELIVERY AND
RETRIEVAL OF SYNCHRONOUS ORBIT PAYLOADS
VIA LASER PROPULSION (SPACE-BASED VEHICLE)

Step No.	Operation
1.	Launch of ground-to-orbit shuttle vehicle with payload and rendezvous with transfer vehicle via chemical propulsion ($\phi_1 \rightarrow \phi_t$).
2.	Transfer payload to laser vehicle and begin primary boosting maneuvers until apoapsis reaches synchronous orbit altitude via laser propulsion ($i = \phi_t$).
3.	Circularize orbit at synchronous orbit altitude via laser propulsion ($i = \phi_t$).
4.	Change inclination to 0° at synchronous orbit altitude via laser propulsion.
5.	Deliver payload to targeted location in synchronous orbit via solar (or chemical) propulsion ($i = 0^\circ$).
6.	Rendezvous with another payload at another location in synchronous orbit via solar (or chemical) propulsion for subsequent delivery to the earth's surface ($i = 0^\circ$).
7.	Move to the initial position in synchronous orbit via solar (or chemical) propulsion that lies on the same meridian as the laser station ($i = 0^\circ$).
8.	Change inclination from 0° to ϕ_t via laser propulsion.
9.	Initiate decircularization maneuver to lower periapsis altitude via laser propulsion ($i = \phi_t$).
10.	Circularize orbit at low initial orbit altitude via laser propulsion to rendezvous with shuttle and transfer payload ($i = \phi_t$).
11.	Deliver payload to earth's surface in shuttle.

then its period P is given by

$$P = 2\pi\sqrt{a^3/\mu} \quad (2)$$

The mean motion n (average orbital angular velocity)

$$\text{is given by: } n = 2\pi/P = \sqrt{\mu/a^3} \text{ (rad/sec)} \quad (3)$$

and the energy E of the orbit is given by

$$E = -\frac{1}{2a} \quad (4)$$

The orbit will be parabolic when $E = 0$.

Let θ denote the earth's rate of rotation about its spin axis. This constant is equal to $7.292115144 \times 10^{-5}$ rad/sec (ref.30) Hence, if P_s denotes the earth's period of rotation, it follows that

$$P_s = 2\pi/\theta = 86,164.099 \text{ seconds} \quad (5)$$

This period is defined as one sidereal day.

Suppose the laser transmitting station S is off the equator at latitude ϕ_t and that the inclination i of the vehicle's orbit is also equal to ϕ_t . If at some time T_0 the vehicle passes directly over S through its zenith, it will make future flyovers through the local zenith of S if and only if there exist two positive integers k_1 and k_2 such that

$$k_1 P_s = k_2 P \quad (6)$$

(We assume k_1 and k_2 have no common divisors other than 1.) The successive station flyovers will occur at times $T_0, T_0 + k_1 P_s, T_0 + 2k_1 P_s \dots$. The time intervals between these flyovers is $k_1 P_s$ or k_1 sidereal days. During this time the vehicle will make k_2 complete orbit revolutions. Since $P_s > P$, it follows that $k_1 < k_2$. Any orbit satisfying equation (6) will be in resonance with S and will be called a resonant orbit. The integers k_1 and

k_2 will be called resonant integers. Thus, the minimum possible time interval between two successive flyovers is one sidereal day, which will occur only if $k_1 = 1$.

When the shuttle rendezvous with the laser transfer vehicle to transfer its payload as prescribed in step 1 of Table 3, the rendezvous orbit should be resonant with S and have $k_1 = 1$. Assuming that this rendezvous orbit is circular, this condition determines the possible altitudes h of the initial parking orbit that corresponds to possible integer values of k_2 . These can be determined directly from (6), using (5) and (2). The result is

$$h = a - \rho_0 = \frac{\mu^{1/3}}{(k_2 \dot{\theta})^{2/3}} - \rho_0$$

where ρ_0 = mean radius of earth = 6371.3 km (ref. 30). These initial orbital altitudes that correspond to various values of k_2 are given in Table 4.

TABLE 4. - INITIAL ORBITAL ALTITUDES OF
RESONANT CIRCULAR ORBITS
(Spherical Gravitational Potential Function)

Altitude h (km)	Altitude h (n-mile)	Semi-Major Axis a (km)	k_2
6.1	3.3	6,377.4	17
269.1	145.3	6,640.4	16
561.1	302.9	6,932.4	15
887.4	479.2	7,258.7	14
1,255.0	677.6	7,626.3	13

It is obvious from figure 1 that the most desirable initial orbital altitude from the point of view of maximizing the payload capabilities of the shuttle is 269.1 km. But if the initial orbital altitude is higher, the time to synchronous orbit will be shorter because each burn over the station will be longer. (See, for example, table 2.)

Suppose that the payload has been transferred to the transfer vehicle and it is approaching the laser transmitter to receive propulsive power for its initial boosting maneuvers to synchronous orbit (step 2 of table 3). As soon as it rises above a specified minimum beam elevation angle α (determined by local atmospheric conditions at the laser transmitting station), power transmission is initiated. (Actually, low power transmission would begin a few seconds before the minimum beam elevation angle is reached in order to "lock on" the vehicle's energy collector. The power would then be brought up to full strength gradually - for example, in 5 to 10 seconds - as the vehicle approaches the minimum beam elevation angle.) The vehicle's thrust vector is kept parallel to the instantaneous velocity vector for maximum efficiency and for maintaining the orbital inclination at $i = \phi_t$.

Let $k_{1,0}$, $k_{2,0}$ and n_0 denote the resonant integers and the mean motion immediately before the first laser propulsion period that corresponds to the initial resonant parking orbit. In view of table 4, we shall assume that $k_{2,0} = 16$ and $k_{1,0} = 1$. Hence, $n_0 = 1.166738 \times 10^{-3}$. The resonant condition (6) can be expressed as

$$n_0 = \left(\frac{k_{2,0}}{k_{1,0}} \right) \theta \quad (7)$$

As soon as the propulsion is started, the semi-major axis

of the vehicle's orbit begins to increase, which causes a decrease in the corresponding mean motion n given by (3). The orbital energy begins to increase according to (4). The propulsion is continued until a new resonant orbit is reached, which is determined when the mean motion becomes equal to $(k_{2,1} \theta)/k_{1,1}$ where $k_{2,1}$ and $k_{1,1}$ are new resonant integers, such that $k_{2,1}/k_{1,1} < k_{2,0}/k_{1,0}$. Hence, the propulsion is always terminated before the vehicle falls below the minimum beam elevation angle. Notice that there are an infinite number of resonant integers $k_{1,1}$ and $k_{2,1}$, such that $k_{2,1}/k_{1,1} < k_{2,0}/k_{1,0}$. The selection of what pair to use for the cutoff is based on minimizing the total time required to drive the orbit's apoapsis altitude to synchronous orbit altitude. Hence, one should choose a pair that will keep the time intervals between station flyovers as short as possible (i.e., one sidereal day) and transmit as much energy as possible during each pass. This means that $k_{1,1}$ should be equal to 1 and $k_{2,1}/k_{1,1}$ should be as small as possible. But $k_{1,1} = 1$ should always take precedence over $k_{2,1}/k_{1,1}$. For example, assume that the minimum beam elevation angle is 15° and assume that when the beam elevation angle is 25° and going down during propulsion, $k_{2,1} = 12$ and $k_{1,1} = 1$, so that $k_{2,1}/k_{1,1} = 12$. Assume also that if the propulsion is continued down to a beam elevation angle of 16° , (still within the power transmission field) it will be possible to reach $k_{2,1} = 23$ and $k_{1,1} = 2$, so that $k_{2,1}/k_{1,1} = 11\frac{1}{2}$. Since more energy would be pumped into the orbit when $k_{2,1}/k_{1,1} = 11\frac{1}{2}$ rather than when $k_{2,1}/k_{1,1} = 12$, one might assume that it would be better to go for the longer burn so that the apoapsis could be driven closer to synchronous orbit. However, this would not be the case because the next station flyover would be 2 sidereal days later because $k_{1,1} = 2$,

instead of only one sidereal day if $k_{1,1} = 1$.

The first propulsion period is terminated when the mean motion n_1 during the first burn decreases to the precise cutoff value given by

$$n_1 = \left(\frac{k_{2,1}}{k_{1,1}} \right) \theta$$

which corresponds to a new higher energy resonant orbit.

(In the example, $k_{2,1} = 12$ and $k_{1,1} = 1$.) After thrust termination, the vehicle resumes its free-fall flight mode until its next pass over the laser transmitting station. Propulsion is resumed immediately after the vehicle rises above the minimum beam elevation angle and continues until the mean motion is decreased to a new resonant value, given by

$$n_2 = \left(\frac{k_{2,2}}{k_{1,2}} \right) \theta$$

Where $k_{2,2}$ and $k_{1,2}$ are new resonant integers selected according to the procedure described above for the first burn.

If the vehicle moves under a spherical gravitational field, the free-fall orbit remains stationary in inertial space. However, in view of the fact that each new coasting orbit is resonant with the laser transmitting station, all of the primary propulsion maneuvers will occur while the vehicle is passing through perigee. Although this will result in better fuel economy - because it is always more efficient to apply propulsion when the vehicle is near its maximum velocity - it will also result in shorter power transmission intervals over the station. The cumulative effect will be a lengthening of the total time

required to reach synchronous orbit altitude to complete step 2.

In general, in the determination of the duration of this i 'th burn in step 2, there will always exist resonant integers $k_{2,i}$ and $k_{1,i}$, that correspond to a resonant orbit, such that $k_{2,i}/k_{1,i} < k_{2,i-1}/k_{1,i-1}$ where the new mean motion n_i is given by

$$n_i = \left(\frac{k_{2,i}}{k_{1,i}} \right) \theta \quad (i = 1, 2, 3, \dots) \quad (8)$$

and where power transmission begins as soon as the vehicle rises above the minimum permissible beam elevation angle and ends after it arcs over the station and falls below the minimum permissible beam elevation angle. This situation will enable a maximum amount of power to be transmitted during the i 'th burn. But the time interval $(k_{1,i} P_s)$ before the next pass over the station will be $k_{1,i}$ sidereal days, which generally will be very long. In mathematical terms, this is because the rational numbers (i.e., quotients of integers) are everywhere dense on the real line. For example, if n_i is the new mean motion resulting from a maximum possible engine burn that is determined by the minimum permissible beam elevation angle α without any regard for resonance, then for any desired degree of accuracy ϵ there will always exist two integers $k_{1,i}$ and $k_{2,i}$ such that

$$|n_i - \left(\frac{k_{2,i}}{k_{1,i}} \right) \theta| < \epsilon$$

Clearly, if ϵ is very small, then both of the integers $k_{1,i}$ and $k_{2,i}$ will, in general, be very large. In

practical terms, this means that although it will always be possible to transmit a maximum amount of energy into the orbit during any burn, the next burn opportunity will appear only after a very long coasting time.

The total time interval T_2 required to carry out the primary propulsion sequence of step 2 is given, approximately, by

$$T_2 = \left(\sum_{i=1}^{N-1} k_{1,i} \right) P_s$$

Where N is equal to the total number of burns required to drive the apoapsis altitude to synchronous orbit altitude. The selection of the resonant integers $(k_{1,i}, k_{2,i})$ is made with the aim of minimizing T_2 .

A typical set of resonant integers $(k_{1,i}, k_{2,i})$ that might correspond to step 2 of the primary boosting maneuvers for a high power laser transmitter is given in table 5 where $N = 7$.

TABLE 5. - EXAMPLE OF RESONANT INTEGERS OCCURRING
DURING THE PRIMARY BOOSTING MANEUVERS
TO SYNCHRONOUS ORBIT

i'th burn	$(k_{1,i}, k_{2,i})$
Initial Orbit 0	(1, 16)
1	(1, 14)
2	(1, 12)
3	(1, 10)
4	(1, 8)
5	(1, 6)
6	(1, 4)
7	Apoapsis altitude reaches synchronous orbit

In this case, the apoapsis altitude of the vehicle's orbit reaches synchronous orbit altitude during the 7'th burn. It should be pointed out that when the apoapsis is at synchronous orbit altitude (35,793 km) and the periapsis is still at the initial orbital altitude of 269.1 km, the ratio $r_s/P = 2.27127$. Hence, $k_{2,i}/k_{1,i} \geq 2.27127$ for every pair of resonant integers where the initial orbital altitude is 269.1 km, i.e., where $(k_{1,0}, k_{2,0}) = (1,16)$.

In the above example, all of the resonant integer coefficients k_{li} are 1, and $T_2 = 6$ sidereal days. In situations where the propulsion acceleration is very low due to low beam powers and/or high payload mass, it will be impossible to have $k_{1,i} = 1$ for all of the burns. For example, in order to obtain (1,15) on the first burn from the initial orbit (1,16), the first propulsive burn will have to be capable of decreasing the orbit's mean motion by an amount δn , given by

$$\delta n = (k_{2,1}/k_{1,1} - k_{2,0}/k_{1,0}) \dot{\theta} = (15-16)\dot{\theta} = -\dot{\theta}$$

If this is not possible, we set $k_{1,1} = 2$ and $k_{2,1} = 31$ and determine if it is possible to change n by the amount $\delta n = -\dot{\theta}/2$ during the first burn. If this is still impossible, we set $k_{1,1} = 3$ and $k_{2,1} = 47$ and determine whether $\delta n = -\dot{\theta}/3$ is possible. This is continued until the smallest positive integer $k_{1,1}$ is found, such that the first power transmission will be capable of changing n by the amount

$$\delta n = (k_{2,1}/k_{1,1} - 16/1)\dot{\theta}$$

Where $k_{2,1} = 16 k_{1,1} - 1$

This testing procedure is carried out by a digital computer which simulates the actual flight profile of the transfer vehicle by detailed numerical integrations. The computer program simultaneously monitors all

dynamical and geometrical aspects of the flight, including the beam angles to the transmitter's local horizon and the effects of the earth's rotation. Specifically, the program will determine the maximum possible change in n that is possible for any particular pass over the station corresponding to a maximum burn time. That is to say, by a burn which starts as soon as the vehicle rises above the minimum allowed beam elevation angle and continues uninterrupted until the vehicle passes directly over the station and falls below the minimum allowed beam elevation angle where the burn is terminated. The program records the time t_i and corresponding vehicle position and velocity vectors \vec{r}_i, \vec{v}_i , every time the vehicle's changing orbit passes through a higher energy resonant orbit corresponding to new resonant integers (with reasonably low integer values). Then, when the minimum beam elevation angle is reached, it is possible to select a specific resonant orbit that will give the most desirable coasting period to the next station flyover. When the most favorable resonant orbit is selected, the corresponding time t_i determines the burn cutoff time, and the state vectors \vec{r}_i and \vec{v}_i determine the new resonant orbit. This is the procedure used to determine the burn cutoff time that will give the most desirable new resonant orbit when the previous resonant orbit had $k_{1,i} = 1$ such as going from $(k_{1,0}, k_{2,0}) = (1,16) \rightarrow (k_{1,1}, k_{2,1})$.

Returning to the example for the first burn, suppose that the most desirable new resonant orbit has $k_{1,1} = 5$. Then $k_{2,1} = 79$ and $\delta n = -\dot{\theta}/5$ and the burn can be represented by $(1,16) \rightarrow (5,79)$. Since $k_{1,1} = 5$, the second burn will be 5 sidereal days later. The procedure for the determination of the duration of the second burn will be different from that described above. In this case, the

burn will be automatically terminated when the mean motion changes by $-\phi/5$ so that $(k_{1,2}, k_{2,2}) = (5, 78)$. In most cases, this will always be possible because the prior burn will not be terminated very close to the minimum allowed beam angle α . Usually, it will be terminated at least 10° above α . This extra margin could be utilized for power transmission on later passes in order to obtain the required δn . The fact that $k_{1,2}$ is still kept at 5 and not changed to 4 follows from the fact that although it will be possible to have $k_{1,2} = 4$ (where $k_{2,2} = 63$ because $79/5 = 15.8 > 15.75 = 63/4 > 15.6 = 78/5$), it may not be possible to have $k_{1,3} = 4$ or $k_{1,4} = 4$ because they would require a minimum δn of $-\phi/4$ instead of $-\phi/5$. But as the vehicle's orbital energy increases after each powered pass, its velocity increases also, which results in shorter and shorter power transmission periods. However, this effect is cancelled somewhat by the fact that since the vehicle will be traveling at a higher rate of speed, the propulsion period required to change the orbit's mean motion by a given amount will be smaller. But these effects are non-linear. Thus each burn will be designed to change n by an amount equal to $-\phi/5$ until after 5 burns are completed when $k_{1,5} = 1$. These 5 initial burns can be represented by the arrows in the series $(k_{1,0}, k_{2,0}) = (1, 16) \rightarrow (5, 79) \rightarrow (5, 78) \rightarrow (5, 77) \rightarrow (5, 76) \rightarrow (5, 75) = (1, 15) = (k_{1,5}, k_{2,5})$. Thus, since each burn is separated by five sidereal days, the total time interval between the first and fifth burns will be equal to $5 \times 4 = 20$ sidereal days. It might be pointed out that if the transmitting station were located on the earth's equator and if the inclination of the vehicle were 0° , a total of $20 \times 15.5 = 310$ passes would be made over the station in the same 20-day time interval instead of only 5 for a non-equatorial station - and a

maximum amount of energy could be transmitted during each pass without regard to any resonance condition. Thus, for a flight profile that remains approximately equal to the non-equatorial case, the payload in the equatorial case could be increased by a factor of at least 70 or 80 (with similar increases in fuel load). This is a payload increase of nearly two orders of magnitude. Perhaps the best location for an equatorial laser transmitter is Mt. Kenya, Kenya, East Africa, because its latitude is only 0.13° south and its elevation is 17,058 feet.

Continuing with the above example, when $(k_{1,5}, k_{2,5}) = (1,15)$ is reached after the 5th burn, the 6'th burn will begin only one sidereal day later. A computer analysis will be carried out for the 6'th burn to determine the smallest possible integer $k_{1,6}$ where $\delta n = -\phi/k_{1,6}$. This is done in exactly the same manner described above for the determination of $k_{1,1}$ for the first burn. If the computer analysis indicates that the smallest possible integer $k_{1,6} = 4$, for example, then the next four burns will be represented by the sequence $(1,15) \rightarrow (4,59) \rightarrow (4,58) = (2,29) \rightarrow (4,57) \rightarrow (4,56) = (1,14)$. But the total time interval between the 6'th and 9'th burns will be $4 + 2 + 4 = 10$ sidereal days and not 12 sidereal days. This is because the resonant orbit defined by $(4,58) = (2,29)$ will require only 2 (and not 4) sidereal days between station flyovers. The greatest common multiple m of $k_{1,i}$ and $k_{2,i}$ is divided out of the resonant integers for every possible pair and represents a reduction between station flyovers by m sidereal days. After $(1,14)$ is reached, a computer determination of $k_{1,10}$ will be made. This process will be continued until the apoapsis altitude reaches synchronous orbit altitude.

The above example illustrates an important fact: if the mean motion n can not be changed by the minimum amount required to have all integers $k_{1,i} = 1$, which is $\delta n = -\phi$, then the flight time to synchronous orbit will be greatly increased. However, we shall see that this situation can be partially corrected by taking advantage of the fact that the earth's gravitation potential function is not spherical but "pear shaped."

After the apoapsis reaches synchronous orbit altitude (35,793 km), the primary boosting sequences (i.e., step 2 in table 3) will be completed. The next propulsion maneuver is designed to circularize the orbit at synchronous orbit altitude in one continuous burn. This corresponds to step 3 in table 3 and will occur when the vehicle passes through its apogee. But this maneuver requires a burn 180° away from perigee. Hence, the earth's rotation will have to position the laser station 180° away from its position during the perigee burns. Hence, after the last periapsis burn is completed (at the instant the apoapsis altitude reaches synchronous orbit altitude), the vehicle will make a total of $m_v + \frac{1}{2}$ orbit revolutions, and the transmitting station will make $m_t + \frac{1}{2}$ revolutions on its axis, where m_v and m_t are integers. This will put the vehicle and transmitter at the same longitude when the vehicle passes through apogee and will result in the vehicle's being at maximum elevation relative to the transmitter's local horizon. The relative positions of the vehicle and transmitter at the beginning of the circularization maneuver are shown in figure 7. If this maximum elevation angle is denoted by β , then

$$\beta = \cos^{-1} \frac{R_s \sin (2\phi_t)}{\sqrt{R_s^2 + p_o^2 - 2p_o R_s \cos (2\phi_t)}}$$

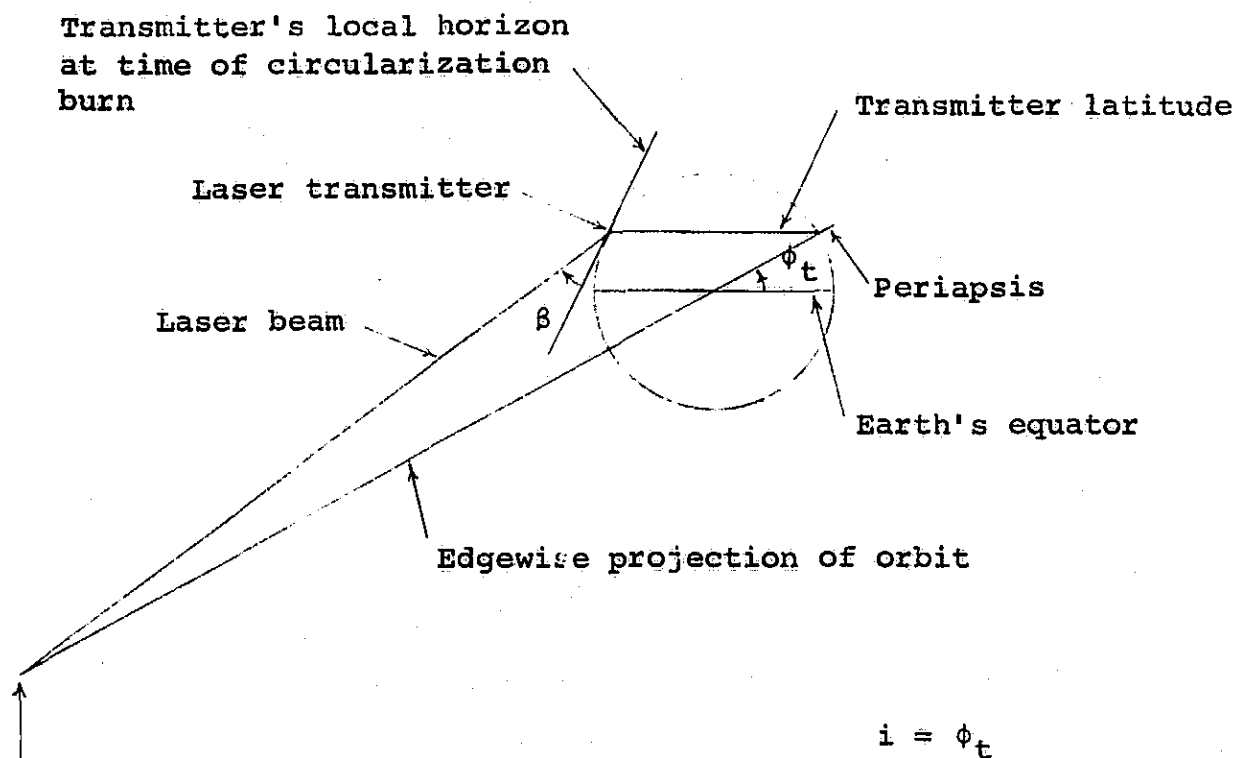


Figure 7. - Relative positions of laser transmitter and laser transfer vehicle at the beginning of the circularization maneuver at synchronous orbit altitude (spherical potential function).

where R_s = distance between synchronous orbit and the center of earth = 42164.2 km; and where ρ_o = earth's mean radius = 6371.3 km. Consequently, if $\phi_t = 31.8^\circ$ then $\beta = 18.14^\circ$.

The integers m_v and m_t can be determined from the equation

$$(m_t + \frac{1}{2})P_s = (m_v + \frac{1}{2})P$$

which can be expressed as

$$\frac{2m_v + 1}{2m_t + 1} = \frac{P_s}{P} = 2.27127$$

where the initial orbit is assumed to be 269.1 km high. A very close integral solution to this equation is $m_v = 12$ and $m_t = 5$ ($25/11 = 2.27273$).

Hence, the circularization maneuver (step 3) will occur $m_t + \frac{1}{2} = 5\frac{1}{2}$ sidereal days (5.485 mean solar days) after the last periapsis burn of step 2. If weather conditions over the transmitter are unfavorable for power transmission, the next transmission opportunity will occur 11 sidereal days later ($16\frac{1}{2}$ sidereal days after the last periapsis burn). In general, these opportunities occur $[(11 k-1)/2] + \frac{1}{2}$ sidereal days after the last periapsis burn where $k = 1, 3, 5, \dots$. The total ΔV for the circularization maneuver will be 1.471 km/sec (if the initial orbital altitude is 269.1 km). The sum of all ΔV 's in the primary boosting maneuvers will be 2.473 km/sec.

After the circularization maneuver is accomplished, the vehicle will remain above the local horizon of the transmitting station. If no further maneuvers are carried out, the vehicle will simply oscillate between a point

directly over the transmitter and a point 18.14° above the transmitter's local horizon.

The plane change maneuver (i.e., step 4) that changes the inclination from ϕ_t to 0° occurs $1/4$ sidereal days (5.98 hours) after the circularization maneuver. If weather conditions are unfavorable for power transmission, the next opportunity will occur $\frac{1}{2}$ sidereal days later ($3/4$ sidereal days after the circularization maneuver). These opportunities occur at $\frac{1}{2}$ sidereal day intervals when the vehicle passes through its ascending or descending node (i.e., every time the vehicle passes over the earth's equator). If $\phi_t = 31.8^\circ$, the maximum beam elevation angle during the plane change maneuver will be 38.89° and the required $\Delta V = 1.685$ km/sec. Hence, if the initial orbital altitude is 269.1 km and if $\phi_t = 31.8^\circ$, then the total ΔV required for transfer to synchronous orbit as described in steps 2, 3, and 4 of table 3 will be 2.437 km/sec. + 1.471 km/sec + 1.685 km/sec = 5.593 km/sec. The maneuvers described in steps 8, 9 and 10 which will bring the vehicle back to the original parking orbit are the reverse of steps 2, 3, and 4 with identical ΔV 's. Hence, the total ΔV required for a complete round trip to synchronous orbit via laser propulsion will be 11.185 km/sec. This is 2.641 km/sec more than that required for ordinary rocket vehicles.

However, the above maneuvers will enable the laser beam to have maximum elevation angles during all of the power transmission periods. This ΔV of 11.185 km/sec actually represents a lower bound, since it was computed on the assumption of impulsive burns at periapsis and apoapsis. Moreover, when we consider the solution corresponding to a "pear-shaped" gravitational potential function, the overall ΔV will be about 300 m/sec to 600 m/sec higher than this value because the burns will not

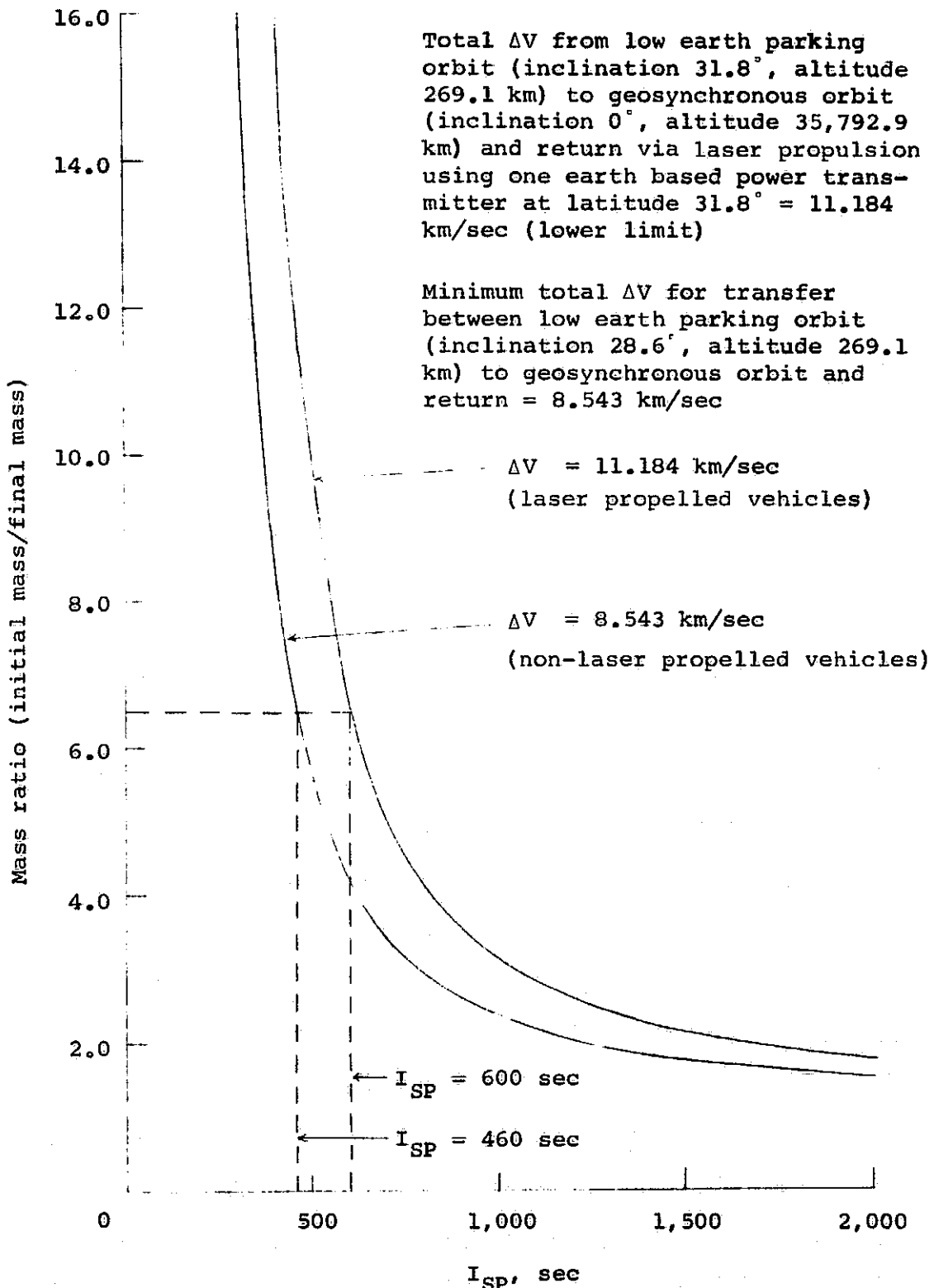


Figure 8. - Mass ratio versus I_{SP} for missions to geosynchronous orbit and return for laser propelled and non-laser propelled vehicles.

occur at periapsis.

Although it may appear that it is much more efficient to employ standard rocket engines that generate the propulsive power aboard this vehicle, the high specific impulse that may be available from a laser rocket engine will more than offset this apparent inefficiency. This can be seen by studying the corresponding mass ratios. In particular, the highest possible I_{SP} that an ordinary chemical rocket engine can generate is about 460 seconds. Hence, in order for a laser transfer vehicle to have the same mass ratios as a chemical orbiter for round trip missions to synchronous orbits, the laser vehicle will have to have an I_{SP} of only 600 seconds.

Figure 8 contains curves of vehicle mass ratios versus engine I_{SP} for round trip missions to synchronous orbit via laser-propelled vehicles with $\Delta V = 11.185$ km/sec and ordinary rockets with $\Delta V = 8.543$ km/sec (chemical, ion, nuclear, etc.). The corresponding mass ratio for the laser vehicle with $I_{SP} = 1,000$ seconds and 2,000 seconds is 3.128 and 1.769 respectively. Since the lowest possible mass ratio for a chemical rocket ($I_{SP} = 460$ seconds) is 6.653, it is clear that the laser transfer vehicle may have a substantial performance advantage over the chemical transfer vehicles. Moreover, if the laser transmitter were located on the equator, the round trip ΔV of 11.185 km/sec could be reduced to only 7.816 km/sec. In this case, the ground-to-orbit shuttle vehicle would make the plane change maneuver during orbit insertion.

2. Analysis based on a "pear-shaped" gravitational potential function

Suppose that the Cartesian inertial frame $\{\}$ introduced above has its origin at the earth's center, its x-y plane in the earth's equatorial plane, and its

positive z axis passing through the north pole. It was pointed out above that if the earth were perfectly spherical and homogeneous, its gravitational potential function $U = \mu/r$ and the orbit, defined as the solution to equation (1), is a conic section. Conic orbits can be defined geometrically in a three-dimensional space by five "classical" orbital elements, namely:

- a (semi-major axis)
- e (eccentricity)
- i (angle of inclination)
- ω (argument of perigee ; angle between line of apsides and ascending line of nodes)
- Ω (longitude of the ascending node; angle between +x-axis and ascending line of nodes)

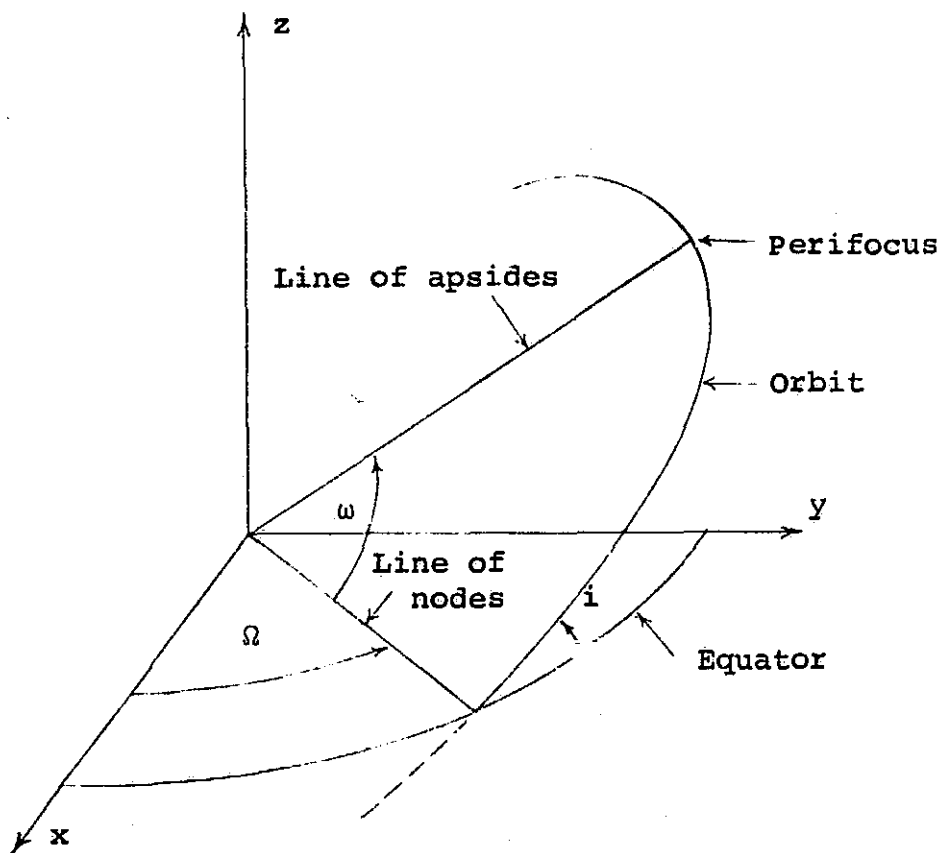
Figure 9 defines the classical angular orbital elements i , ω , and Ω relative to ℓ . If $U = \mu/r$, then all of these elements are constants.

However, the earth is actually an oblate spheroid, and its potential function is actually given by (ref. 31)

$$U = \frac{\mu}{r} \left[1 + \frac{J_2}{2r^2} (1 - 3 \sin^2 \delta) + \frac{J_3}{2r^3} (3 - 5 \sin^2 \delta) \sin \delta \right. \\ \left. - \frac{J_4}{8r^4} (3 - 30 \sin^2 \delta + 35 \sin^4 \delta) + \epsilon \right]$$

where $\sin \delta = \frac{z}{r}$ and where J_2 , J_3 and J_4 are constants defined by (ref. 30).

$$J_2 = +1082.70 \pm 0.3 \times 10^{-6} \\ J_3 = -2.56 \pm 0.2 \times 10^{-6} \\ J_4 = -1.58 \pm 0.5 \times 10^{-6}$$



ω = argument of perigee

Ω = longitude of the ascending node

i = orbit inclination

Figure 9. - Definition of the angular classical orbital elements i, ω, Ω , the line of apsides and the line of nodes.

The term ϵ is very small and includes all higher order terms. This "pear-shaped" gravitational field causes the orbital elements to change with the passage of time. It can be shown (ref. 32) that, omitting small second order terms,

$$\frac{da}{dt} = 0$$

$$\frac{de}{dt} = 0$$

$$\frac{di}{dt} = 0$$

$$\frac{d\omega}{dt} = \frac{3nJ_2 p_0^2}{4p^2} [5 \cos^2 i - 1] \left(\frac{\text{radians}}{\text{sec}} \right) \quad (9)$$

$$\frac{d\Omega}{dt} = - \frac{3nJ_2 p_0^2}{2p^2} \cos i \left(\frac{\text{radians}}{\text{sec}} \right) \quad (10)$$

$$\frac{dM}{dt} = \bar{n} = n + \frac{3nJ_2 p_0^2 (3 \cos^2 i - 1)}{4(1-e^2)^{3/2} a^2} \left(\frac{\text{radians}}{\text{sec}} \right) \quad (11)$$

where

$$p = a(1-e^2) = \text{orbit's semi-parameter}$$

$$n = \sqrt{\mu/a^3} = \text{orbit's mean motion}$$

$$M = n(t-t_p) = \text{orbit's mean anomaly}$$

Hence, the orbits of space vehicles about the earth are not conics that are stationary with respect to the inertial frame $\{\}$ but conics that move relative to $\{\}$. In particular, the orbit's line of apsides will rotate at a rate $\frac{d\omega}{dt}$ in the same direction as the vehicle's motion, while the line of nodes rotates in a retrograde direction at the rate $\frac{d\Omega}{dt}$. These lines are defined in figure 9. Notice that if

the orbit's inclination $i = \cos^{-1} \sqrt{1/5} = 63.435^\circ$, then

$\frac{d\omega}{dt} = 0$ and there would be no movement of the line of apsides. On the other hand, if $i = 0^\circ$ there would be no line of nodes and hence no movement of the line of nodes (the expression given above by $\frac{d\Omega}{dt}$ does not hold if $i = 0^\circ$).

Table 6 describes the values of $\frac{d\omega}{dt} = \dot{\omega}$ and $\frac{d\Omega}{dt} = \dot{\Omega}$ for various earth orbits. In addition to the above parameters, the table also contains several others, defined by:

$Q = a(1+e) =$ apoapsis distance (km)

$q = a(1-e) =$ periapsis distance (km)

$Q_h = Q - \rho_0 =$ apoapsis altitude above earth's surface (km)

$q_h = q - \rho_0 =$ periapsis altitude above earth's surface (km)

$\dot{\omega} = \frac{d\omega}{dt}$ (converted to degrees per mean solar day)

$\dot{\Omega} = \frac{d\Omega}{dt}$ (converted to degrees per mean solar day)

The information given in table 6 describes how fast an orbit's line of apsides and the line of nodes move during one mean solar day for various orbital parameters. Notice that for relatively low orbital altitudes (e.g., less than 1,000 km) the orbital motion is quite rapid. This motion will be utilized to increase the altitude of the laser transfer vehicle as it passes over the

Motion of the Line of Apsides and the
Line of Nodes for Various Orbits

ORIGINAL PAGE IS
OF POOR QUALITY

a	e	p	Q	q	Q _h	q _h	i=0°			i=30°		
							ω	Ω	h	ω	Ω	h
6,583	.0008	6,583	6,588	6,578	210	200	17.8350	12.2616	-7.7228			
6,728	.0223	6,725	6,878	6,578	500	200	16.5403	11.3715	-7.1622			
6,978	.0573	6,955	7,378	6,578	1,000	200	14.6408	10.0656	-6.3397			
8,978	.2673	8,336	11,378	6,578	5,000	200	6.9836	4.8012	-3.0240			
6,883	.0007	6,883	6,888	6,878	510	500	15.2592	10.4907	-6.6074			
7,128	.0351	7,119	7,378	6,878	1,000	500	13.5353	9.3055	-5.8609			
9,128	.2465	8,573	11,378	6,878	5,000	500	6.4408	4.4281	-2.7890			
11,628	.4085	9,688	16,378	6,878	10,000	500	3.5078	2.4116	-1,5189			
7,383	.0007	7,383	7,388	7,378	1,010	1,000	11.9383	8.2076	-5.1694			
9,378	.2113	8,951	11,378	7,378	5,000	1,000	5.6735	3.9005	-2.4567			
11,878	.3789	10,173	16,378	7,378	10,000	1,000	3.0814	2.1185	-1.3343			
16,878	.5639	11,531	26,378	7,378	20,000	1,000	1.4159	0.9734	-0.6131			
31,878	.7686	13,048	56,378	7,378	50,000	1,000	0.4260	0.2929	-0.1845			
56,878	.8703	13,799	106,378	7,378	100,000	1,000	0.1598	0.1099	-0.0692			
106,878	.9310	14,247	206,378	7,378	200,000	1,000	0.0582	0.0400	-0.0252			
156,878	.9530	14,409	306,378	7,378	300,000	1,000	0.0320	0.0220	-0.0139			
11,383	.0004	11,383	11,388	11,378	5,010	5,000	2.6234	1.8036	-1.1360			
13,878	.1801	13,428	16,378	11,378	10,000	5,000	1.4004	0.9628	-0.6064			
18,878	.3973	15,898	26,378	11,378	20,000	5,000	0.6297	0.4329	-0.2727			
33,878	.6641	18,935	56,378	11,378	50,000	5,000	0.1847	0.1269	-0.0799			
58,878	.8068	20,557	106,378	11,378	100,000	5,000	0.0684	0.0470	-0.0302			
108,878	.8955	21,567	206,378	11,378	200,000	5,000	0.0247	0.0170	-0.0107			
158,878	.9284	21,941	306,378	11,378	300,000	5,000	0.0135	0.0073	-0.0059			
16,383	.0003	16,383	16,388	16,378	10,010	10,000	0.7335	0.5043	-0.3176			
21,378	.2339	20,209	26,378	16,378	20,000	10,000	0.3234	0.2223	-0.1400			
36,378	.5498	25,382	56,378	16,378	50,000	10,000	0.0924	0.0635	-0.0400			
61,378	.7332	28,386	106,378	16,378	100,000	10,000	0.0337	0.0232	-0.0146			
111,378	.8530	30,348	206,378	16,378	200,000	10,000	0.0121	0.0083	-0.0039			
161,378	.8985	31,094	306,378	16,378	300,000	10,000	0.0066	0.0045	-0.0029			
26,383	.0002	26,383	26,388	26,378	20,010	20,000	0.1384	0.0952	-0.0599			
41,378	.3625	35,940	56,378	26,378	50,000	20,000	0.0389	0.0261	-0.0165			
66,378	.6026	42,274	106,378	26,378	100,000	20,000	0.0135	0.0093	-0.0059			
116,378	.7733	46,777	206,378	26,378	200,000	20,000	0.0048	0.0033	-0.0021			
166,378	.8415	48,574	306,378	26,378	300,000	20,000	0.0026	0.0012	-0.0011			
56,383	.0001	56,383	56,388	56,378	50,010	50,000	0.0097	0.0067	-0.0042			
81,378	.3072	73,698	106,378	56,378	100,000	50,000	0.0033	0.0023	-0.0014			
131,378	.5709	88,562	206,378	56,378	200,000	50,000	0.0011	0.0008	-0.0005			
181,378	.6892	95,232	306,378	56,378	300,000	50,000	0.0006	0.0004	-0.0002			

laser transmitter during the primary boosting sequence. This will result in longer power transmission times and consequently, greater velocity increments during each pass. The cumulative effect of these increased velocity increments will result in a significantly shorter time interval required to reach synchronous orbit altitude compared to a purely spherical gravitation field.

We shall now derive a formula, analogous to equation (8), for the determination of resonant orbits where the orbit's line of apsides and the line of nodes precess under the influence of an oblate spheroid central body. As in the case of a spherical central body, this formula will provide the means for determining the duration of each successive engine burn, during the primary boosting maneuvers to synchronous orbit, such that the resulting orbits at the instant of engine cutoff will be resonant with the laser transmitting station.

The constant motion of an orbit's line of nodes due to the motion of the orbital plane about the earth's rotation axis (see figure 9) can be viewed with respect to the earth's surface as being due to a speed-up of the earth's rotation to a new value given by $\dot{\theta} - \dot{\Omega}$. (The value of $\dot{\Omega}$ is negative.) This will produce an apparent period for the earth's rotation P_s^1 given by

$$P_s^1 = \frac{2\pi}{\dot{\theta} - \dot{\Omega}} \quad (12)$$

By assuming that the earth's rotational period is P_s^1 instead of P_s , the orbital plane will appear stationary relative to the fixed stars (i.e., relative to $\{\}$).

Suppose that the line $L(t)$ generated by the station's local zenith and the center of the earth O at some instant t , intersects the stationary orbit at a point A when the vehicle is also at that point (see figure 10). We can assume that the station lies on this

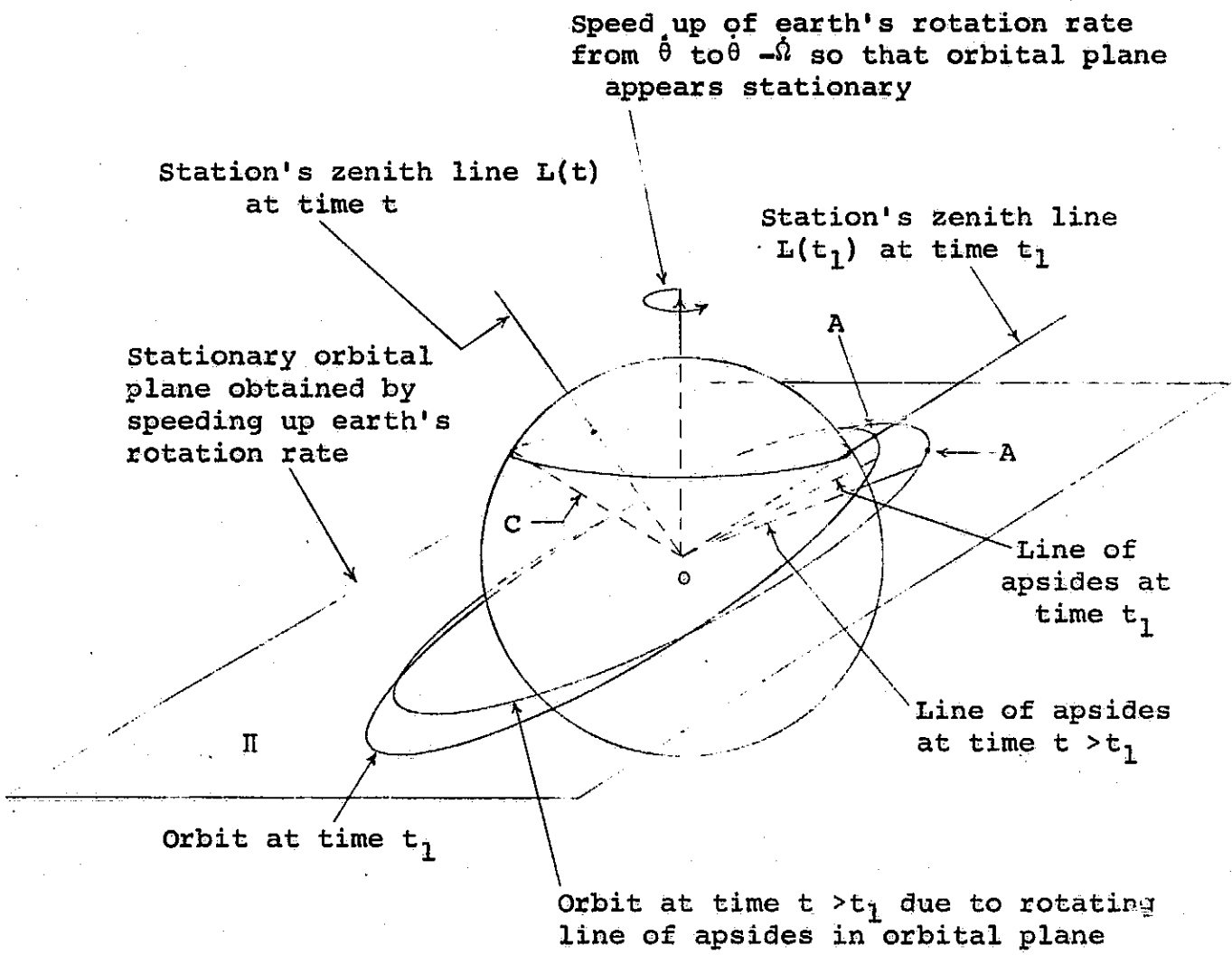


Figure 10. - Station-vehicle synchronization geometry for precessing orbit.

line. The line $L(t)$ traces out a cone C relative to $\{\}$ that has its vertex fixed at the earth's center 0. This cone C passes through (or is tangent to) the stationary orbital plane at line $L(t_1)$ fixed in this plane (i.e., fixed in $\{\}$). The station's zenith line $L(t)$ will be coincident with $L(t_1)$ in the orbital plane at intervals of time equal to P_s^1 seconds where P_s^1 is given by (12). Hence, it will be coincident with $L(t_1)$ at times $t_1, t_1 + P_s^1, t_1 + 2P_s^1, t_1 + 3P_s^1, \dots$. But since the orbit itself is rotating within the stationary orbital plane at a rate ω radians/sec, the zenith line $L(t)$ will intersect different points of the orbit after each revolution of the station.

Let \bar{n} and \bar{P} denote the orbit's anomalistic mean motion and anomalistic period respectively (ref. 33). Then

$$\bar{P} = \frac{2\pi}{\bar{n}}$$

This is the time interval between two successive perifocal passages. However, since the perifocal point is itself rotating about the earth's center 0 in the stationary orbital plane at a rate ω radians per second where the time for one complete revolution is $2\pi/\omega$, it follows that the time interval P^1 that the vehicle requires between two successive intersections of the fixed line $L(t_1)$ is given by

$$P^1 = \frac{2\pi}{\bar{n} + \omega} \quad (13)$$

At the time t_1 the vehicle is passing through the station's zenith line $L(t_1)$. Thus, in order for the vehicle to pass through the station's zenith during every revolution of the station, P_s^1 and P^1 must be related by the equation

$$P_s^1 = kP^1$$

where k is a positive integer. The integer k is approximately equal to the number of perifocal passages, (i.e., orbit revolutions) the vehicle makes between successive station flyovers. However, this integer is exactly equal to the number of times the vehicle moves around the earth during the time interval P_s^1 .

In order for the vehicle to pass through the station's zenith at intervals of k_1 revolutions of the laser station, where k_1 is a positive integer, there must exist a second integer k_2 such that

$$k_1 P_s^1 = k_2 P^1 \quad (14)$$

This equation is analogous to equation (6) derived for non-precessing orbits. Upon substituting equations (12) and (13) into this equation, we obtain

$$\bar{n}_i + \dot{\omega}_i = \frac{k_{2,i}}{k_{1,i}} (\theta - \Omega_i) \quad (15)$$

where the subscript i refers to the value of the corresponding quantity after the i 'th engine burn ($i = 0, 1, 2, \dots$). This equation is analogous to equation (8).

The actual transfer of payloads to and from synchronous orbit is carried out according to table 3. In particular, the primary boosting maneuvers of step 2 (table 3) are carried out by exactly the same methods already described for the case of a spherical potential function. For example, in the case of a spherical potential function, each integration step during the primary thrusting maneuvers required the calculation of the orbit's instantaneous semi-major axis a and instantaneous mean motion n_i given by equation (3) in order to terminate the burn when the desired solution to equation (8) is reached. In the case of the "pear-shaped" potential function, the orbit's

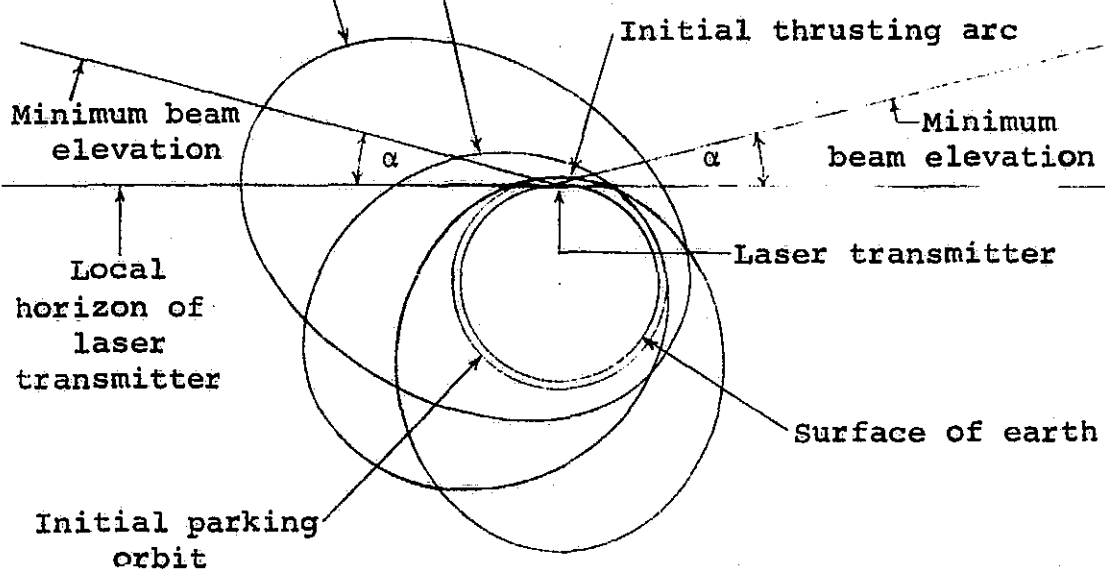
instantaneous semi-major axis a is also computed during each integration step. But in addition to calculating the instantaneous mean motion n_i , the orbit's instantaneous anomalistic mean motion \bar{n}_i is also calculated by equation (11). Moreover, the instantaneous values of $\dot{\omega}_i$ and Ω_i are also calculated by equations (9) and (10) so that the burn can be terminated as soon as the desirable solution to equation (15) is reached. This is the only difference that results from replacing the spherical potential function with the "pear-shaped" potential function during step 2 of the primary boosting maneuvers.

Figure 11 describes the rotation of the orbit's line of apsides in its orbital plane Π between successive thrusting maneuvers and the thrusting field of the laser transmitter (defined by the minimum beam elevation angle) as it intersects Π when the vehicle passes through its zenith. Notice that as the orbit is progressively rotated in Π , more of its arc falls into the transmitter's thrusting field. This results in a greater thrusting time during each successive flyover. Thus, the time required to reach synchronous orbit is significantly reduced. Since orbit rotation does not occur with a spherical potential function, the duration of successive thrusting maneuvers does not increase. Although this results in greater propulsion efficiency, since the burns will always occur during periapsis passage, this benefit is offset by the longer flight times. If the vehicle acceleration is very small during the thrusting maneuvers because of low beam power and/or high payload mass, this shortening of flight time to synchronous orbit will be significant.

The determination of the time interval between the last primary boosting maneuver of step 2 and the circularization maneuver of step 3 will be different for

Thrusting arc corresponding to
120° rotation of line of apsides

Thrusting arc corresponding to
60° rotation of line of apsides



II

Stationary orbital plane containing precessing orbits II

Figure 11. - Higher energy resonant orbits during primary boosting maneuvers based on pear-shaped potential function resulting in increasing thrusting arcs.

the case of a "pear-shaped" potential function. This is because the periapsis altitude at the end of the primary boosting maneuvers will be much greater than the initial orbital altitude. (In the spherical case these altitudes are nearly equal.) In addition, the vehicle's true anomaly could have any value at the end of the last boosting maneuver. (In the spherical case, the vehicle's true anomaly will be close to zero.) We shall now give a simple method for calculating this time interval for the "pear-shaped" potential field.

It will be convenient to begin the circularization maneuver of step 3 when the vehicle passes through apogee. Thus, at the time t_2 when the last boosting burn of step 2 is terminated (when the apoapsis reaches synchronous orbit altitude), the time interval Δt to the next apogee passage is calculated. The orbit's anomalistic period \bar{P} at cutoff is also calculated. The time t is then advanced by discrete jumps equal to

$$t(k) = t_2 + \Delta t + k\bar{P}$$

where $k = 1, 2, 3, \dots$. These times correspond to successive apogee passages. The position vector of the vehicle relative to the transmitting station and its elevation angle $\beta(k)$ relative to the station's local horizon is calculated for each value of k . The burn for step 3 is started when an integer k is found such that $\beta(k) > \alpha$ where α is equal to some pre-determined minimum allowed beam elevation angle and such that β will increase (locally) when time t is allowed to increase continuously from $t(k)$. As in the spherical case, the burn is carried out in one continuous burn until the orbit has been circularized at synchronous orbit altitude. This will complete step 3. The numerical results show that

the beam elevation angle during this maneuver will be greater than the one resulting from the corresponding maneuver formulated on the basis of a spherical potential function (as previously described). This result, however, is actually inherent in this method.

If the vehicle acceleration is very low due to low beam powers and/or high payload mass, the plane change maneuver of step 4 will take place by a series of burns with thrust vector normal to the vehicle's instantaneous velocity vector. Each burn occurs when the vehicle approaches one of its nodes. This burn sequence is continued until the vehicle's inclination is zero. As in the spherical potential case, the laser propulsion maneuvers for steps 8, 9, and 10 (that return the vehicle to the initial parking orbit) are essentially the reverse of steps 2, 3, and 4.

3. Numerical comparison of trajectories to synchronous orbit using spherical and pear-shaped potential functions

Two computer programs were constructed according to the above algorithms to numerically simulate round-trip trajectories to synchronous orbit by laser propelled shuttle orbiters. One program was based on the spherical potential function and the other on the pear-shaped potential function. Each program took the vehicle through steps 2, 3, 4, 8, 9, and 10 of Table 3 automatically (using detailed numerical integrations) without interruption for a complete flight simulation. The coasting periods were computed by closed form conic equations which, in the case of the pear-shaped potential, were rotated in \mathbb{R}^3 by rotation matrices determined by the precession equations (9) and (10). The mathematical formulation was based on the vector methods developed for gravity thrust

trajectories (ref. 34). Since the details involve astrodynamical concepts not particularly relevant to the central aim of this paper they shall not be discussed here. However, they proved to be very convenient for this study.

In order to evaluate the possible benefits of using the pear-shaped potential function over the spherical function, the two programs were run with identical initial conditions. These initial conditions were:

vehicle dry mass = 4,648 kg
propulsive power = 60 MW
engine I_{SP} = 700 seconds
engine thrust = 17,481 N (3,930 lbs.)
initial orbital altitude = 269.1 km
initial orbital inclination = 31.8°
payload up = 3,000 kg
payload down = 0 kg

As expected, the most striking difference between the trajectories appeared during the primary boosting maneuvers of step 2 (Table 3). The results, corresponding to spherical and pear-shaped potential functions, are shown in Tables 7 and 8 respectively. These tables and subsequent tables will use the following notation:

Duration = burn duration (seconds)

$(k_{1,i}, k_{2,i})$ = resonant integers

T = time at beginning of burn interval (measured from start of first burn in days)

Fuel = amount of fuel burned during a burn interval (kg)

Apoapsis = apoapsis distance after a burn interval

is completed (measured from earth's center in km)

Periapsis = periapsis distance after a burn interval is completed (measured from earth's center in km)

TABLE 7. - PRIMARY BOOSTING MANEUVERS OF LASER PROPELLED INTERORBITAL TRANSFER VEHICLE
 WITH 3,000 kg PAYLOAD MOVING UNDER SPHERICAL POTENTIAL FUNCTION
 (total initial mass = 30,475 kg, $I_{sp} = 700$ sec, propulsive power = 60 MW, $\beta_1 = 15^\circ$)

Burn No.	Duration (sec)	(k_1, i, k_2, i)	T (days)	Fuel (kg)	Apoapsis (km)	Periapsis (km)	a (km)	e	D_1 (km)	D_2 (km)	β_2 (deg)
0	-	(1, 16)	-	-	6,640	6,640	0,000	-	-	-	-
1	140.5	(2, 31)	0.0000	357.7	6,926	6,639	0,021	831.5	351.7	48.70	48.70
2	139.0	(1, 15)	1.9945	354.1	7,229	6,636	0,043	827.5	353.2	47.81	47.81
3	137.3	(2, 29)	2.9918	349.7	7,548	6,633	0,065	828.5	349.6	47.90	47.90
4	135.7	(1, 14)	4.9862	345.7	7,887	6,631	0,087	824.1	350.2	47.19	47.19
5	134.2	(2, 27)	5.9835	341.7	8,246	6,628	0,109	810.7	357.0	45.40	45.40
6	132.8	(1, 13)	7.9781	338.1	8,628	6,625	0,131	802.1	361.7	44.09	44.09
7	131.5	(2, 25)	8.9753	335.0	9,034	6,623	0,154	804.2	359.3	43.97	43.97
8	130.2	(1, 12)	10.9699	331.6	9,469	6,620	0,177	798.6	361.7	43.08	43.08
9	129.1	(2, 23)	11.9672	328.8	9,935	6,617	0,200	786.3	371.1	41.19	41.19
10	128.1	(1, 11)	13.9617	326.3	10,435	6,615	0,224	781.3	375.6	40.11	40.11
11	127.1	(2, 21)	14.9589	323.7	10,975	6,612	0,248	768.9	385.6	38.40	38.40
12	126.3	(1, 10)	16.9535	321.6	11,558	6,610	0,272	763.2	391.3	37.31	37.31
13	125.6	(2, 19)	17.9508	319.8	12,193	6,607	0,297	768.6	389.4	37.15	37.15
14	125.0	(1, 9)	19.9453	318.3	12,885	6,605	0,322	750.4	407.5	34.79	34.79
15	124.4	(2, 17)	20.9426	316.8	13,645	6,602	0,348	755.3	406.5	34.55	34.55
16	124.2	(1, 8)	22.9371	316.3	14,482	6,600	0,374	739.4	426.6	32.29	32.29
17	123.0	(2, 15)	23.9344	315.5	15,412	6,598	0,400	729.5	441.0	30.76	30.76
18	123.7	(1, 7)	25.9289	315.1	16,450	6,595	0,428	729.2	448.1	29.93	29.93
19	123.9	(2, 13)	26.9262	315.6	17,619	6,593	0,455	721.4	465.0	28.41	28.41
20	124.1	(1, 6)	28.9207	315.9	18,949	6,591	0,484	724.7	471.3	27.75	27.75
21	124.7	(2, 11)	29.9180	317.5	20,476	6,589	0,513	718.6	491.0	26.26	26.26
22	125.5	(1, 5)	31.9125	319.6	22,254	6,586	0,543	708.3	517.0	24.56	24.56
23	126.6	(2, 9)	32.9098	322.5	24,354	6,584	0,574	703.7	540.2	23.20	23.20
24	128.3	(1, 4)	34.9043	326.6	26,885	6,582	0,607	695.2	573.7	21.51	21.51
25	130.4	(2, 7)	35.9016	332.0	30,002	6,580	0,640	693.8	604.2	20.15	20.15
26	133.3	(1, 3)	37.8962	339.5	33,964	6,578	0,675	688.4	647.8	18.49	18.49
27	137.3	(2, 5)	38.8934	349.6	39,206	6,576	0,713	675.6	711.2	16.51	16.51
28	63.0	-	40.8881	460.4	42,164	6,575	0,730	675.1	208.6	80.22	80.22

Total fuel burned = 9,054.9 kg

ORIGINAL PAGE IS
 OF POOR QUALITY

TABLE 8. - PRIMARY BOOSTING MANEUVERS OF LASER PROPELLED INTERORBITAL TRANSFER VEHICLE

WITH 3,000 kg PAYLOAD MOVING UNDER PEAR-SHAPED POTENTIAL FUNCTION

(total initial mass = 33,748 kg, $l_{sp} = 700$ sec, propulsive power = 60 MW, $\beta_1 = 15^\circ$)

Burn No.	Duration (sec)	(k_1, i, k_2, i)	T (days)	Fuel (kg)	Apoapsis (km)	Periapsis (km)	a (km)	e	D_1 (km)	D_2 (km)	β_2 (deg)
0	-	(1, 16)	-	6,640	6,640	6,640	0,000	-	-	-	-
1	74.8	(2, 31)	0.0000	190.6	6,775	6,640	6,708	0.010	831.5	365.5	46.13
2	164.1	(1, 15)	1.9560	417.9	7,085	6,638	6,862	0.033	847.5	472.3	32.67
3	160.6	(2, 29)	2.9354	409.1	7,409	6,640	7,024	0.055	868.5	447.0	35.48
4	158.9	(1, 14)	4.8968	404.5	7,742	6,650	7,196	0.076	999.1	372.2	51.74
5	157.1	(2, 27)	5.8787	399.9	8,093	6,663	7,378	0.097	1,083.5	351.2	65.72
6	156.9	(1, 13)	7.8447	399.6	8,454	6,688	7,571	0.117	1,282.1	404.5	83.79
7	308.5	(1, 12)	8.8286	785.7	9,264	6,728	7,996	0.159	1,530.1	939.4	21.41
8	303.6	(1, 11)	9.8145	773.2	10,201	6,764	8,482	0.203	1,719.2	802.5	31.11
9	300.0	(1, 10)	10.8022	764.1	11,296	6,799	9,047	0.249	1,926.5	689.7	44.85
10	296.9	(1, 9)	11.7915	756.1	12,593	6,834	9,713	0.296	2,122.3	631.2	61.07
11	295.1	(1, 8)	12.7822	751.4	14,160	6,869	10,514	0.347	2,321.6	627.9	78.13
12	294.2	(1, 7)	13.7742	749.2	16,097	6,903	11,500	0.400	2,494.1	667.3	89.17
13	294.8	(1, 6)	14.7674	750.7	18,567	6,936	12,752	0.456	2,663.4	724.5	79.66
14	296.9	(1, 5)	15.7616	756.2	21,846	6,967	14,406	0.516	2,791.6	769.3	75.70
15	301.8	(1, 4)	16.7567	768.4	26,452	6,995	16,723	0.582	2,905.1	794.8	74.88
16	310.4	(1, 3)	17.7529	790.4	33,511	7,020	20,265	0.654	2,973.7	785.3	79.99
17	252.2	-	18.7499	642.1	42,423	-	24,732	0.715	3,004.8	1,040.1	52.25

Total fuel burned = 10,509 kg

THIS PAGE IS
OF POOR QUALITY

a = orbit's semi-major axis after a burn interval is completed (km)

e = orbit's eccentricity after a burn interval is completed

D_1 = distance between laser transmitter and vehicle at beginning of power transmission (km)

D_2 = distance between laser transmitter and transmission interval (km)

β_1 = beam elevation angle with respect to the transmitter's local horizon at beginning of power transmission (deg) - this angle is always 15° during the primary boosting maneuvers

β_2 = beam elevation angle at end of power transmission interval with respect to transmitter's local horizon (deg)

Figure 5 describes the effect of the primary boosting maneuvers of a laser transfer vehicle moving under a spherical potential function and figure 11 describes the effect of the primary boosting maneuvers of a laser transfer vehicle moving under a pear-shaped potential function. Notice that in the spherical case (Table 7) the power transmission intervals generally decrease with each new burn while in the pear-shaped case (Table 8) they increase to almost double their initial values. The total time required to boost the orbit's apoapsis to synchronous orbit altitude is only 18.7 days for the pear-shaped case which required 10,509 kg of propellant. In the spherical case, 9,055 kg of propellant was used over a time period of 40.9 days. Although 1,454 kg of additional propellant is consumed in the pear-shaped case (because of the non-periapsis propulsion), the flight time is reduced by more than 50%. The time reduction relationship between the spherical and pear-shaped cases is

highly non-linear so that if the payload is doubled the time reduction will be much greater than 50%. The circularization and plane change maneuvers for insertion into synchronous orbit are given in Table 9.

Of course, the actual trajectories will always correspond to the pear-shaped potential because it is the actual potential function of the earth. However, it is important to analyze the trajectory differences that are introduced when using the two potential functions. If these differences are minor, then the spherical potential could be used as it simplifies the analysis. But in view of the above calculations, these differences are very significant and represent a definite improvement in performance. Consequently, all laser propelled transfer trajectories between low initial orbits and synchronous orbits computed in the parametric mission analysis studies will use the high accuracy pear-shaped potential function. It should be emphasized, however, that the method for determining the resonant integers ($k_{1,i}, k_{2,i}$) for the pear shaped potential is the same as that discussed in the case of the spherical potential function.

C. Laser Propelled Injection Maneuvers

In addition to determining the performance capabilities of laser propelled transfer vehicles on missions to synchronous orbit, it is also important to consider the capabilities of these same laser propelled vehicles in injecting payloads onto interplanetary escape trajectories. Since a fair proportion of all shuttle flights in the 1980s and 1990s will require lifting second stage injection vehicles along with their payloads

TABLE 9. - CIRCULARIZATION AND PLANE CHANGE MANEUVERS OF LASER PROPELLED
INTERORBITAL TRANSFER VEHICLES
WITH 3,000 kg PAYLOAD

(I_{SP} = 700 sec, propulsive power = 60 MW)

Parameter	Circularization Maneuver		Plane Change Maneuver		
	Spherical	Pear-Shaped	Spherical	Pear-Shaped	
Burn No.	29	18	30	19	20
Duration (sec)	1645.9	1719.3	1498.2	1214	372
T (days)	46.3427	20.3038	46.5935	21.0139	21.5303
Fuel (kg)	4191	4378	3815	3092	947
D ₁ (km)	39402	39724	37003	37059	37237
θ ₁ (deg)	18.20	18.59	49.07	53.33	50.37
D ₂ (km)	39611	39796	36874	37181	37228
θ ₂ (deg)	18.08	19.40	51.09	51.27	50.50
Total fuel burned during both maneuvers (spherical) = 8005 kg					
Total fuel burned during both maneuvers (pear-shaped) = 8417 kg					

for injection onto interplanetary trajectories (ref. 21), it would be very economical if such injections could also be accomplished by a "standard" laser propelled transfer vehicle.

It has been estimated that by 1980 there will be 250 nuclear powered electric generating plants on line within the United States. Although the total annual tonnage of the resulting waste products will not be great (about 2 tons per GW per year) they will be highly radioactive with half-lives running into the thousands of years. Safe disposal on earth will be extremely difficult if not impossible over these geologic time periods. But this disposal problem could be completely and permanently solved by simply injecting the waste materials onto interplanetary trajectories that will take them directly into the sun. The required injection energies can be significantly lowered by using transfer trajectories to Jupiter where that planet's strong gravitational field can be utilized to redirect the payload directly into the sun without requiring any additional major propulsive maneuvers (ref. 20), enabling a substantial increase in payload. The potential long-range economical benefits in this method of disposal may be very great if an economical injection vehicle could be developed. Recognizing that the possibility of injecting scientific payloads to Mars and Venus is an important possible application of laser propelled shuttle orbiters, we shall restrict ourselves in this report to the investigation of laser propelled injections to Jupiter. Obviously, if a significant payload can be injected onto an interplanetary trajectory to Jupiter via laser propulsion, then it will be possible to inject much more massive payloads to Mars or to Venus by these vehicles because

the injection C_3 's (C_3 is the square of the hyperbolic excess velocity) required to reach these planets will be much lower. We shall assume that the Jupiter injection $C_3 = 120 \text{ km}^2/\text{sec}^2$.

1. The determination of optimum pre-injection orbits for laser propelled injection maneuvers

The escape mass during an injection maneuver can be increased if the maneuver is carried out when the vehicle approaches the periapsis point of a highly eccentric pre-injection orbit. However, the geometrical constraints on laser propelled vehicles impose constraints on the pre-injection orbits. For example, since the injection vehicle will place itself in the desired pre-injection orbit by laser propulsion before the actual injection maneuver takes place, all of the pre-injection orbits will have to be resonant with the laser transmitter on the earth's surface. In order to increase the propulsion efficiency of the injection maneuver, the pre-injection orbit will be highly eccentric and the injection maneuver will begin when the vehicle approaches perigee where its velocity is maximum. The greater the eccentricity, the greater the propulsion efficiency. Thus, optimum pre-injection orbits will have very high apoapsis altitudes. In view of Table 6, these orbits will have almost no movement of the line of apsides or the line of nodes and the potential function can be taken as spherical. Hence, in view of the resonance condition, the period P of the pre-injection orbit must be related to the earth's rotational period P_s by equation (6) where k and k_1 are integers. For highly eccentric orbits $P > P_s$ and hence $k_1 > k$. The time interval between successive transmitter flyovers in the pre-injection orbit will be $k_1 P_s$ or simply

k_1 sidereal days. In order to make k_1 as small as possible without reducing the synchronization ratio P/P_s (and eccentricity) the integer k will always be 1. Hence, the resonance equation for pre-injection orbits becomes

$$k_1 P_s = P \quad (16)$$

Consequently, when the vehicle is in its free-fall, pre-injection orbit, it will always pass through its perigee when it passes directly over the laser transmitter.

Notice that if k_1 is an even integer, the vehicle will also pass through the transmitter's meridian plane when it passes through apogee. Since the transmitting station is not on the earth's equator, the vehicle will not pass directly over the station when it passes through apogee as it will during periapsis passage. However, it will be fairly high in the sky above the station's local horizon because of its high apoapsis altitude. The elevation angle β can be computed from the equation

$$\beta = \cos^{-1} \frac{Q \sin (2\phi_2)}{\sqrt{Q^2 + p_0^2 - 2p_0 Q \cos (2\phi_2)}}$$

where Q denotes the apoapsis' distance from the earth's center.

When equation (2) is substituted into the resonance equation (16), the semi-major axis a of the pre-injection orbit is determined by

$$a = \left[\mu \left(\frac{k_1 P_s}{2\pi} \right)^2 \right]^{1/3} \quad (17)$$

Although the injection propulsion efficiency increases with increasing synchronization ratio, it becomes impractical to use synchronization ratios higher

than about 12 because of the long time intervals between successive station flyovers. If weather conditions are unfavorable for the injection maneuver, the next opportunity will occur P/P_s sidereal days later. But launch windows for injections to Jupiter with $C_3 \leq 120 \text{ km}^2/\text{sec}^2$ are only about 60 days long. Unless the injection occurs within the launch window it will be impossible to reach Jupiter with the prescribed injection C_3 , and the flight will have to be postponed until the next launch window. But this would mean a delay of about 400 days because launch windows to Jupiter are separated by approximately 400 days. In order to increase the probability of finding favorable weather conditions for the injection maneuver, the period of the pre-injection orbit should be such that a maximum of at least 10 passes per window is available. Hence, for a 60-day window, the synchronization ratio should be equal to 6.

Unlike the preliminary boosting maneuvers to the pre-injection orbit, the injection maneuver will be carried out in one long continuous burn which, when started, must be continued until the required injection C_3 is reached. It would be impractical to provide the extra fuel necessary for retrieving the vehicle once it attains a significant velocity above escape velocity. Extremely long-range transmission distances are very desirable because they will allow more energy to be transmitted to the vehicle, increasing the injected payload capability. Hence the atmosphere above the transmitter will have to be extremely clear during the injection maneuver.

After selecting a desirable synchronization ratio P/P_s , the semi-major axis of the pre-injection orbit is determined by equation (17). Since the inclination of the orbit is equal to the latitude of the laser transmitter,

the pre-injection orbit will be completely determined when the eccentricity and time of periapsis passage are determined. The latter is determined by the required interplanetary transfer trajectory, so the eccentricity is the only parameter remaining to be determined. This variable will be determined such that the injection mass is maximum for any given value of I_{SP} and propulsive power. In order to determine the maximum injection mass, we shall assume that the thrust vector is always aligned with the vehicle's instantaneous velocity vector. Also, due to the high injection C_3 , there will be no attempt to retrieve the laser propelled transfer vehicle by retro propulsion once the desired escape velocity is reached. It will be injected along with the payload.

Let D_{max} be equal to the maximum possible, full power, transmission distance which occurs when the beam diameter at the vehicle is equal to the vehicle's main reflector diameter. (see figures 3A, 3B and 3C) We shall assume that the reflector's diameter is 50 meters (164 feet) and $D_{max} = 50,000$ km. At this range, the reflector subtends an angle of 10^{-6} radians or .206 arc-seconds at the transmitter. If the distance between the vehicle and the transmitter is equal to D_{max} when it first appears above the transmitter's minimum beam elevation angle α while approaching perigee, the time spent within the full power transmission field of the transmitter during the injection maneuver will be maximum. This will maximize the energy transmitted to the vehicle during the injection maneuver. It should be noted, however, that in practice, the power transmission would probably not be terminated when the vehicle reaches D_{max} . In this case, the maximum injection payloads determined here will be lower bounds.

For any given value of the synchronization ratio P/P_s , the initial conditions $t = t_1$, $\beta = \alpha$, $D = D_{\max}$ will uniquely determine the eccentricity. This can be shown as follows:

When P/P_s is given, the semi-major axis is determined by equation (17), consequently, the vehicle's position vector $\vec{R}(e, t)$ is a function of only time t and eccentricity e . Let $\vec{\rho}(t)$ denote the position vector of the laser transmitter that is rotating about the earth's rotation axis. The position vector \vec{D} of the vehicle relative to the transmitter is given by

$$\vec{D} = \vec{R}(e, t) - \vec{\rho}(t) = \vec{D}(e, t)$$

Hence, the initial conditions $t = t_1$, $\beta = \alpha$, $D = D_{\max}$ can be expressed by the equations

$$\begin{aligned} \hat{\rho}(t_1) \cdot \hat{D}(e, t_1) &= \sin \alpha \\ D(e, t_1) &= D_{\max} \end{aligned} \tag{18}$$

where

$$\hat{\rho} = \frac{\vec{\rho}}{|\vec{\rho}|}, \quad \hat{D} = \frac{\vec{D}}{D}$$

This is a system of two scalar equations in two unknowns t_1 and e . It is convenient to measure time with respect to the pre-injection orbits' time of periapsis passage where $t = 0$.

Hence, $t_1 < 0$. The solutions to (18) corresponding to various values of P/P_s determine the optimum pre-injection orbits. They are given in Table 10. Figure 12 describes the optimum pre-injection orbit for $P/P_s = 6$. The angle θ_i is defined by the equation

$$\theta_i = \dot{\theta} t_i \quad (i = 1, 2)$$

The time t_2 corresponds to the time at which the injection maneuver is terminated. Note that in Table 10 the

TABLE 10. - OPTIMUM PRE-INJECTION ORBITS FOR LASER PROPELLED INJECTION MANEUVERS

($\alpha = 17^\circ$, $D_{\max} = 50,000$ km, $\phi_t = 31.8^\circ$)

Synchronization Ratio P/P _S	Semi-Major Axis a (km)	Eccentricity e	Apoapsis Q _h (km)	Altitude Periapsis q _h (km)	Begin Propulsion t ₁ (sec)	Longitude of Transmitter When Propulsion Begins θ ₁ (deg)
6	139,223	.8651	253,294	12,409	-13,605	-56.84°
8	168,657	.8895	312,306	12,265	-13,317	-55.64°
10	195,709	.9052	366,500	12,176	-13,140	-54.90°
12	221,003	.9164	417,149	12,114	-13,019	-54.39°

Pre-injection orbit $P/P_s = 6$
(inclination = 31.8 deg)

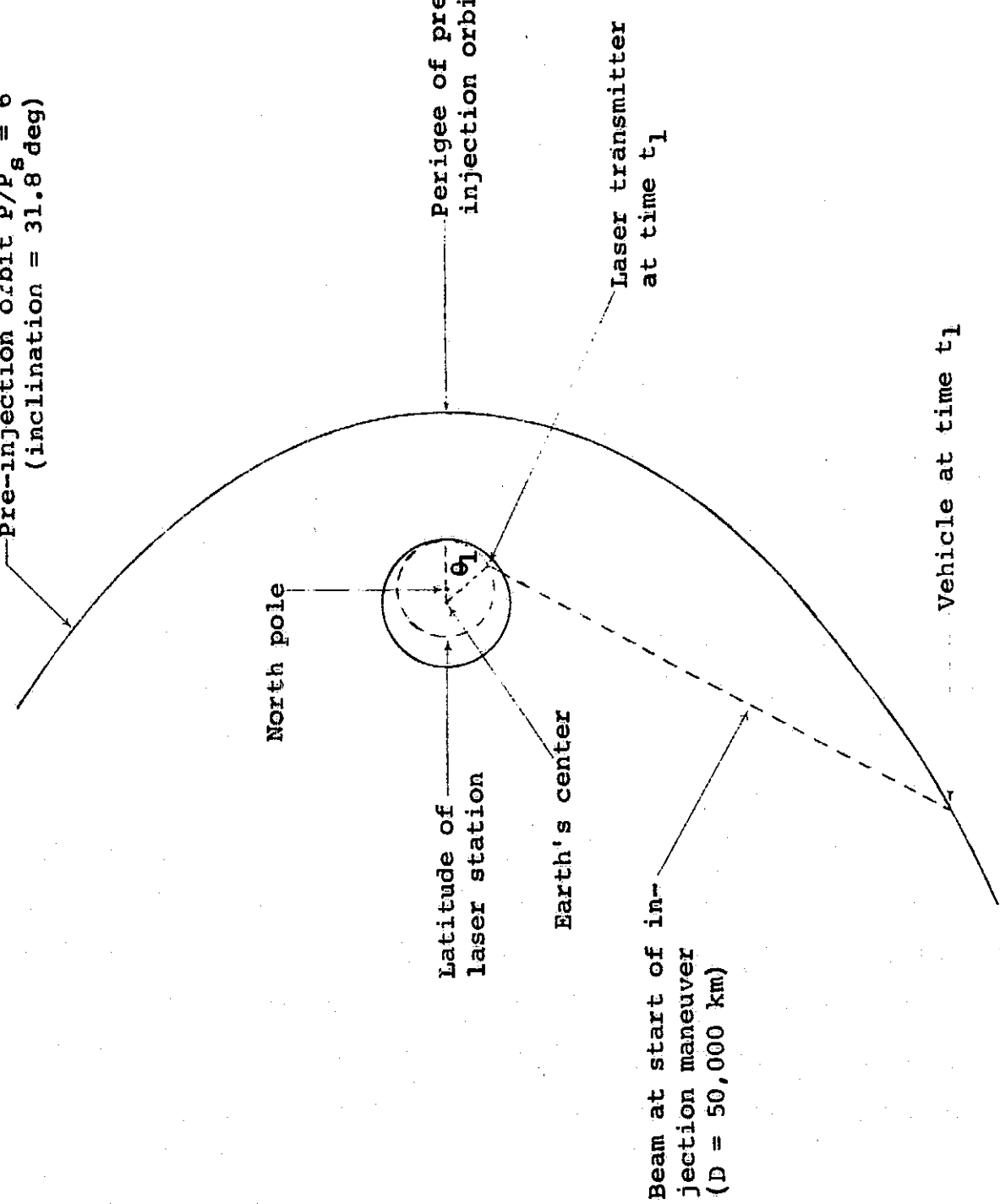


Figure 12. - Optimum pre-injection orbit for maximum energy transmission during injection maneuver.

minimum beam elevation angle α is set at 17° instead of 15° . This is because the vehicle's elevation angle β actually begins to decrease after rising slightly above 15° for a few hundred seconds, then drops to a low of about 13.4° before it begins to climb monotonically above 15° (until reaching its maximum of 90° at perigee). This initial decrease in β will also occur during the injection maneuver unless the propulsive acceleration is very high. This is due to the fact that during this time, the earth's rotation causes the line of sight to fall at a faster rate than the rate of increase caused by the vehicle's orbital motion. But by beginning the injection maneuver as soon as the vehicle's elevation angle reaches 17° instead of 15° , the beam will only fall to a minimum of about 15.4° before the monotonic increase begins. This will prevent the beam from dropping below the 15° limit.

2. The determination of optimum injection maneuvers which will maximize injection mass for prescribed values of I_{SP} and propulsive power

The above analysis only determines the optimum pre-injection orbit which corresponds to a specified value of the synchronization ratio P/P_s . These orbits are completely independent of engine I_{SP} and propulsive power. Suppose that a laser propelled vehicle with a prescribed I_{SP} and propulsive power is in an optimum pre-injection orbit. The optimum injection maneuver which will maximize injection mass can be computed as follows:

Let m_0 and m_f denote the vehicle's dry mass and propellant mass respectively, at time t_1 when the injection maneuver begins. (As mentioned above, the thrust vector is aligned with the vehicle's instantaneous

velocity vector.) An integration process that simulates the thrusting maneuver begins at time t_1 when the vehicle is 50,000 km from the transmitter and has an elevation angle of 17° . The integration simulating the propulsion maneuver continues until the required injection C_3 is reached, which in our case is $120 \text{ km}^2/\text{sec}^2$. If the fuel is exhausted before the required injection energy is reached, or if the transmission distance D is less than D_{\max} when the required C_3 is reached, the time t is reset to t_1 , m_f will be increased and the integration is initiated again. An integration-iteration process is carried out which will determine m_f such that when the required injection energy is reached, the transmission distance D is precisely equal to the maximum, full power transmission distance D_{\max} . This will allow a maximum amount of energy to be transmitted to the vehicle during the injection maneuver, resulting in a maximum injected mass.

Let m_f^* denote the solution to the above integration-iteration process. Let m_b denote the mass of fuel actually burned during this optimum injection maneuver. Consequently, the maximum payload mass m_p can be calculated by the equation

$$m_p = m_f^* - m_b \quad (18)$$

The total injected mass M is given by

$$M = m_o + m_b + m_p \quad (19)$$

For some combinations of I_{SP} and propulsive power, it is impossible to reach the required C_3 without continuing the propulsion beyond the maximum full power transmission distance D_{\max} . In these cases we shall assume that the required injection is impossible. However,

this is actually not the case because after D_{max} is reached, power transmission will still be possible although it will be decreasing inversely by the square of the distance. Likewise, the maximum payload mass m_p determined by (18) will be less than the actual maximum. It will, in fact, represent a lower bound on the maximum payload. As mentioned above, we shall also assume that the laser injection vehicle and payload are brought up and placed in the optimum pre-injection orbit by its own laser propulsion system. Thus, the flight begins from the initial shuttle parking orbit.

An extensive parametric analysis was carried out to determine the optimum combinations of synchronization ratios, I_{SP} , and propulsive powers needed to maximize injected payload and minimize fuel expenditure.

D. Optimum Specific Impulses of
Laser Propelled Vehicles for
Achieving Maximum ΔV_s During
One Burn Maneuvers

Since laser propelled vehicles must remain within the operational range and line of sight of the power transmitter during all propulsive maneuvers, these maneuvers are limited to relatively short periods of time. This time constraint does not exist for vehicles that develop their own propulsive power. These limitations are particularly evident during the primary boosting maneuvers to synchronous orbit (or to the pre-injection orbits) and during an injection maneuver since the injection must be achieved during one pass over the transmitter in one continuous burn. Thus, the specific impulses of laser propelled vehicles should be selected with these limitations in mind. Although the final selection of I_{SP} will be based on parametric performance studies to be

considered later (and on physical limitations of the engines) it is useful to derive theoretical optimum values of the specific impulse, propulsive power, duration of thrusting period, final mass, and resulting ΔV s for one burn maneuvers.

1. The determination of optimum I_{SP} that will deliver a given ΔV in least time

Suppose that a particular maneuver requires a specified ΔV . We shall determine the optimum engine I_{SP} that will enable the maneuver to be executed in the smallest possible time interval, and the duration of this time interval.

Let T denote the thrusting time of a particular propulsive maneuver that is required to achieve a specified ΔV . We shall assume that the thrust vector is kept aligned with the vehicle's instantaneous velocity vector at all times. If \dot{m} denotes the mass flow rate (also assumed to be constant) it follows from the rocket equation that

$$\frac{M + \dot{m}T}{M} = \exp(\Delta V/u) \quad (20)$$

where M denotes the total vehicle mass after the burn is terminated. For the time being, M is assumed to have a specified value. Hence, it follows directly from (20) that

$$T = \frac{M}{\dot{m}} [\exp(\Delta V/u) - 1] \quad (21)$$

The propulsive power p (which is also assumed to be constant) is related to u and \dot{m} by the equation

$$p = 1/2 \dot{m} u^2 \quad (22)$$

Therefore, by substituting this equation into (21) we obtain

$$T(u) = Ku^2 [\exp(\Delta V/u) - 1] \quad (23)$$

where $K = M/2p = \text{constant}$. By defining the function $F(u)$ by

$$F(u) = u^2 [\exp(\Delta V/u) - 1] \quad (24)$$

equation (23) can be expressed as

$$T(u) = KF(u) \quad (25)$$

In order to determine the optimum exhaust velocity u_o that will minimize T for any specified values for M , p , and ΔV , we solve the equation

$$\frac{dT}{du} = K \frac{dF}{du} = 0 \quad (26)$$

where

$$\frac{dF}{du} = 2u [\exp(\Delta V/u) - 1] + u^2 \exp(\Delta V/u) (-\Delta V/u^2)$$

By introducing a new variable x defined by

$$x = \Delta V/u \quad (27)$$

the solution to (26) can be obtained by solving the equation

$$(1 - \frac{1}{2}x) \exp x = 1$$

The solution is $x = x_o = 1.593624$. The fact that this solution will indeed minimize T can be proved by noting that

$$\left. \frac{d^2 T}{du^2} \right|_{x_0} = K \frac{d^2 F}{dx^2} \left(\frac{dx}{du} \right)^2 \Big|_{x_0} = \frac{K \Delta V^2}{x_0^3} [\exp x_0 - 2] \left(\frac{dx}{du} \right)^2 > 0$$

Therefore, the optimum exhaust velocity u_0 which will minimize T for any given ΔV is given by

$$u_0 = \Delta V / x_0 \quad (28)$$

It is a rather significant and remarkable fact that this optimum exhaust velocity is completely independent of the vehicle's mass M at the end of the burn and the propulsive power p . The corresponding optimum specific impulse is given by

$$I_{SP}(\text{optimum}) = \frac{u_0}{g} = 63.9871 (\text{sec}^2/\text{km}) \Delta V \quad (29)$$

where ΔV is given in units of km/sec.

The actual minimum power transmission time can be calculated by substituting (28) back into (23). The result is

$$T_{\min} = 772069.3 (M/p) \Delta V^2 \text{ seconds} \quad (30)$$

where ΔV , p and M are given in units of km/sec, watts and kg respectively.

It is interesting to apply this equation to the problem of propelling a rocket from rest, on the earth's surface, to orbital velocity via laser propulsion (ref.13). The minimum ΔV required for such a launch is approximately 8.22 km/sec (including gravity losses). Hence, the minimum propulsion time required for the launch is

$$T_{\min} = 5.2167 \times 10^7 (M/p)$$

when the standard ascent profile is used (to minimize g losses) the maximum possible transmission time that is

possible (before the vehicle drops below the transmitter's horizon) is about five minutes (300 seconds). Hence, the minimum required power to payload mass ratio is

$$p/M \text{ (minimum)} = 174 \text{ (KW/kg)}$$

In view of (29) the corresponding $I_{SP} = 526$ sec.

If the inefficiencies in converting beamed power to propulsive power are neglected, the total energy E transmitted to a laser propelled vehicle during the maneuver is given by

$$E = pT$$

Hence, in view of (30) the minimum energy required to produce a given ΔV is given by

$$E_{min} = 772069.3 M \Delta V^2$$

The corresponding optimum I_{SP} is given by (29).

2. The determination of optimum I_{SP} that maximizes ΔV

Suppose that the thrusting time T , final mass M and propulsive power p have prescribed values. The optimum I_{SP} that will maximize ΔV for these prescribed values can be determined by finding the maximum of $\Delta V(u)$ given by the equation

$$\Delta V(u) = u \log \left(1 + \frac{T}{2Ku} \right) \quad (31)$$

This equation follows directly from (23) where $K = M/2p$. The solution can be obtained by solving the equation

$$\frac{d\Delta V}{du} = \log \left(1 + \frac{T}{2Ku} \right) + u \cdot \left(\frac{1}{1 + \frac{T}{2Ku}} \right) \left(\frac{-2T}{Ku^2} \right) = 0$$

By introducing a new variable y defined by

$$y = 1 + \frac{T}{Ku^2} \quad (32)$$

the above equation becomes

$$\frac{d\Delta V}{du} = \log y - \frac{2(y-1)}{y} = 0$$

The solution to this equation is $y_0 = 4.921554$. The fact that this solution maximizes ΔV can be proved by noting that

$$\left. \frac{d^2 \Delta V}{du^2} \right|_{y_0} = \left(\frac{1}{y_0} - \frac{2}{y_0^2} \right) \left(\frac{-2T}{Ku^3} \right) < 0$$

Upon substituting y_0 into equation (32) we obtain

$$u = \sqrt{\frac{T}{K(y_0-1)}} \quad (33)$$

When this result is substituted into equation (31) it follows that

$$\frac{\Delta V}{u} = \log y_0 = 1.593624 = x_0$$

or

$$\Delta V = x_0 u \quad (34)$$

Notice that this equation is the same as (28). Hence, the I_{SP} which maximizes ΔV for given values of p , T and M will also be equal to the I_{SP} which minimizes T . We expect this result because if T were not the minimum, for the maximum ΔV , then it follows from equation (31) that ΔV could be increased by increasing T without changing u , p or M , which is impossible because ΔV is maximum.

In view of equation (33) the optimum exhaust velocity u_0 can be expressed by

$$u_0 = .7141442 \sqrt{\frac{T_p}{M}} \quad (35)$$

and

$$I_{SP}(\text{optimum}) = .0728223 \sqrt{\frac{T_p}{M}} \quad (36)$$

3. The determination of optimum I_{SP} that maximizes final mass

In this case we assume that the thrusting time T , ΔV , and the propulsive power have been specified. Hence, it follows from equation (25) that the total mass M after the propulsive maneuver is given by

$$M(u) = \frac{2pT}{F(u)}$$

Since $F(u)$ is minimum when $u = u_0$, the maximum burn out mass is

$$M(\text{maximum}) = \frac{2pT}{F(u_0)} = 1.29522 \frac{pT}{\Delta V^2} \quad (37)$$

Neglecting energy conversion inefficiencies, the total energy E transmitted to the vehicle is given by $E = pT$. Consequently,

$$M(\text{maximum}) = \frac{1.29522E}{\Delta V^2} \quad (38)$$

The above results can be summed up as follows:
The optimum I_{SP} given by (29) will:

- minimize T if M , p , and ΔV are given
- maximize ΔV if T , M , and p are given (in this case u is given by (33) and $I_{SP} = u/g$)
- maximize M if T , ΔV , and p are given
- minimize p if M , T , and ΔV are given

(e) minimize the required transmitted energy E if M and ΔV are given.

A curve of the optimum I_{SP} versus ΔV is shown in figure 13.

It is interesting to note that the optimum exhaust velocity u_0 will always produce the same mass ratio regardless of ΔV . This result follows directly from equation (28).

$$\text{Mass Ratio} = \exp(\Delta V/u_0) = \exp x_0 = y_0 \approx 4.9$$

This mass ratio is too high for ΔV maneuvers ≤ 10 km/sec because the optimum $I_{SP} \leq 640$ sec. However, round trip missions to synchronous orbit by laser propelled shuttle orbiters require a total $\Delta V \approx 11.6$ km/sec (starting from an initial orbital altitude of 478 km). The optimum I_{SP} corresponding to this ΔV is 742 seconds.

Suppose that the payload mass up to synchronous orbit is the same as the payload mass down and that the entire round trip requires a total of N burns $\Delta V_1, \Delta V_2, \Delta V_3, \dots, \Delta V_N$ corresponding to N different burn durations $\Delta T_1, \Delta T_2, \Delta T_3, \dots, \Delta T_N$. Then the total ΔV and total burn time T is given by

$$\Delta V = \sum_{i=1}^N \Delta V_i$$

$$T = \sum_{i=1}^N \Delta T_i$$

If the initial mass is M_0 and if the mass at the end of the i 'th burn is M_i , the total mass ratio M_0/M_N is given by

$$\begin{aligned} M_0/M_N &= (M_0/M_1) (M_1/M_2) \dots (M_{N-1}/M_N) \\ &= \exp(\Delta V_1/u) \exp(\Delta V_2/u) \dots \exp(\Delta V_N/u) \end{aligned}$$

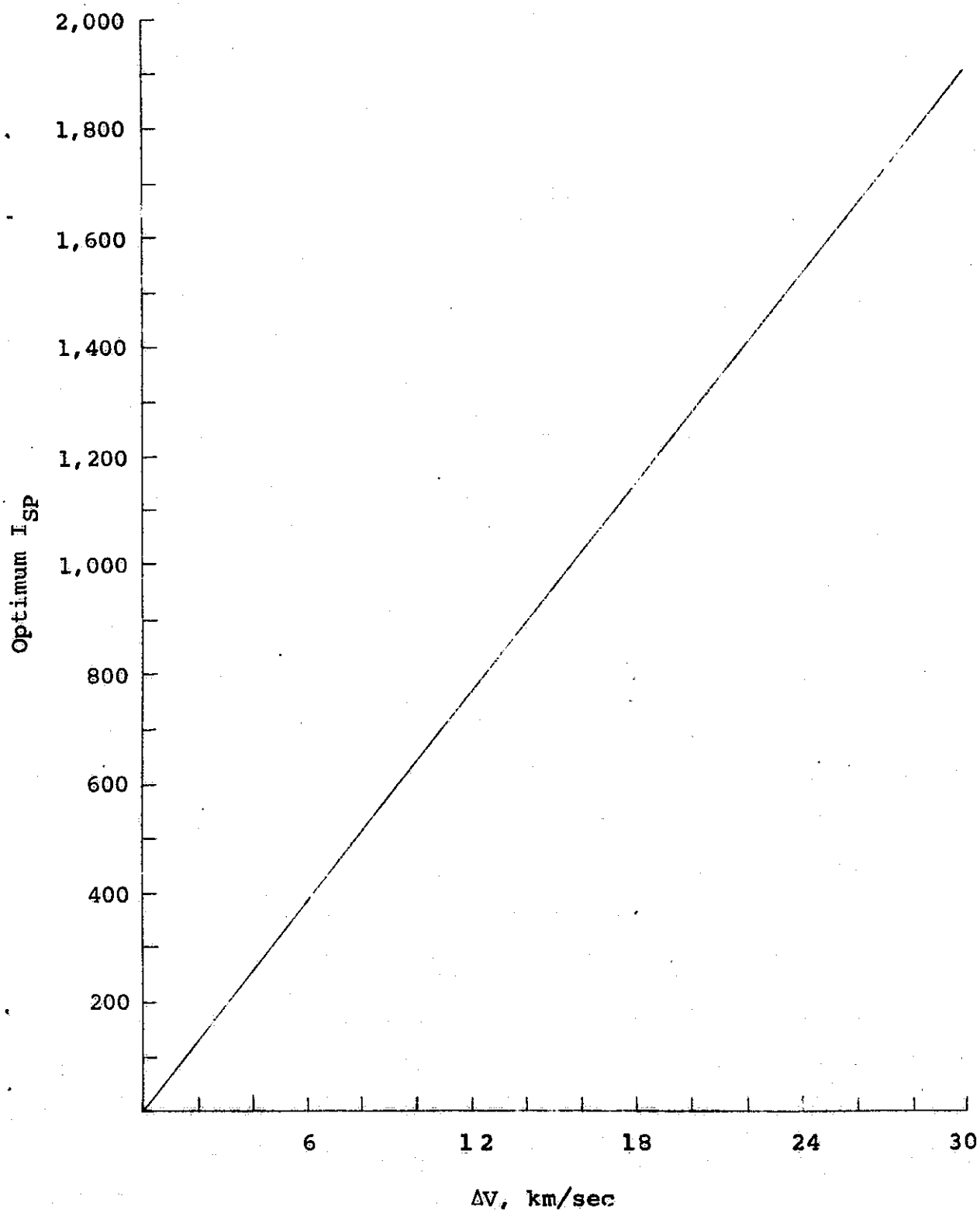


Figure 13. - Optimum I_{sp} versus ΔV for laser propelled rocket vehicles

$$\begin{aligned}
 N &= \exp\left[\left(\sum_{i=1}^N \Delta v_i\right)/u\right] \\
 &= \exp(\Delta v/u)
 \end{aligned}$$

Consequently, for any given propulsive power, T will be minimum if $I_{SP} \approx 742$ seconds. In view of the restricted power transmission times during the primary boosting maneuvers it appears that this I_{SP} may in fact minimize the total round trip flight time to synchronous orbit.

However, minimizing the round trip flight time to synchronous orbit is of secondary importance, the most important aspect being how much mass can be delivered with reasonable flight times and initial masses. To answer this requires a detailed parametric mission analysis. This analysis has been conducted for laser propelled transfer vehicles on round-trip missions to synchronous orbit and on injection missions with escape energy $C_3 = 120 \text{ km}^2/\text{sec}^2$.

RESULTS AND DISCUSSION

Since the transmitted laser radiation is coherent it can be focused to produce an extremely high flux. If a gas is opaque (or can be made absorbing), to the laser radiation and injected into the high flux region, the gas will be heated to extremely high temperatures. By expelling the hot gas through an appropriately shaped rocket nozzle, an extremely high I_{SP} exhaust jet can be produced. Hence, the I_{SP} can be varied over a wide range of values, for example, 500 sec to 5,000 sec, by decreasing the flux and increasing the absorption region or

vice-versa. This, in essence, is the laser rocket engine (refs. 15, 20). Other configurations based on ablating a solid surface by a high intensity laser beam have been proposed (refs. 16, 17), but these may not be suitable for the extremely long-range transmission distances envisioned in this paper.

Unless stated otherwise, the laser propelled transfer vehicle is assumed to be earth based. In this configuration, the shuttle vehicle carries the laser transfer vehicle and payload from the earth's surface to the initial parking orbit inside its cargo bay. The vehicle's dry mass, less fuel tanks, is assumed to be 3,700 kg (8,157 lbs.). The mass of the fuel tanks, which must be added to this mass in order to calculate the vehicle's true dry mass, is assumed to be 5% of the fuel mass. For example, the dry mass of a laser transfer vehicle with 10,000 kg capacity fuel tanks is 4,200 kg.

A. Parametric Analysis of Missions to Synchronous Orbit

It has been determined that the total ΔV required for laser propelled shuttle orbiters to deliver payloads to synchronous orbit (35,793 km high, 0° inclination) from an initial 478 km high, 31.8° circular parking orbit, averages about 5.631 km/sec using the pear-shaped gravitational potential function. Hence, the round trip will require a total ΔV of about 11.262 km/sec. (These values vary about ± 300 meters/sec depending upon payload mass.) The total payload that can be delivered to this initial parking orbit by the ground-to-orbit shuttle vehicle is 27,216 kg (60,000 lbs.).

If M_0 denotes the total initial mass corresponding to a one-way mission to synchronous orbit, the final mass, M can be computed by

$$M = M_0 \exp(-\Delta V/u)$$

The fuel burned in the mission $m_b = M_0 - M$. Hence, the vehicle's dry mass $m_0 = 3,700 \text{ kg} + .05 m_b \text{ kg}$ and the payload mass $m_p = M - m_b$.

Figures 14 and 15 describe the payload capabilities of laser propelled transfer vehicles with various I_{SP} on three different missions to synchronous orbit. They were calculated with the aid of the above equation and other equations that are obvious modifications of it. All of the missions began from a 478 km high, 31.8° circular parking orbit with a total initial mass of 27,216 kg. The first mission was designed to transfer a maximum payload from the initial orbit to synchronous orbit where the vehicle runs out of fuel and is expended. The second mission is identical except that the vehicle carried just enough fuel to be able to return to the initial orbit empty. The third mission was designed to transfer a maximum payload to synchronous orbit and retrieve another payload of equal mass to this initial orbit. It should be emphasized that these performance curves are independent of propulsive power and do not require any detailed trajectory calculations for their construction. However, in practical applications, propulsive powers will play a very important role as they will have a great effect on flight times.

Figure 14 is a graph of payload versus I_{SP} . In view of the curvatures of the graphs it appears that the optimum I_{SP} should be above 1,500 seconds. A laser transfer vehicle with $I_{SP} = 1,750$ seconds will be capable of

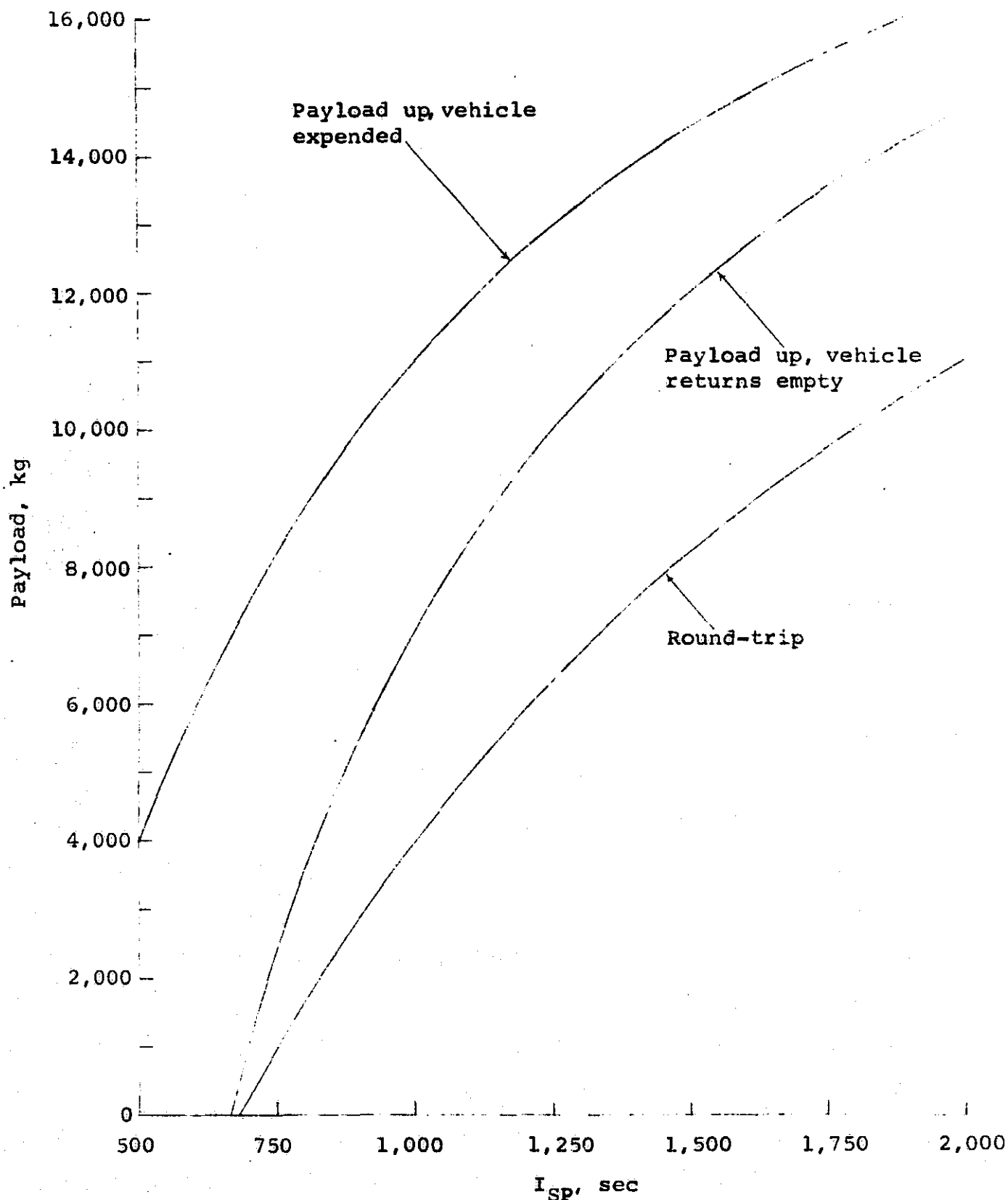


Figure 14. - Maximum payload capabilities to synchronous orbit of ground based laser propelled transfer vehicle (478 km, 31.8° initial parking orbit, 27,216 kg initial mass).

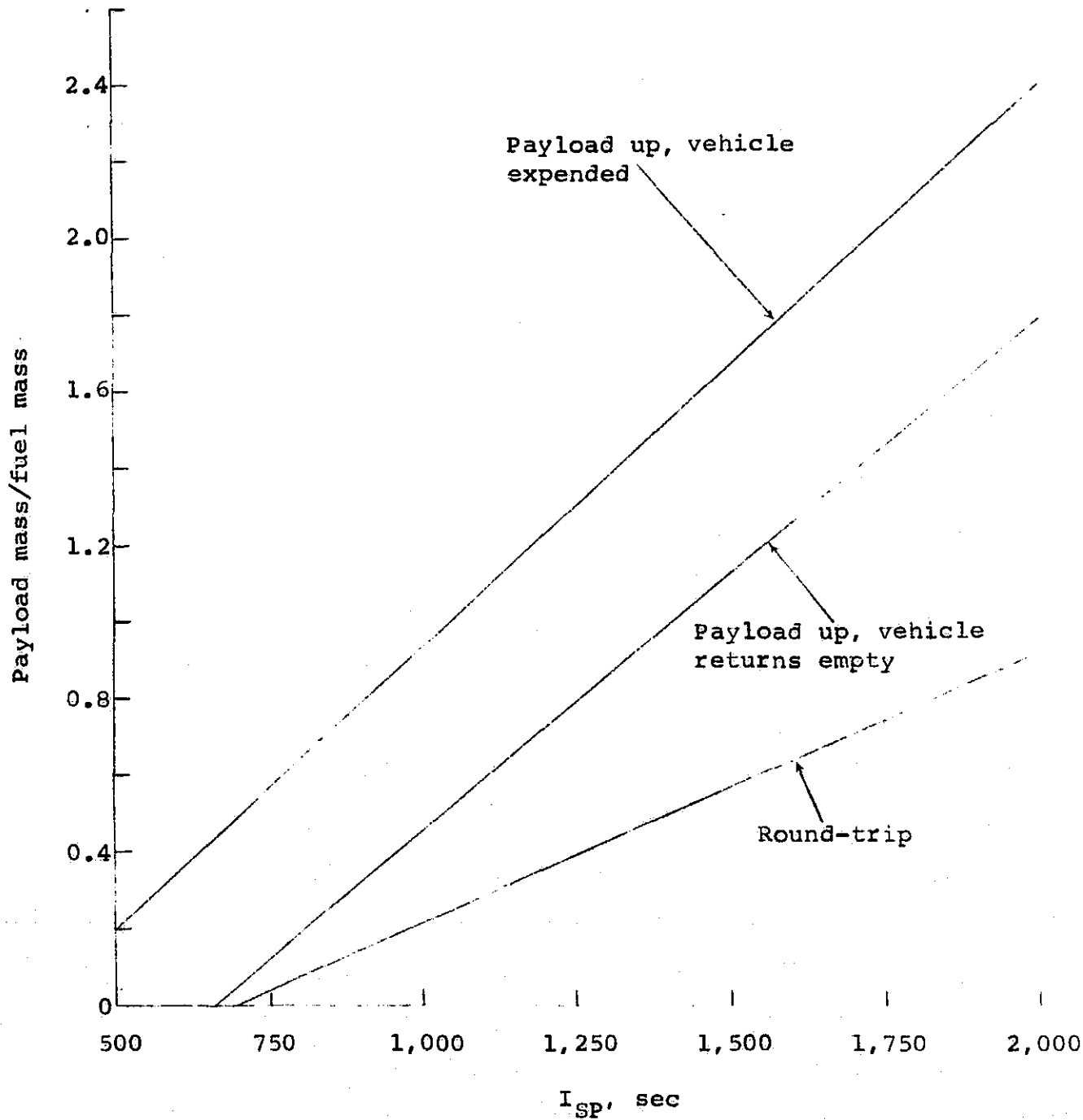


Figure 15. - Payload/fuel ratios for missions to synchronous orbit via ground based laser propelled transfer vehicle (478 km, 31.8° initial parking orbit; 27,216 kg initial mass).

transferring payloads of mass 15,522 kg (34,220 lbs.) on the first mission, 13,557 kg (29,890 lbs.) on the second and 9,765 kg (21,528 lbs.) on the third. When we compare these values with the corresponding payload capabilities of previously proposed transfer vehicles given in Table 1 it is clear that the laser transfer vehicle offers a considerable advance in payload capability. Figure 15 shows curves of payload/fuel versus I_{SP} for the three missions.

The parametric study involving round-trip integrated trajectories to synchronous orbit covered a range of specific impulses and propulsive powers. Two initial orbital altitudes were used in order to study how they affect the overall performance characteristics. In particular, the trajectory calculations were based on all possible combinations of I_{SP} = 500 sec, 1,000 sec, 1,500 sec, 2,000 sec; propulsive powers = 20 MW, 40 MW, 65.4 MW; initial orbital altitudes = 176.3 km, 478.0 km. These initial conditions were combined with various payloads, to and from synchronous orbit, which ranged from 2,000 kg to 30,000 kg. A total of about 160 complete round-trip trajectories were computed. The results appear in Tables 11, 12, 13, 14, 15, and 16. Some of the notations appearing in tables require definition. They are:

\sum Burn₁ = total thrusting time of primary boosting maneuvers (sec)

No. of Burns₁ = number of burns in primary boosting sequence

Fuel₁ = fuel burned during primary boosting sequence (kg)

T_1 = total time required to complete primary boosting sequence (days)

Revs₁ = total number of complete orbit revolutions made by vehicle during primary boosting sequence

Burn₂ = thrusting time to circularize orbit at synchronous orbit altitude - one burn maneuver (sec)

Fuel₂ = fuel burned during Burn₂ (kg)

Burn₃ = total thrusting time to carry out plane change maneuver ($31.8^\circ \rightarrow 0^\circ$) (sec)

Fuel₃ = fuel burned during Burn₃ (kg)

Time Up = total time required to reach synchronous orbit (days)

Fuel Up = total fuel burned reaching synchronous orbit (kg)

Burn₄ = thrusting time to carry out plane change at synchronous orbit altitude for the return leg ($0^\circ \rightarrow 31.8^\circ$) - one burn maneuver (sec)

Fuel₄ = fuel burned during Burn₄ (kg)

Burn₅ = thrusting time to carry out decircularization maneuver - one burn maneuver (sec)

Fuel₅ = fuel burned during Burn₅ (kg)

Σ Burn₆ = total thrusting time to circularize orbit to initial orbital altitude (sec)

No. of Burns₆ = number of burns in Burn₆ sequence

Fuel₆ = fuel burned during Burn₆ sequence (kg)

T₆ = total time required to complete Burn₆ maneuvers (days)

Revs₆ = total number of complete orbit revolutions made by vehicle during Burn₆ maneuvers

Fuel Down = total fuel burned returning from synchronous orbit (kg)

Time Down = total time required to return from synchronous orbit (days)

Total Fuel = total fuel burned during complete round-trip mission to synchronous orbit (kg)

Total Time = total time required for complete round-trip mission to synchronous orbit -zero stay time at synchronous orbit (days)

TABLE I3. - PERFORMANCE DATA FOR ROUND-TRIP MISSIONS TO SYNCHRONOUS ORBIT VIA LASER PROPELLED INTERORBITAL TRANSFER VEHICLE

Initial Inclination = 31.6°; Minimum Beam Elevation = 15°

Propulsive Power = 40 MN; Initial Orbital Altitude = 176.3 km

TABLE I 4. - PERFORMANCE DATA FOR ROUND-TRIP MISSIONS TO SYNCHRONOUS ORBIT VIA LASER PROPELLED INTERORBITAL TRANSFER VEHICLE

Proulsive Power = 40 [W] Orbital Altitude = 478.0 km

Each line in Tables 11-16 corresponds to a complete round-trip trajectory to synchronous orbit. Much additional data, such as beam angles and transmission distances at the start and end of each burn (such as that shown in Table 8 for the primary boosting maneuvers) have been suppressed because it is too numerous. The variables shown in Tables 8 and 9 corresponding to the transfer to synchronous orbit, however, are typical. The minimum beam elevation angle is kept at 15° for all trajectories.

The tables have been grouped into three pairs corresponding to the three different propulsive powers; 20 MW, 40 MW and 65.4 MW. The two tables in each pair correspond to the two different initial orbital altitudes; 176.3 km and 478.0 km. Hence, the trajectories in each of the six tables correspond to the same propulsive power and the same initial orbital altitude. The varying parameters in each table are I_{SP} , payload up, and payload down. Notice that for a fixed initial orbital altitude (176.3 km or 478.0 km) many of the transfer times up to synchronous orbit with different values of propulsive power, payload, and I_{SP} are nearly equal. This discrete characteristic of transfer time is due to the nature of the propulsive maneuvers and their dependence on vehicle-transmitter synchronization. These discrete transfer times up to synchronous orbit are illustrated graphically in figures 16, 17 and 18.

In order to compare the effects of I_{SP} , propulsive power, and initial orbital altitude on the transfer time to synchronous orbit, as illustrated in the figures, the payloads up and down were unchanged. These payloads were: 6,000 kg (13,228 lbs.) up and 3,000 kg (6,614 lbs.) down.

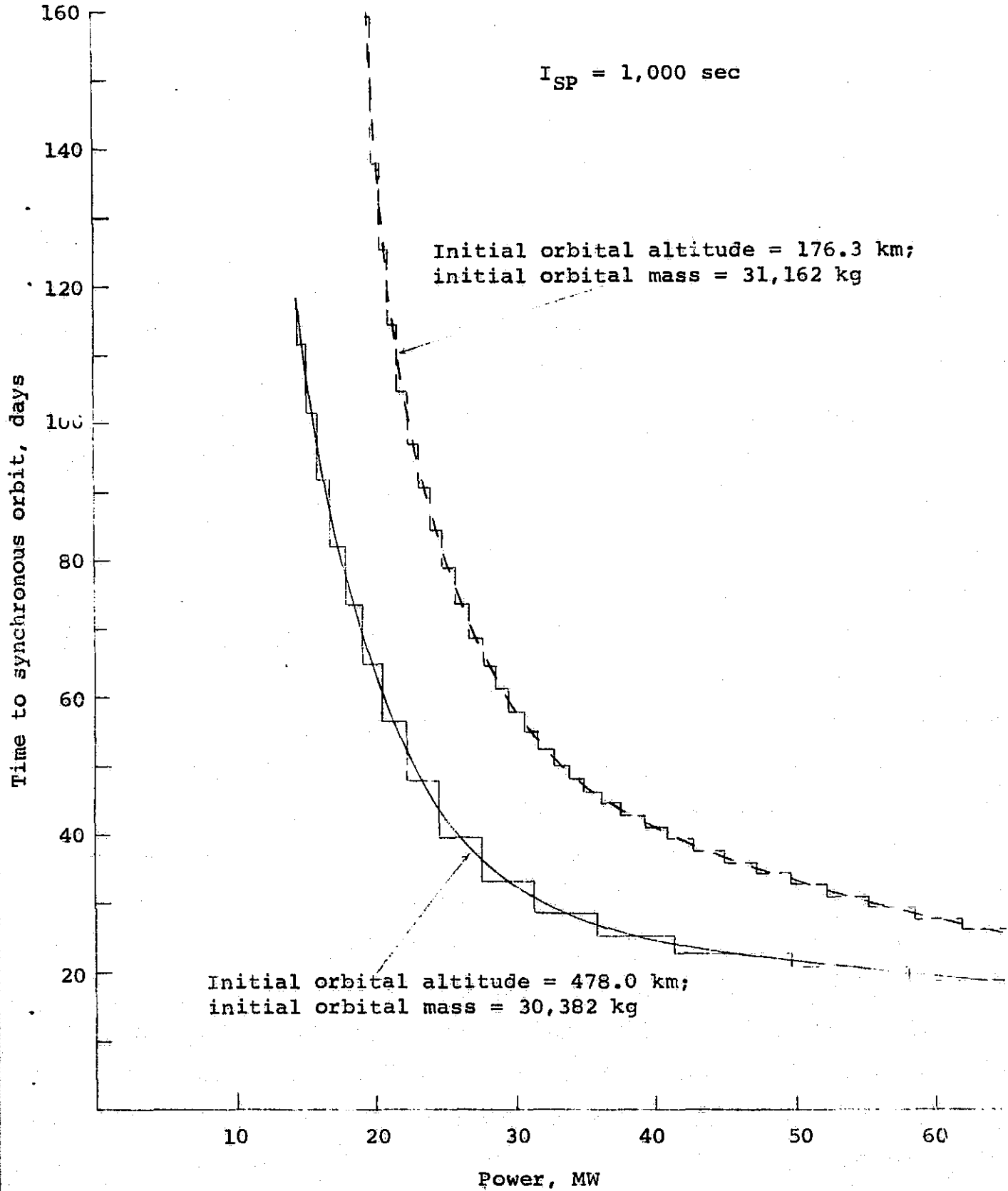


Figure 16. - Flight time to synchronous orbit via laser propelled transfer vehicle (6,000 kg payload up; 3,000 kg payload down).

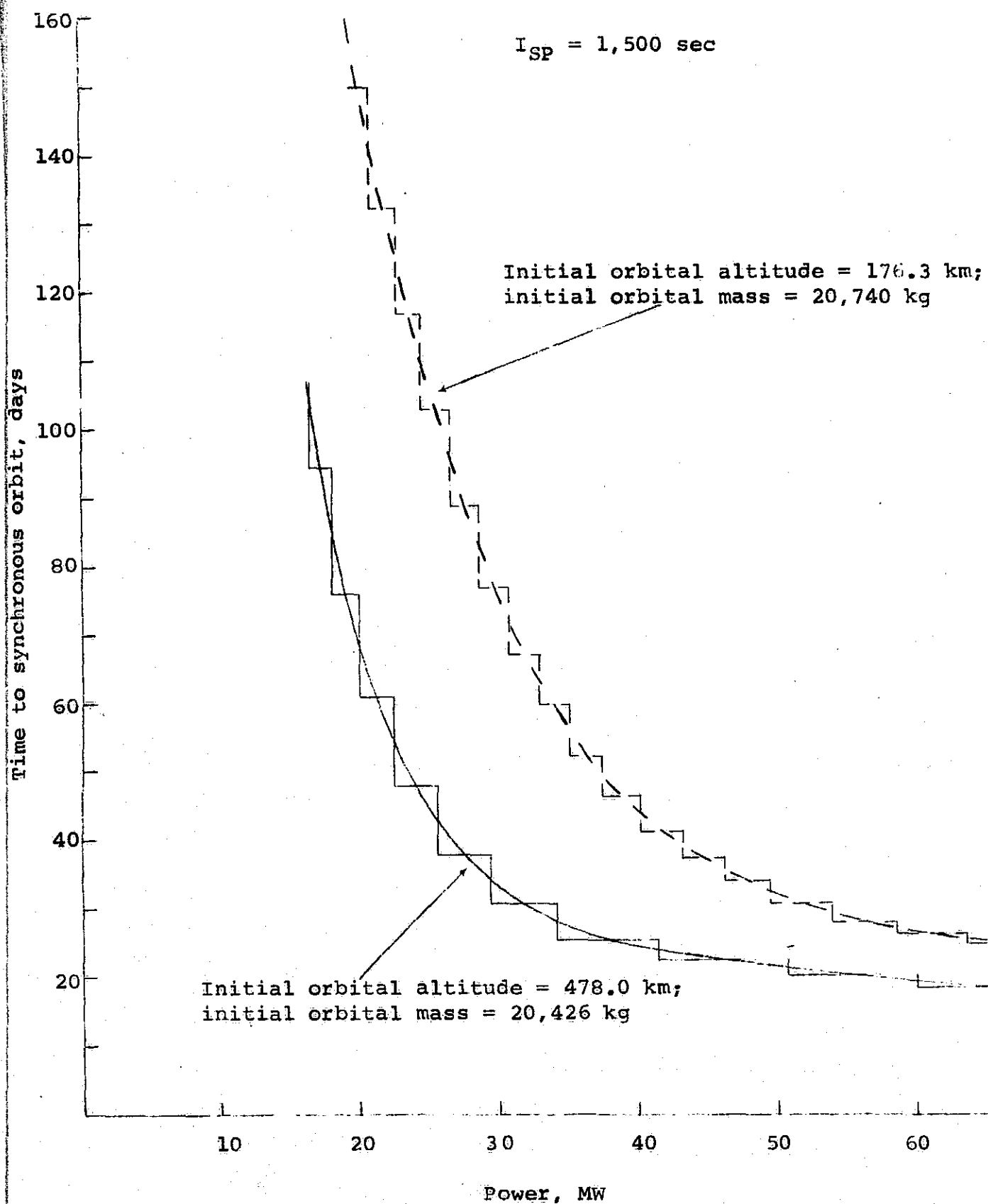


Figure 17. - Flight time to synchronous orbit via laser propelled transfer vehicle (6000 kg payload up; 3,000 kg payload down).

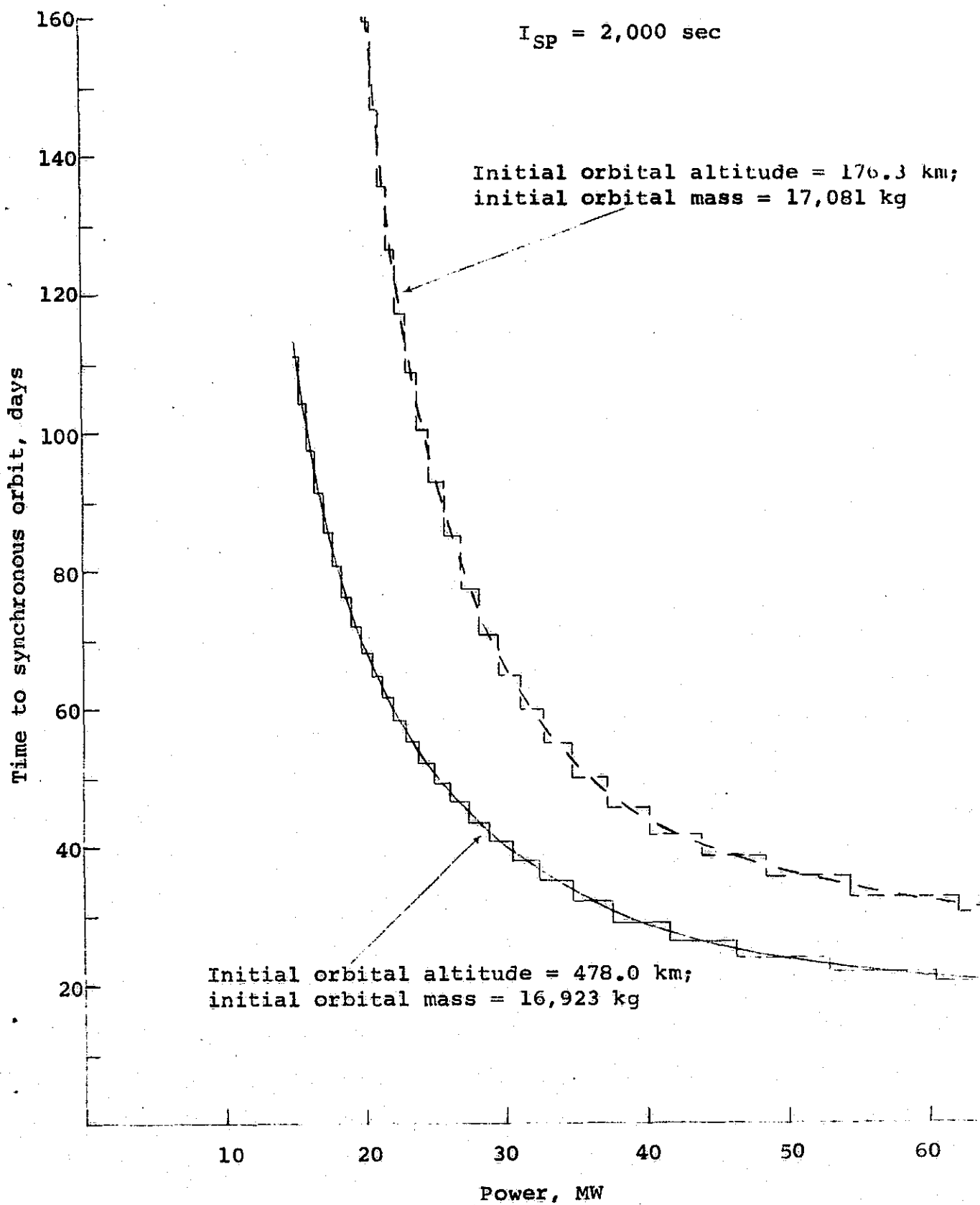


Figure 18. - Flight time to synchronous orbit via laser propelled transfer vehicle (6,000 kg payload up; 3,000 kg payload down).

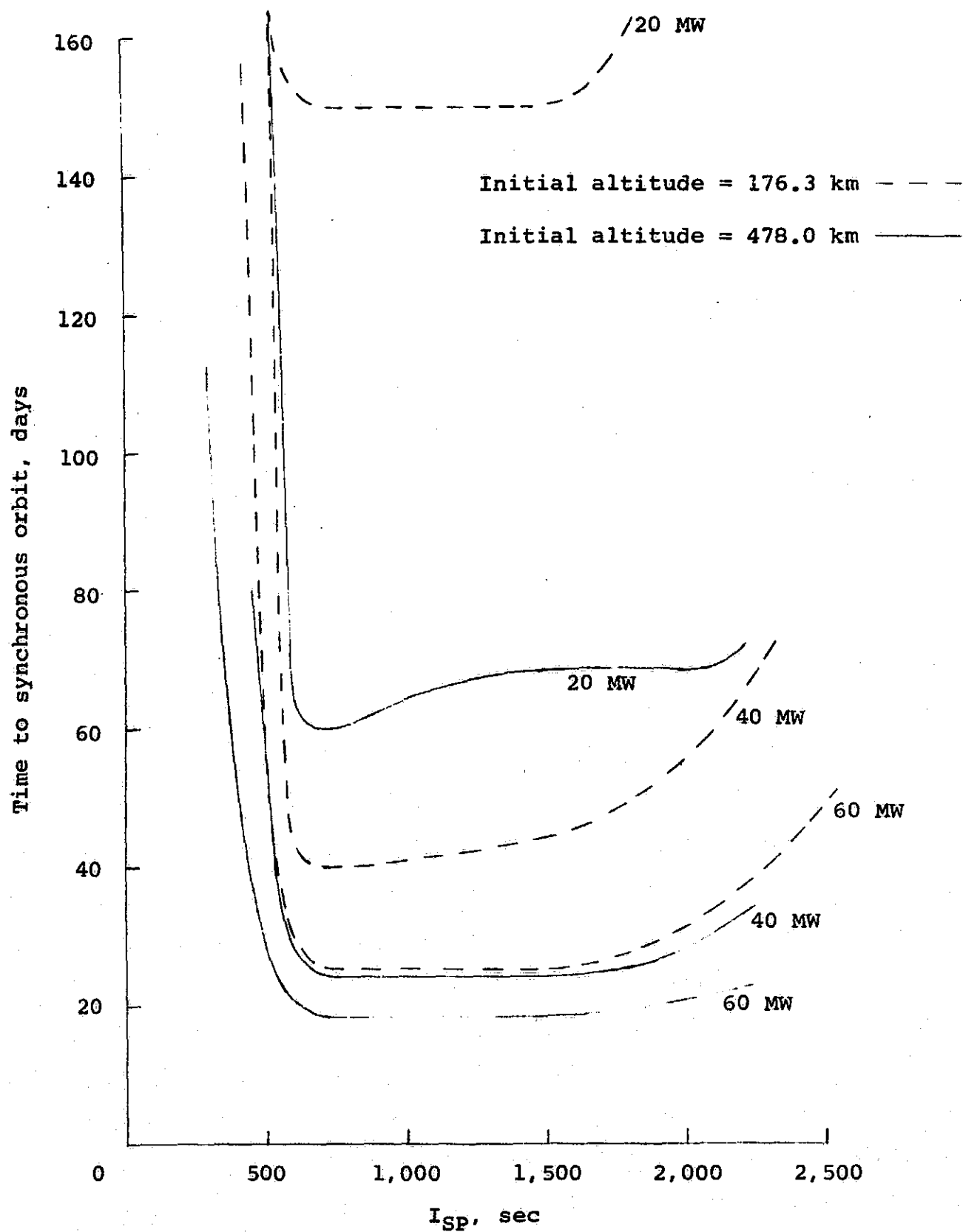


Figure 19. - Flight time to synchronous orbit versus I_{SP} via laser propelled transfer vehicle (6,000 kg up; 3,000 kg down).

Figures 16, 17, and 18 correspond to I_{SP} values of 1,000 sec, 1,500 sec and 2,000 sec respectively. Each of the figures has two curves corresponding to the two initial orbital altitudes, 176.3 km and 478.0 km. Since the I_{SP} for each curve is constant, each curve corresponds to a constant total initial orbital mass. (The initial orbital mass is independent of propulsive power.) In the case of 176.3 km initial orbital altitudes, the initial masses corresponding to $I_{SP} = 1,000$ sec, 1,500 sec, and 2,000 sec are 31,162 kg, 20,740 kg and 17,081 kg respectively. In the case of 478.0 km initial orbital altitudes, these initial masses are 30,382 kg, 20,426 kg. and 16,923 kg respectively. Consequently, by choosing an I_{SP} of 2,000 sec instead of 1,000 sec the initial orbital mass can be cut almost in half. This will result in a substantial increase in performance. Figure 19 illustrates the dependence of flight time to synchronous orbit on I_{SP} .

Figures 16, 17, and 18 illustrate how sensitive the transfer time to synchronous orbit is to changes in the initial orbital altitude and propulsive power. The curvatures of these curves reveal that the flight times can be significantly shortened if propulsive powers above approximately 40 MW are used with initial orbital altitudes of 478 km or greater. A change in I_{SP} from 1,000 sec to 2,000 sec will result in a substantial increase in payload capability, while having very little effect on the flight time. For example, in the case of 65.4 MW of propulsive power, if the I_{SP} is increased from 1,000 sec to 2,000 sec, then the flight time only increases from 18.611 days to 20.590 days but the initial mass decreases from 30,382 kg to 16,923 kg.

It should be pointed out that the step functions around each of the curves do not correspond to actual data

points as their construction would have required many more data points than were available. Rather, they are drawn to illustrate the step function nature of the curves which is apparent from Tables 11-16. However, the curves they surround were constructed from actual data points found in the tables. Figures 20, 21 and 22 illustrate the functional dependence of flight time to synchronous orbit on the payload mass (where the vehicle returns to the initial orbit empty).

Table 16, which is based on a propulsive power of 65.4 MW and an initial orbital altitude of 478 km, illustrates the very high performance potential of a laser propelled transfer vehicle. Operating with an I_{SP} between 1,500 sec to 2,000 sec, this vehicle may, in fact, be too powerful to be compatible with one ground-to-orbit shuttle vehicle in which the transfer vehicle and the payload are brought up to the initial parking orbit together in the shuttle's cargo bay. Thus, there arises the possibility of utilizing two shuttles per mission. In this configuration, the transfer vehicle would be brought up by one shuttle along with part of the payload and the other shuttle would bring up all of the remaining payload. In this way, payloads exceeding 30,000 kg could be transferred to synchronous orbit without requiring any in-orbit-refuelings or vehicle assembly. (The last few trajectories of Table 16 with $I_{SP} \geq 1,500$ sec describe missions in which the payload up is 30,000 kg.) The flight times to synchronous orbit would be 40-60 days. In fact, if one shuttle containing one transfer vehicle with $I_{SP} = 2,000$ sec is loaded with enough fuel so that the total mass of the vehicle and fuel equals the shuttle's maximum payload capability to the 478 km, 31.8° initial parking orbit (27,216 kg), then the transfer vehicle would have the capability of delivering a 55,000 kg (121,250 lbs.)

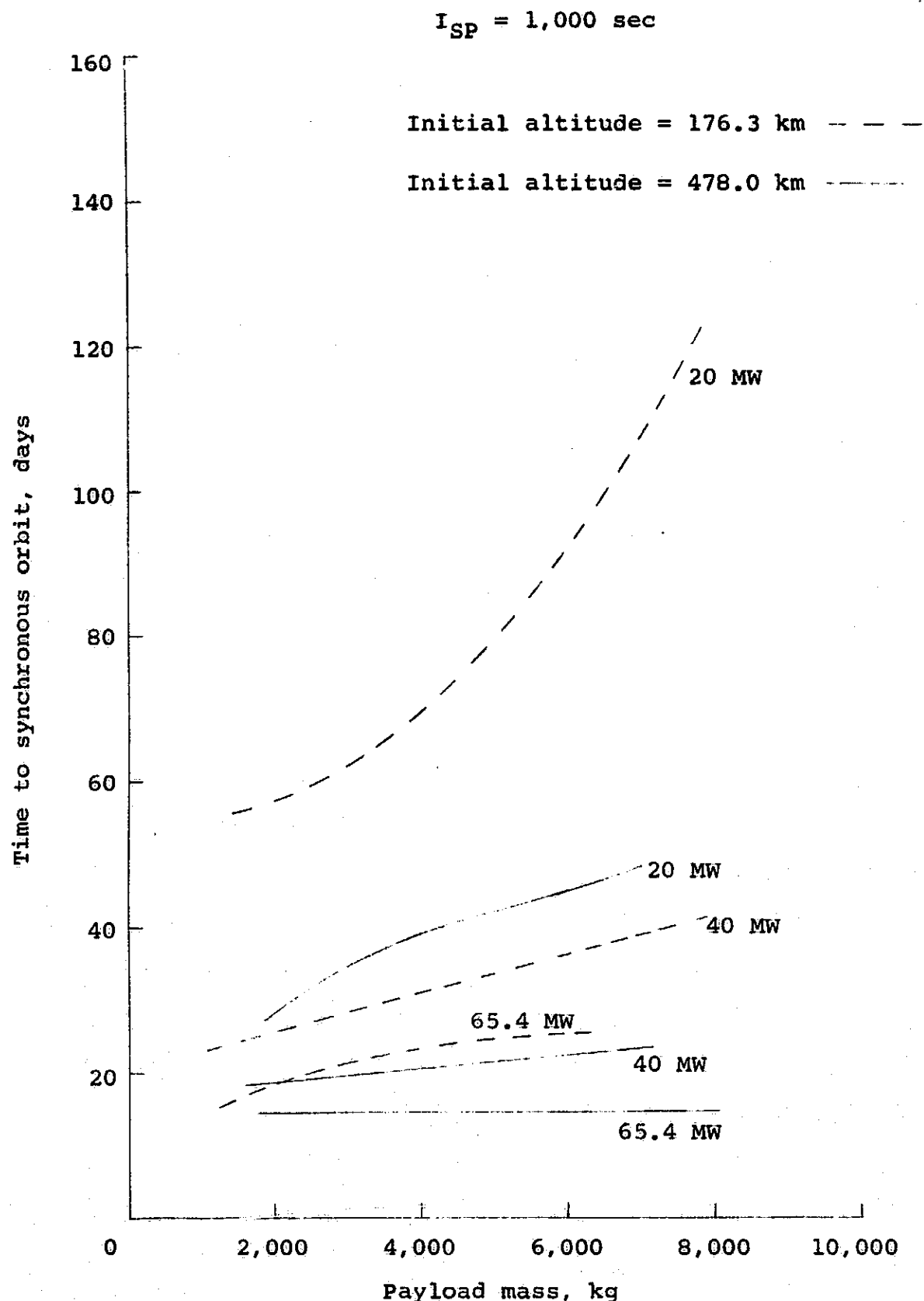


Figure 20. - Flight time to synchronous orbit versus payload mass via laser propelled transfer vehicle (vehicle returns empty).

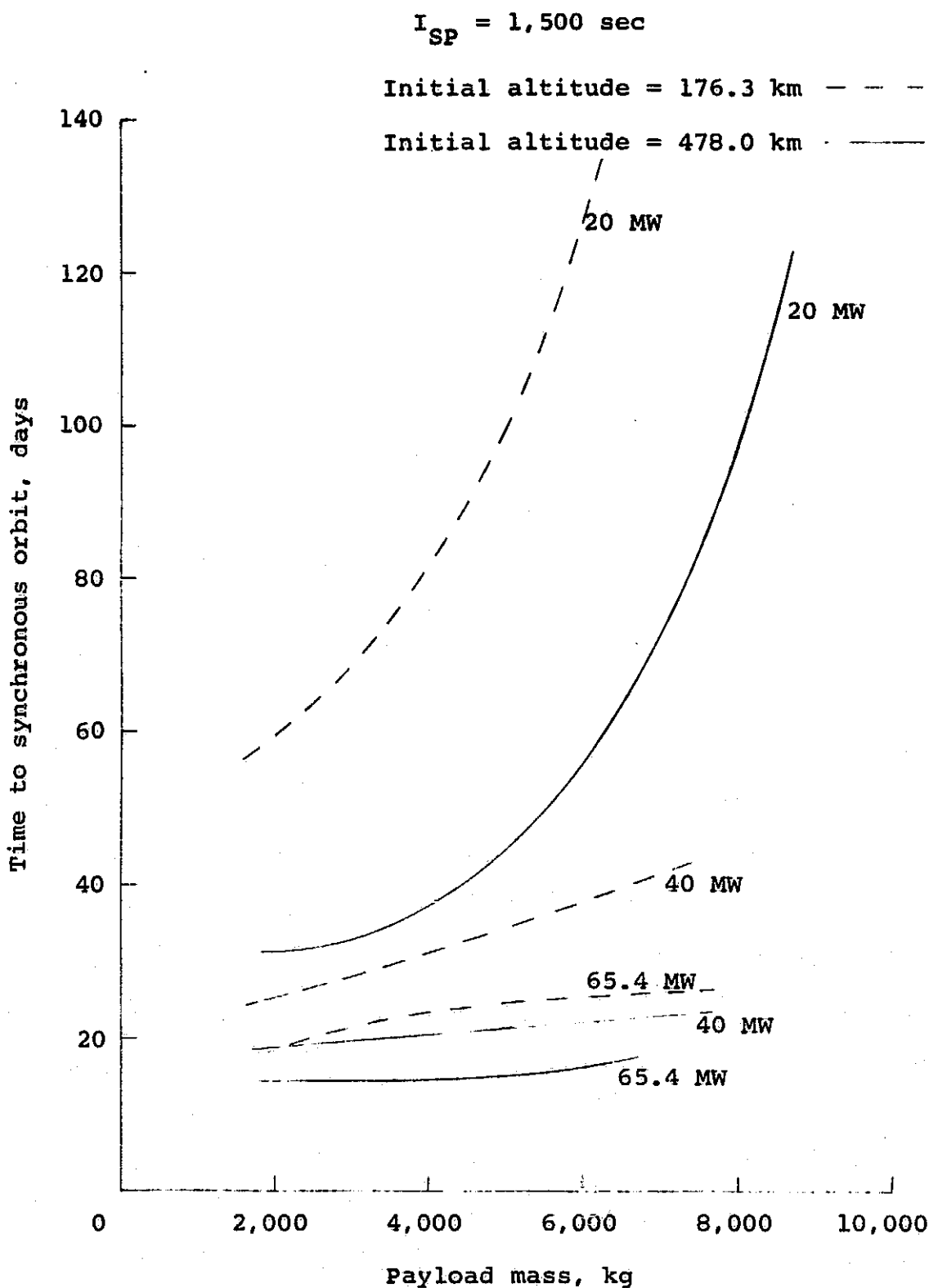


Figure 21. - Flight time to synchronous orbit versus payload mass via laser propelled transfer vehicle (vehicle returns empty).

$I_{SP} = 2,000$ sec

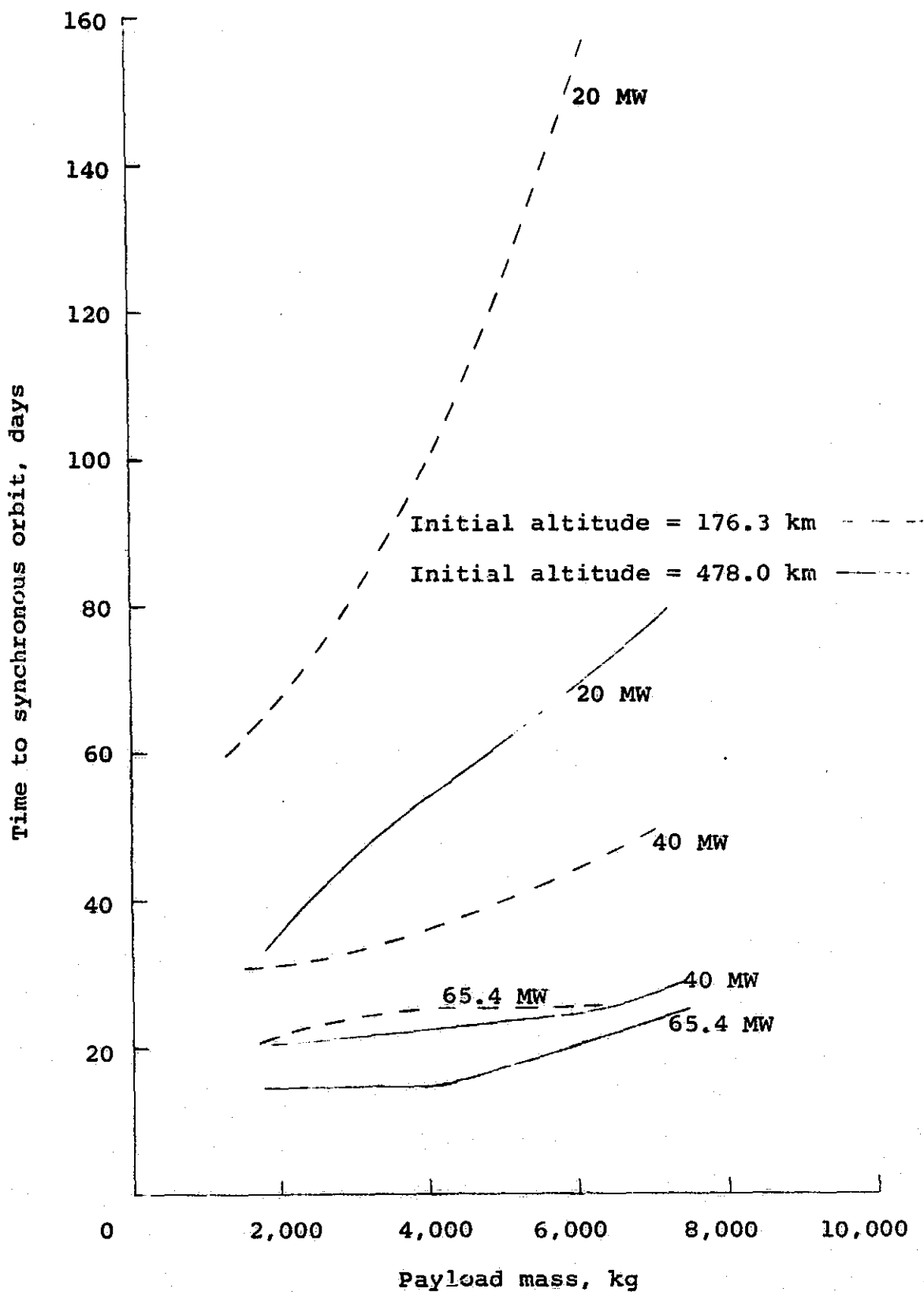


Figure 22. - Flight time to synchronous orbit versus payload mass via laser propelled transfer vehicle (vehicle returns empty).

payload to synchronous orbit and returning empty to the initial parking orbit. This 55,000 kg payload would be brought up by two shuttles containing only useful payload (i.e., no transfer vehicles or fuel). The flight time to synchronous orbit would be about 80 to 90 days. Of course, this flight time could be reduced by using higher initial orbital altitudes or higher propulsive powers. This would represent another possible configuration for a ground based laser propelled transfer vehicle. When payloads of this magnitude can be transported economically, the door is open to large manned space stations at synchronous orbit. The possible utility of such stations are limitless.

More advanced versions of the laser propelled transfer vehicle could be space based. In this configuration, the vehicle would not be carried up to the initial parking orbit along with the payload at the beginning of each mission and would not have to be returned to the earth's surface when the mission is completed. Its fuel could be replenished by simply replacing empty tanks (cartridge fashion) with full tanks, brought up by the shuttle along with the payload. Complicated altitude control systems based on small vernier gas jet thrusters (that constantly require refueling) would be replaced by a relatively simple system based on electrically driven reaction wheels, that, for all practical purposes, never wear out (ref. 35). The vehicle's electrical systems derive power from small rechargeable energy storage systems (such as batteries or flywheels) that are charged by thermionic or thermoelectric converters from wasted heat generated during the propulsion maneuvers. (Small solar arrays could also be provided.) A laser propelled transfer vehicle should be much easier to operate in a purely space-based mode than other vehicles, using chemical or nuclear propulsion, because it will be much simpler, mechanically, since it will not carry any major energy generating system.

By employing a space based laser transfer vehicle, the payload capabilities of the shuttle that would ordinarily carry it could be increased by about 4,000 kg and used for satellite payloads. The laser vehicle's frame could be telescoping so that it could be stored in a relatively small volume along with the retractable reflector. It would be very tedious to assemble the vehicle in orbit before each mission.

A space based laser transfer vehicle can be designed to accommodate many detachable cartridge type fuel tanks that could be added when extremely massive payloads require transfer to synchronous orbit. In these cases, the payload will be towed by a long (low mass) nylon cable that is attached to the vehicle by a "Y" shaped beam. Each arm could be attached to the orbiter near each end of the reflector's rotation axis (see figures 3A and 3B). The stem of the beam would be attached to the tow cable which could have a length of 1 kilometer or more depending on the physical dimensions of the payload. The long cable would prevent the payload from getting into the path of the laser beam. The orbiting solar power station proposed by Glaser (ref. 36) would be an extreme example of a massive payload that could be towed to synchronous orbit by a space based laser transfer vehicle. Previous methods proposed for the transfer to synchronous orbit involve utilization of the station's solar array to power a system of perhaps thousands of small low thrust electric propulsion engines. Unfortunately, since the station's mass is very large (14,000 tons, or 1.27×10^7 kg), the transfer to synchronous orbit would take about 6 months (ref. 36). But this method would expose the solar array to the radiation of the Van Allan Belt for an extended period. The effects of this radiation on the solar cells

would cause their efficiency to drop 50% or more. If the transfer were made by a laser transfer vehicle, the solar array could be protected from the radiation by a light-weight shield which would be removed upon reaching synchronous orbit.

Although the results of the parametric analysis shown in Tables 11-16 clearly demonstrate the high performance capabilities of a laser propelled transfer vehicle, it should be emphasized that these results correspond to a laser transmitter located off the equator at latitude 31.8° . If the transmitter were located on the equator, and if the initial parking orbit had zero inclination, the orbiter would fly directly over the transmitter on each and every orbit revolution. Thus, for low initial orbits, power could be transmitted 15 or 16 different times during a span of only one sidereal day. Moreover, a maximum amount of energy could be transmitted on each pass without having to terminate the transmission when a new resonant orbit is reached (before the beam reaches the minimum beam elevation angle). The result will be a significant reduction in the time required to reach synchronous orbit. The magnitude of this reduction can be estimated from the tables. For example, by consulting Table 12, we find that the time required to complete the first leg of a round-trip mission to synchronous orbit involving the transfer of a 6,000 kg payload up and a 3,000 kg down is 68.972 days if the initial parking orbit is 478 km and $p = 20$ MW, and $I_{SP} = 1,500$ sec. But 63.186 days of this time is spent carrying out the primary boosting maneuvers which require 31 individual burns. During this time the vehicle makes a total of 692 complete orbit revolutions. If the transmitter were located on the equator, and if

the initial parking orbit had zero inclination, these 31 burns could be accomplished in only 31 orbit revolutions instead of 692. Hence, the time required to carry out these 31 maneuvers of the primary boosting sequence would be reduced from 63.186 days to only 4.091 days. Of course, the fact that the performance of a laser propelled transfer vehicle can be significantly increased by placing the power transmitter on the equator does not subtract from its outstanding performance capabilities using an off-equator transmitter.

B. Parametric Analysis of $C_3 = 120$
 km^2/sec^2 Injection Maneuvers

The parametric analysis of laser propelled injection maneuvers with $C_3 = 120 \text{ km}^2/\text{sec}^2$ was based on computing integrated injection trajectories with varying initial conditions which were generated by taking all possible combinations of $I_{SP} = 500 \text{ sec}, 750 \text{ sec}, 1,000 \text{ sec}, 1,250 \text{ sec}, 1,500 \text{ sec}, 1,750 \text{ sec}, 2,000 \text{ sec}$; propulsive power = 20 MW, 30 MW, 40 MW, 50 MW, 60 MW, 65.4 MW; and synchronization ratio = 6, 8, 10, 12. This combination represents a set of 168 injection trajectories. The results appear in Tables 17, 18, 19, and 20. These tables correspond to pre-injection orbits defined by $P/P_s = 6, 8, 10$, and 12 respectively (see Table 10). Each injection maneuver is performed in one long, continuous burn that ranges from 3.6 hours to 4.1 hours in duration. Although these burn times are quite long, the vehicle's distance to the transmitter never exceeds 50,000 km during the propulsion period. An example of a typical injection profile corresponding to $I_{SP} = 1,500 \text{ sec}$, $p = 50 \text{ MW}$ and $P/P_s = 6$ is shown in figure 19.

TABLE 17. - LASER PROPELLED INJECTION MANEUVERS

Pre-Injection Orbit: $a = 139,223$ km; $e = .8651$; $P = 5.9836$ days; $P/P_g = 6$
 $\theta_1 = 17^\circ$; $\theta_1 = -56.84^\circ$; Escape $C_3 = 120$ km²/sec²; $V_\infty = 10.95$ km/sec

Injection parameters							Escape mass	
Power (MW)	I _{SP}	Thrust (lbs.)	Duration (hrs.)	Fuel Burned (kg)	θ_2 (deg)	θ_2 (deg)	Total (kg)	Payload (kg)
20.0	500	1,833.9	4.0469	24,238.2	59.62	4.03	6,607.9	1,696.0
	750	1,222.6	3.8404	10,222.8	61.66	.92	5,649.2	1,438.1
	1,000	917.0	3.7381	5,597.2	62.57	-.62	4,761.4	781.6
	1,250	733.6	3.6779	3,524.5	63.08	-1.52	4,076.6	200.4
	1,500	917.0	3.6382	3,631.8	63.40	-2.12	5,326.0	1,444.4
	1,750	786.0	3.6097	2,647.3	63.62	-2.55	4,709.5	877.1
30.0	2,000	687.7	3.5883	2,014.8	63.78	-2.86	4,217.1	416.3
	500	2,750.9	4.0467	36,355.8	59.62	4.03	9,912.0	4,394.2
	750	1,833.9	3.8406	15,335.0	61.66	.92	8,473.7	4,006.9
	1,000	1,375.4	3.7380	8,395.6	62.57	-.62	7,142.4	3,022.6
	1,250	1,100.4	3.6777	5,286.5	63.08	-1.52	6,114.9	2,150.6
	1,500	917.0	3.6382	3,631.8	63.40	-2.12	5,326.0	1,444.4
40.0	1,750	786.0	3.6097	2,647.3	63.62	-2.55	4,709.5	877.1
	2,000	687.7	3.5883	2,014.8	63.78	-2.86	4,217.1	416.3
	500	3,667.9	4.0469	48,476.4	59.62	4.03	13,215.7	7,091.9
	750	2,445.2	3.8404	20,445.7	61.66	.92	11,298.4	6,576.1
	1,000	1,833.9	3.7381	11,194.4	62.57	-.62	9,522.9	5,263.1
	1,250	1,467.1	3.6779	7,049.0	63.08	-1.52	8,153.2	4,100.7
50.0	1,500	1,222.6	3.6380	4,842.1	63.40	-2.12	7,101.4	3,159.3
	1,750	1,048.0	3.6097	3,529.8	63.62	-2.55	6,279.3	2,402.8
	2,000	917.0	3.5886	2,686.7	63.78	-2.86	5,622.7	1,788.4
	500	4,584.8	4.0468	60,594.7	59.62	4.03	16,520.0	9,790.3
	750	3,056.5	3.8404	25,557.2	61.66	.92	14,123.0	9,145.1
	1,000	2,292.4	3.7381	13,993.1	62.57	-.62	11,903.5	7,503.8
60.0	1,250	1,833.9	3.6779	8,811.4	63.08	-1.52	10,191.4	6,050.8
	1,500	1,528.3	3.6379	6,052.4	63.40	-2.12	8,876.8	4,874.2
	1,750	1,309.9	3.6094	4,411.8	63.62	-2.55	7,849.2	3,928.6
	2,000	1,146.2	3.5888	3,358.6	63.78	-2.86	7,028.3	3,160.4
	500	5,501.8	4.0467	72,711.6	59.62	4.03	19,823.8	12,488.2
	750	3,667.9	3.8406	30,670.1	61.66	.92	16,947.3	11,713.8
65.4	1,000	2,750.9	3.7380	16,791.2	62.57	-.62	14,284.8	9,745.2
	1,250	2,200.7	3.6775	10,572.6	63.08	-1.52	12,229.4	8,000.8
	1,500	1,833.9	3.6382	7,263.5	63.40	-2.12	10,652.0	6,588.8
	1,750	1,571.9	3.6097	5,294.7	63.62	-2.55	9,418.9	5,454.2
	2,000	1,375.4	3.5883	4,029.6	63.78	-2.86	8,434.2	4,532.7
	500	5,999.7	4.0472	79,301.0	59.62	4.03	21,620.6	13,955.6
	750	3,999.8	3.8402	33,442.2	61.66	.92	18,480.0	13,107.8
	1,000	2,999.8	3.7382	18,312.0	62.57	-.61	15,578.7	10,963.1
	1,250	2,399.9	3.6781	11,531.2	63.08	-1.52	13,336.4	9,059.8
	1,500	1,999.9	3.6381	7,920.7	63.40	-2.12	11,616.1	7,520.1
	1,750	1,714.2	3.6097	5,773.7	63.62	-2.55	10,271.4	6,282.7
	2,000	1,499.9	3.5886	4,394.8	63.78	-2.86	9,197.3	5,277.6

TABLE 18. - LASER PROPELLED INJECTION MANEUVERS

Pre-Injection Orbit: $a = 168,656$ km; $e = .8895$; $P = 7.9782$ days; $P/P_s = 8$
 $\theta_1 = 17^\circ$; $\theta_1 = -55.64^\circ$; Escape $C_3 = 120$ km 2 /sec 2 ; $V_\infty = 10.95$ km/sec

Injection parameters							Escape mass	
Power (MW)	I_{SP}	Thrust (lbs)	Duration (hrs.)	Fuel Burned (kg)	θ_2 (deg)	θ_2 (deg)	Total (kg)	Payload (kg)
20.0	500	1,833.9	4.0248	24,105.8	57.95	4.90	6,698.2	1,792.9
	750	1,222.6	3.8266	10,186.3	59.97	1.92	5,718.5	1,509.2
	1,000	917.0	3.7289	5,583.5	60.88	.45	4,817.8	838.6
	1,250	733.6	3.6704	3,517.4	61.38	-.43	4,122.9	247.0
	500	2,750.9	4.0246	36,157.3	57.95	4.90	10,047.4	4,539.5
	750	1,833.9	3.8268	15,280.3	59.97	1.92	8,577.7	4,113.6
30.0	1,000	1,375.4	3.7288	8,375.0	60.88	.45	7,226.9	3,108.1
	1,250	1,100.4	3.6702	5,275.8	61.39	-.43	6,184.4	2,220.6
	1,500	917.0	3.6323	3,625.9	61.71	-.01	5,385.4	1,504.1
	1,750	786.0	3.6044	2,643.4	61.93	-.42	4,760.8	928.6
	2,000	687.7	3.5852	2,013.1	62.08	-.71	4,264.4	463.7
	500	3,667.9	4.0260	48,225.9	57.93	4.90	13,382.2	7,270.9
40.0	750	2,445.2	3.8328	20,405.2	59.93	1.95	11,421.1	6,700.8
	1,000	1,833.9	3.7303	11,171.2	60.85	0.46	9,625.8	5,367.2
	1,250	1,467.1	3.6772	7,047.8	61.36	-.42	8,235.4	4,183.0
	1,500	1,222.6	3.6470	4,854.1	61.68	-.99	7,169.0	3,226.3
	1,750	1,048.0	3.6307	3,550.3	61.90	-.39	6,335.6	2,458.1
	2,000	917.0	3.6035	2,697.8	62.07	-.71	5,675.2	1,840.3
50.0	500	4,584.8	4.0282	60,316.3	57.93	4.90	16,727.5	10,011.8
	750	3,056.5	3.8270	25,468.3	59.96	1.92	14,286.3	9,312.8
	1,000	2,292.4	3.7341	13,978.2	60.85	0.46	12,028.2	7,629.3
	1,250	1,833.9	3.6743	8,802.8	61.36	-.42	10,296.1	5,156.0
	1,500	1,528.3	3.6388	6,053.8	61.68	-.00	8,964.8	4,962.1
	1,750	1,309.9	3.6093	4,411.7	61.91	-.40	7,928.6	4,008.0
60.0	2,000	1,146.2	3.6105	3,378.9	62.06	-.70	7,091.8	3,222.9
	500	5,501.8	4.0279	72,373.4	57.93	4.90	20,075.0	12,756.4
	750	3,667.9	3.8286	30,574.5	59.94	1.93	17,136.7	11,908.0
	1,000	2,750.9	3.7303	16,756.7	60.85	0.46	14,438.7	9,900.8
	1,250	2,200.7	3.6721	10,556.8	61.36	-.43	12,355.8	8,127.9
	1,500	1,833.9	3.6336	7,254.3	61.68	-.00	10,761.7	6,699.0
65.4	1,750	1,571.9	3.6126	5,298.9	61.91	-.41	9,511.9	5,546.9
	2,000	1,375.4	3.5918	4,033.6	62.07	-.71	8,517.1	4,615.4
	500	5,999.7	4.0292	78,950.0	57.93	4.91	21,891.6	14,244.2
	750	3,999.8	3.8285	33,340.5	59.96	1.92	18,692.1	13,325.1
	1,000	2,999.8	3.7313	18,278.0	60.85	0.46	15,744.0	11,130.1
	1,250	2,399.9	3.6723	11,512.9	61.36	-.42	13,475.5	9,199.9
70.0	1,500	1,999.9	3.6373	7,918.8	61.68	-.00	11,733.1	7,637.2
	1,750	1,714.2	3.6140	5,780.6	61.90	-.40	10,372.0	6,383.0
75.0	2,000	1,499.9	3.6030	4,412.3	62.07	-.71	9,283.5	5,362.8

ORIGINAL PAGE IS
OF POOR QUALITY

TABLE 19. - LASER PROPELLED INJECTION MANEUVERS

Pre-Injection Orbit: $a = 195,709$ km; $e = .9052$; $P = 9.9727$ days; $P/P_{\text{a}} = 10$
 $\theta_1 = 17^\circ$; $\theta_2 = -54.90^\circ$; Escape $C_3 = 120 \text{ km}^2/\text{sec}^2$; $V_{\infty} = 10.95 \text{ km/sec}$

Injection parameters							Escape mass	
Power (MW)	I_{SP}	Thrust (lbs.)	Duration (hrs.)	Fuel Burned (kg)	θ_2 (deg)	θ_2 (deg)	Total (kg)	Payload (kg)
20.0	500	1,833.9	4.0101	24,018.2	56.92	5.42	6,755.7	1,854.8
	750	1,222.6	3.8172	10,161.1	58.93	2.52	5,762.3	1,554.2
	1,000	917.0	3.7217	5,572.7	59.83	1.08	4,852.4	873.8
	1,250	733.6	3.6649	3,512.0	60.34	.23	4,151.9	276.3
	500	2,750.9	4.0100	36,025.8	56.92	5.42	10,133.5	4,632.2
	750	1,833.9	3.8174	15,242.5	58.93	2.52	8,643.3	4,181.2
30.0	1,000	1,375.4	3.7216	8,358.7	59.83	1.08	7,278.8	3,160.8
	1,250	1,100.4	3.6647	5,267.8	60.34	.23	6,227.9	2,264.5
	1,500	917.0	3.6276	3,621.2	60.66	-.34	5,422.6	1,541.5
	1,750	786.0	3.6008	2,640.8	60.88	-.74	4,793.8	961.7
	2,000	687.7	3.5806	2,010.5	61.04	-1.03	4,291.8	491.3
	500	3,667.9	4.0101	48,036.4	56.92	5.42	13,511.3	7,409.4
40.0	750	2,445.2	3.8172	20,322.3	58.93	2.52	11,524.6	6,808.5
	1,000	1,833.9	3.7217	11,145.4	59.83	1.08	9,704.8	5,447.6
	1,250	1,467.1	3.6649	7,024.1	60.34	.23	8,303.8	4,252.6
	1,500	1,222.6	3.6274	4,828.0	60.66	-.34	7,230.2	3,288.8
	1,750	1,048.0	3.6008	3,521.1	60.88	-.74	6,391.7	2,515.6
	2,000	917.0	3.5810	2,681.0	61.04	-1.03	5,722.4	1,888.3
50.0	500	4,584.8	4.0101	60,044.6	56.92	5.42	16,889.3	10,187.1
	750	3,056.5	3.8168	25,400.0	58.93	2.51	14,404.0	9,434.0
	1,000	2,292.4	3.7218	13,931.8	59.83	1.08	12,131.1	7,734.5
	1,250	1,833.9	3.6649	8,780.3	60.34	.23	10,379.6	6,240.6
	1,500	1,528.3	3.6273	6,034.8	60.66	-.34	9,037.8	5,036.0
	1,750	1,309.9	3.6005	4,401.0	60.88	-.74	7,989.7	4,069.7
60.0	2,000	1,146.2	3.5815	3,351.7	61.04	-1.03	7,153.5	3,285.9
	500	5,501.8	4.0097	72,046.3	56.93	5.41	20,265.8	12,963.5
	750	3,667.9	3.8174	30,484.9	58.93	2.52	17,286.6	12,062.3
	1,000	2,750.9	3.7216	16,717.3	59.83	1.08	14,557.5	10,021.7
	1,250	2,200.7	3.6647	10,535.6	60.34	.23	12,455.8	8,229.0
	1,500	1,833.9	3.6276	7,242.4	60.66	-.34	10,845.1	6,783.0
65.4	1,750	1,571.9	3.6009	5,281.7	60.88	-.74	9,587.5	5,623.5
	2,000	1,375.4	3.5806	4,021.1	61.04	-1.03	8,583.7	4,682.6
	500	5,999.7	4.0099	78,571.7	56.92	5.42	22,101.4	14,472.8
	750	3,999.8	3.8173	33,242.7	58.93	2.52	18,851.2	13,489.1
	1,000	2,999.8	3.7215	18,230.2	59.83	1.08	15,875.1	11,263.6
	1,250	2,399.9	3.6651	11,490.5	60.34	.23	13,582.7	9,308.2
	1,500	1,999.9	3.6275	7,897.6	60.66	-.34	11,826.7	7,731.8
	1,750	1,714.2	3.6008	5,759.6	60.88	-.74	10,455.2	6,467.2
	2,000	1,499.9	3.5810	4,385.4	61.04	-1.03	9,360.4	5,441.1
	1,800	3,056.5	3.5962	9,971.9	60.92	-0.80	18,738.1	14,539.5

TABLE 20. - LASER PROPELLED INJECTION MANEUVERS

Pre-Injection Orbit: $a = 221,003$ km; $e = .9164$; $P = 11.9672$ days; $P/P_g = 12$
 $\theta_1 = 17^\circ$; $\theta_1 = -54.39^\circ$; Escape $C_3 = 120$ km 2 /sec 2 ; $V_\infty = 10.95$ km/sec

Injection parameters							Escape mass	
Power (MW)	I_{SP}	Thrust (lbs.)	Duration (hrs.)	Fuel Burned (kg)	θ_2 (deg)	θ_2 (deg)	Total (kg)	Payload (kg)
20.0	500	1,833.9	3.9997	23,955.4	56.22	5.77	6,795.9	1,898.1
	750	1,222.6	3.8102	10,142.6	58.21	2.92	5,792.8	1,585.7
	1,000	917.0	3.7165	5,564.8	59.11	1.51	4,876.8	898.5
	1,250	733.6	3.6606	3,507.9	59.62	.67	4,172.1	296.7
	30.0	2,750.9	3.9995	35,931.6	56.22	5.77	10,194.0	4,697.4
	750	1,833.9	3.8104	15,214.7	58.21	2.92	8,689.1	4,228.4
40.0	1,000	1,375.4	3.7163	8,346.9	59.11	1.51	7,315.3	3,197.9
	1,250	1,100.4	3.6604	5,261.7	59.62	.67	6,258.2	2,295.1
	1,500	917.0	3.6240	3,617.6	59.94	.12	5,448.4	1,567.5
	1,750	786.0	3.5976	2,638.5	60.16	-.28	4,816.3	984.3
	2,000	687.7	3.5778	2,008.9	60.32	-.57	4,311.8	511.3
	500	3,667.9	4.0000	47,914.6	56.21	5.77	13,592.8	7,497.1
50.0	750	2,445.2	3.8102	20,285.2	58.21	2.92	11,585.6	6,871.4
	1,000	1,833.9	3.7165	11,129.7	59.11	1.51	9,753.5	5,497.1
	1,250	1,467.1	3.6605	7,015.8	59.62	.67	8,344.0	4,293.2
	1,500	1,222.6	3.6238	4,823.2	59.94	.12	7,264.6	3,323.4
	1,750	1,048.0	3.5976	3,518.0	60.16	-.28	6,421.7	2,545.8
	2,000	917.0	3.5781	2,678.8	60.32	-.57	5,748.9	1,915.0
60.0	500	4,584.8	3.9996	59,887.6	56.22	5.77	16,990.1	10,295.8
	750	3,056.5	3.8103	25,356.7	58.21	2.92	14,482.0	9,514.2
	1,000	2,292.4	3.7165	13,912.2	59.11	1.51	12,191.9	7,796.3
	1,250	1,833.9	3.6607	8,770.0	59.62	.67	10,430.1	6,291.6
	1,500	1,528.3	3.6237	6,028.8	59.94	.12	9,080.8	5,079.4
	1,750	1,309.9	3.5973	4,397.1	60.16	-.28	8,027.2	4,107.4
65.4	2,000	1,146.2	3.5784	3,348.8	60.32	-.57	7,186.1	3,318.7
	500	5,501.8	3.9995	71,863.2	56.22	5.77	20,388.0	13,094.8
	750	3,667.9	3.8104	30,429.4	58.21	2.92	17,378.2	12,156.7
	1,000	2,750.9	3.7163	16,693.7	59.11	1.51	14,630.6	10,095.9
	1,250	2,200.7	3.6604	10,523.3	59.62	.67	12,516.3	8,290.2
	1,500	1,833.9	3.6240	7,235.2	59.94	.12	10,896.8	6,835.0
75.0	1,750	1,571.9	3.5976	5,277.0	60.16	-.28	9,632.5	5,668.7
	2,000	1,375.4	3.5778	4,017.9	60.32	-.57	8,623.5	4,722.6
	500	5,999.7	3.9999	78,375.2	56.21	5.77	22,235.7	14,616.9
	750	3,999.8	3.8103	33,182.2	58.21	2.92	18,951.2	13,592.1
	1,000	2,999.8	3.7167	18,206.6	59.11	1.52	15,956.6	11,346.3
	1,250	2,399.9	3.6609	11,477.1	59.62	.67	13,648.8	9,374.9
85.0	1,500	1,999.9	3.6239	7,889.7	59.94	.12	11,883.0	7,788.5
	1,750	1,714.2	3.5976	5,754.5	60.16	-.28	10,504.3	6,516.6
	2,000	1,499.9	3.5781	4,381.9	60.32	-.57	9,403.8	5,484.7

ORIGINAL PAGE IS
OF POOR QUALITY

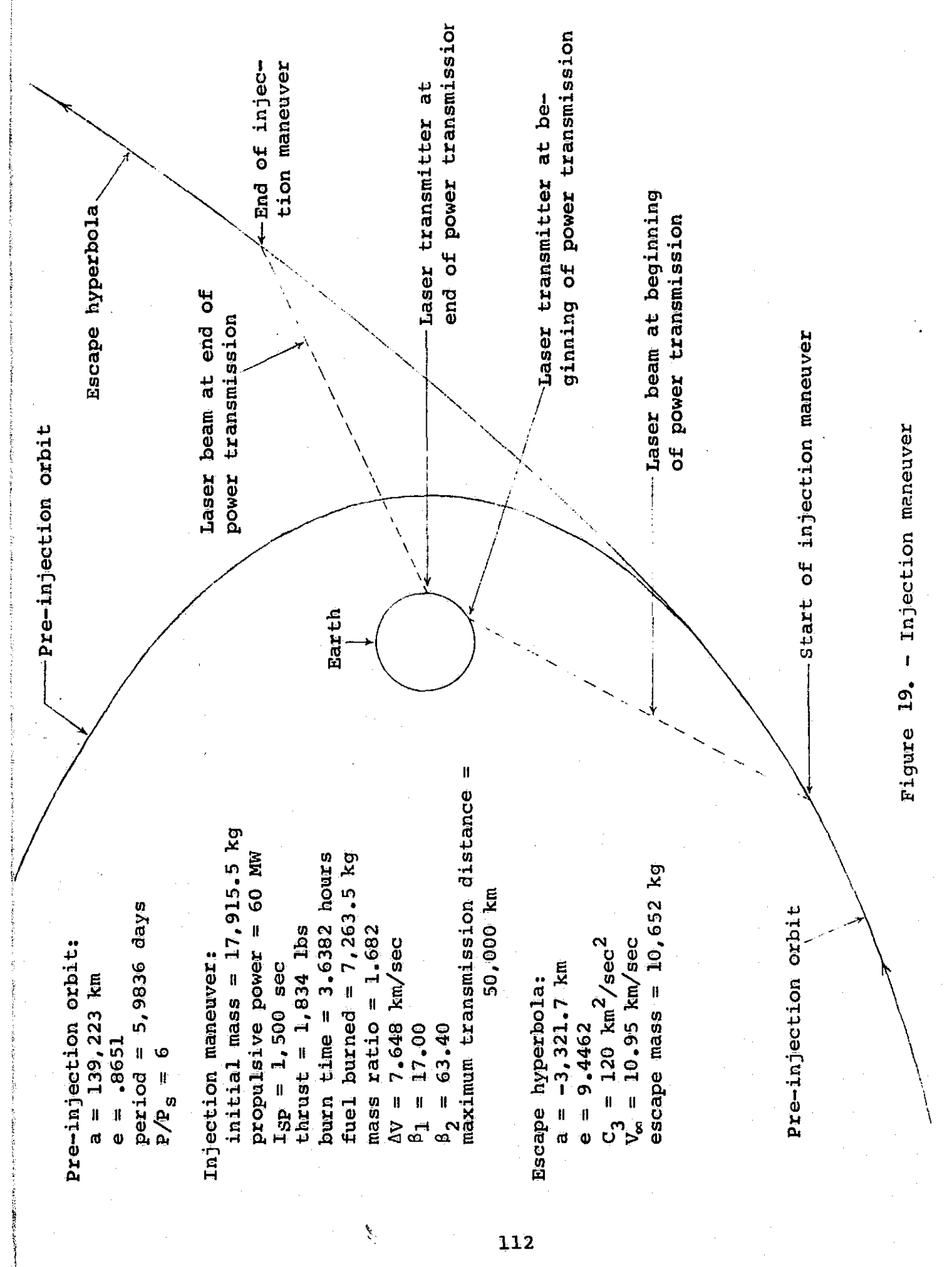


Figure 19. - Injection maneuver

Notice that there are no entries in Tables 17-20 corresponding to a propulsive power of 20 MW when $I_{SP} \geq 1,500$ sec. This result occurs because 20 MW of propulsive power is not high enough to allow the total injection mass to be greater than the vehicle's dry mass. In view of the theoretical investigation of the previous section regarding the determination of optimum I_{SP} which will maximize burn-out mass, it is obvious that this optimum I_{SP} must be below 1,500 sec. The optimum I_{SP} corresponding to various injection trajectories can be obtained by first determining the ΔV s generated during the various injection maneuvers (corresponding to the different initial conditions) and applying equation (29). The results are given in Table 21. Notice that the ΔV s corresponding to fixed values of P/P_s and I_{SP} do not change when P changes. Also, ΔV does not change very much for fixed P/P_s when I_{SP} changes. The optimum I_{SP} values were computed by (29) using the ΔV s corresponding to $I_{SP} = 500$ sec because these will be closer to the resulting ΔV s when the optimum I_{SP} s are used during the injection maneuvers. The table indicates that the optimum I_{SP} which will maximize injection mass corresponding to $P/P_s = 6, 8, 10$ and 12 is 483 sec, 479 sec, 476 sec and 473 sec respectively.

Performance curves describing the maximum possible total injection mass for various values of propulsive power and I_{SP} are shown in figures 24 and 25. The solid curves correspond to injections with $P/P_s = 6$ and the dotted curves correspond to injections with $P/P_s = 12$. Similar curves corresponding to pre-injection orbits with $P/P_s = 8$ and 10 have not been plotted but they would lie between the $P/P_s = 6$ and $P/P_s = 12$ curves. These curves confirm our theoretical results which show that the

TABLE 21. - OPTIMUM I_{SP} THAT MAXIMIZES INJECTION MASS
FOR $C_3 = 120 \text{ km}^2/\text{sec}^2$ VIA LASER PROPULSION

P (MW)	P/P _s	I _{SP} = 500,	ΔV(km/sec)						Optimum I _{SP}
			750,	1000,	1250,	1500,	1750,	2000,	
20	6	7.555	7.598	7.623	7.637	-	-	-	483
	8	7.482	7.524	7.547	7.562	-	-	-	479
	10	7.435	7.476	7.500	7.514	-	-	-	476
	12	7.402	7.443	7.466	7.480	-	-	-	473
30	6	7.555	7.598	7.622	7.637	7.648	7.655	7.660	483
	8	7.481	7.524	7.547	7.561	7.572	7.579	7.584	479
	10	7.435	7.476	7.499	7.514	7.524	7.531	7.536	476
	12	7.402	7.443	7.466	7.480	7.490	7.497	7.502	473
40	6	7.555	7.598	7.622	7.637	7.648	7.655	7.660	483
	8	7.487	7.538	7.555	7.579	7.606	7.636	7.628	479
	10	7.435	7.476	7.500	7.514	7.524	7.531	7.536	476
	12	7.402	7.443	7.466	7.480	7.490	7.497	7.503	473
50	6	7.555	7.598	7.623	7.637	7.647	7.654	7.661	483
	8	7.489	7.527	7.562	7.638	7.590	7.592	7.642	479
	10	7.435	7.476	7.500	7.514	7.524	7.530	7.537	476
	12	7.402	7.443	7.466	7.480	7.490	7.497	7.503	473
60	6	7.555	7.598	7.622	7.637	7.648	7.655	7.660	483
	8	7.488	7.531	7.555	7.570	7.580	7.599	7.604	479
	10	7.435	7.476	7.499	7.514	7.525	7.531	7.536	476
	12	7.402	7.443	7.466	7.480	7.491	7.497	7.502	473
65.4	6	7.555	7.598	7.622	7.638	7.648	7.655	7.661	483
	8	7.490	7.530	7.557	7.570	7.587	7.602	7.627	479
	10	7.435	7.476	7.499	7.514	7.524	7.531	7.536	476
	12	7.402	7.443	7.466	7.480	7.490	7.497	7.503	473

ORIGINAL PAGE IS
OF POOR QUALITY

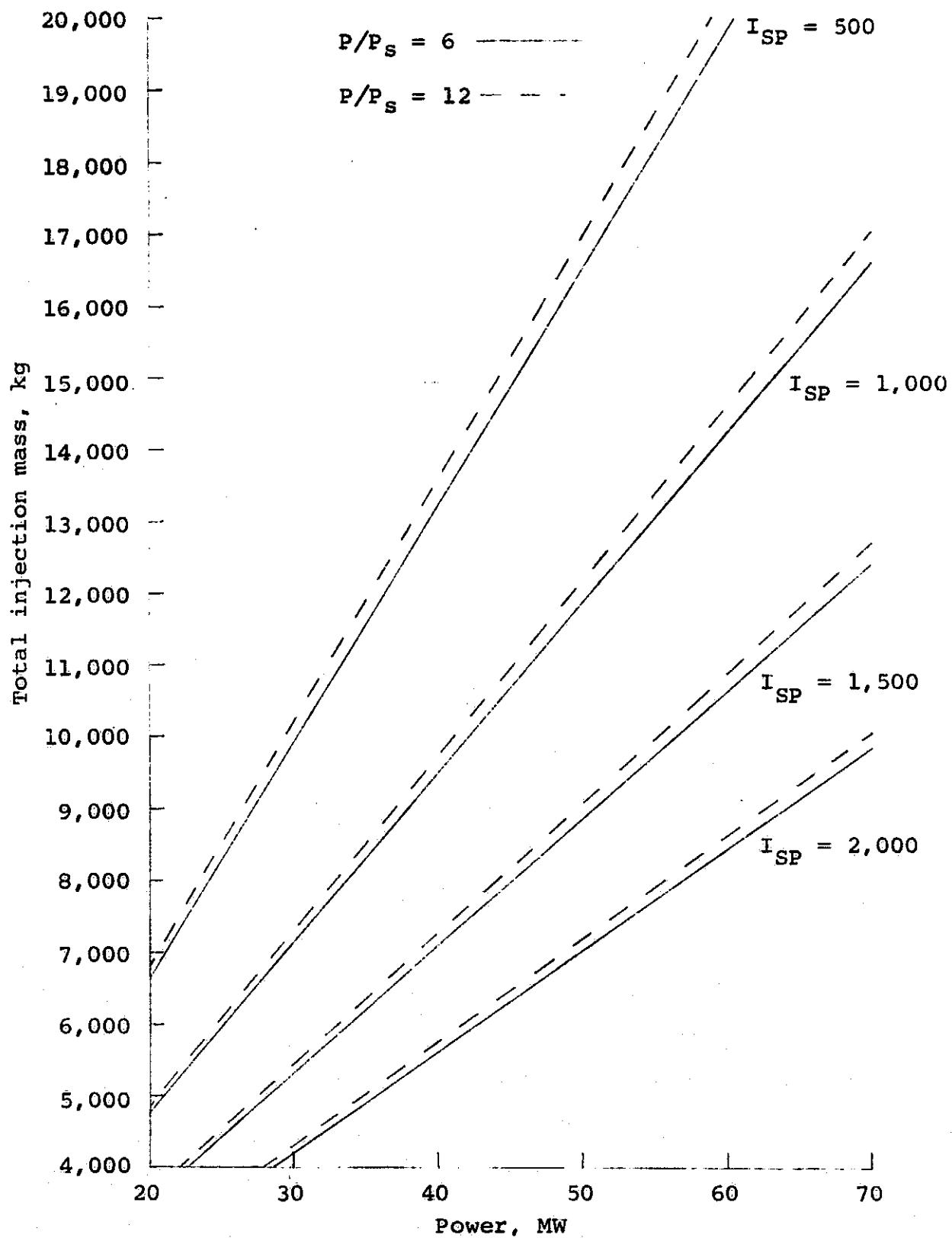


Figure 24. - Injection performance capabilities of laser propelled transfer vehicle ($C_3 = 120 \text{ km}^2/\text{sec}^2$; maximum laser transmission distance = 50,000 km).

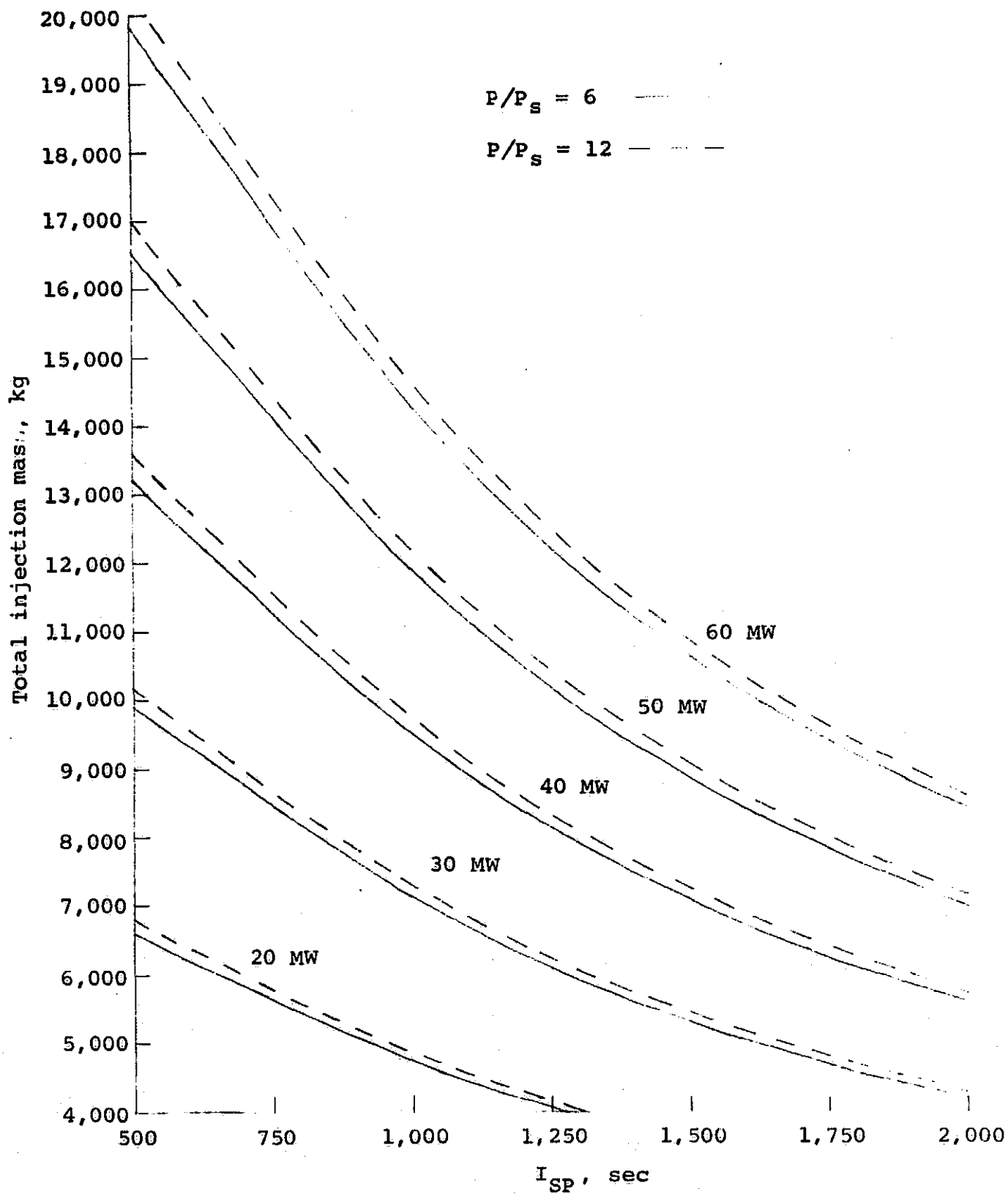


Figure 25. - Injection performance capabilities of laser propelled transfer vehicle ($C_3 = 120 \text{ km}^2/\text{sec}^2$; maximum laser transmission distance = 50,000 km).

optimum I_{SP} which maximizes total injected mass is less than 500 sec (see eq. 29 where $\Delta V = 7.6$ km/sec). Since no injection trajectories were calculated with I_{SP} below 500 sec, it is impossible to observe any maximum injection mass in the curves of figures 24 and 25.

The available injection payload mass is obtained by subtracting the vehicle's dry mass (3,700 kg + 5% of total initial fuel mass) from the total injection mass. These payloads are given in Tables 17-20 and are plotted in figures 26 and 27. The curves in figure 27 give a fairly good picture of the fact that the injected payload is maximum when I_{SP} is near 500 sec. Figures 24 and 25 show that the injected mass is directly proportional to the propulsive power. This result also follows from equation (23). But figures 24-27 do not show the required fuel expenditure, which is substantial for low values of I_{SP} .

One possible definition for optimum I_{SP} is that which maximizes the payload/fuel ratio. Figure 28 contains curves of the injected payload mass divided by the fuel burned during the injection maneuver versus I_{SP} for various propulsive powers. The figure shows that these optimum I_{SP} 's depend upon the propulsive power. These values are approximately 900 sec, 1,375 sec and 1,860 sec for propulsive powers corresponding to 20 MW, 30 MW and 40 MW respectively. These optimum I_{SP} 's for propulsive powers ≥ 50 MW are above 2,000 sec.

Since we are assuming that the laser vehicle and payload are brought up from the earth's surface inside the cargo bay of one shuttle and boosted to the pre-injection orbit by preliminary thrusting maneuvers that begin from the initial parking orbit via laser propulsion, it is important to determine the total initial mass. If this total initial mass exceeds the ground-to-orbit payload capabilities of the shuttle, the payload and laser transfer

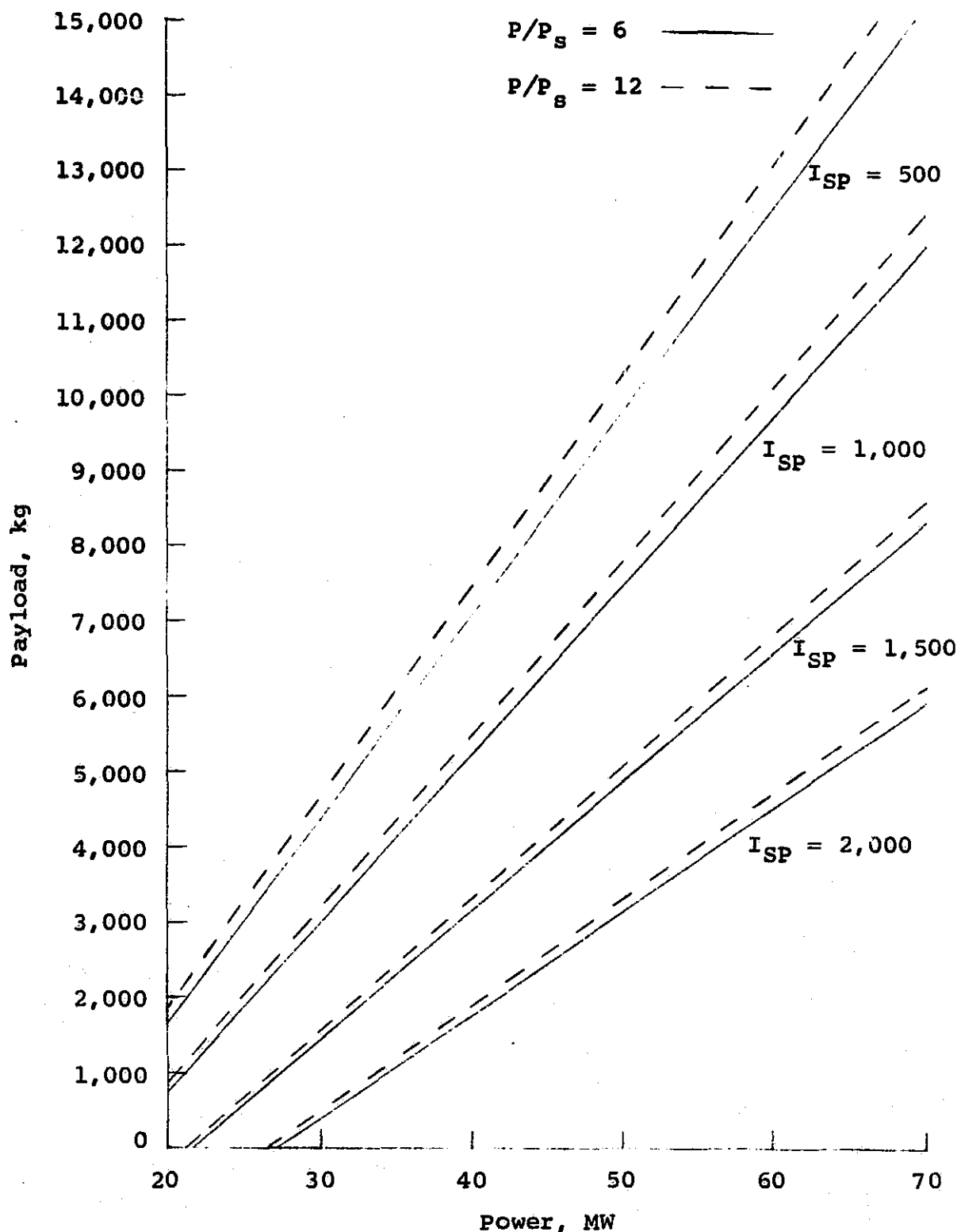


Figure 26. - Injection performance capabilities of laser propelled transfer vehicle ($C_3 = 120 \text{ km}^2/\text{sec}^2$; maximum laser transmission distance = 50,000 km).

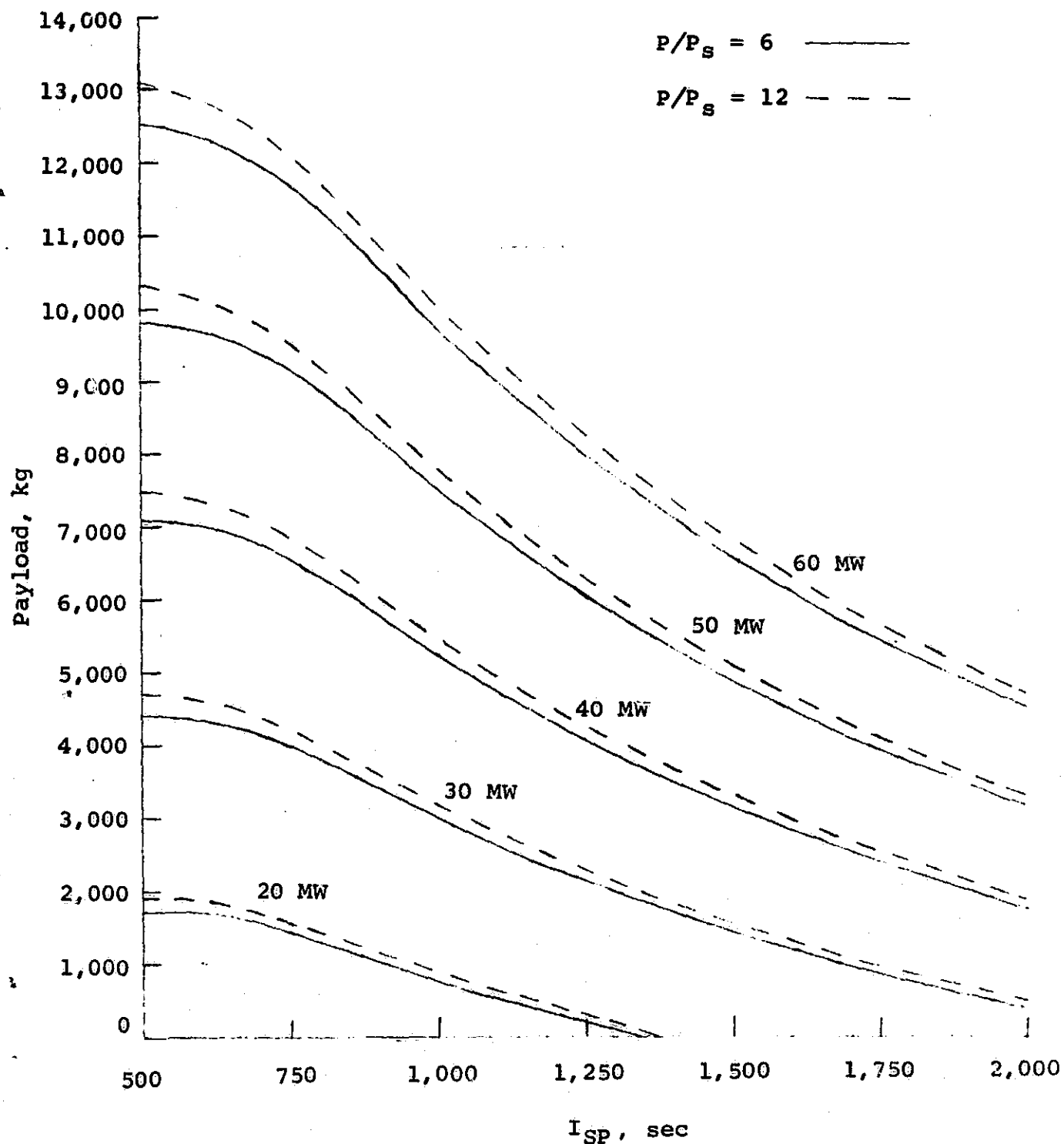


Figure 27. - Injection performance capabilities of laser propelled transfer vehicle ($C_3 = 120 \text{ km}^2/\text{sec}^2$; maximum laser transmission distance = 50,000 km).

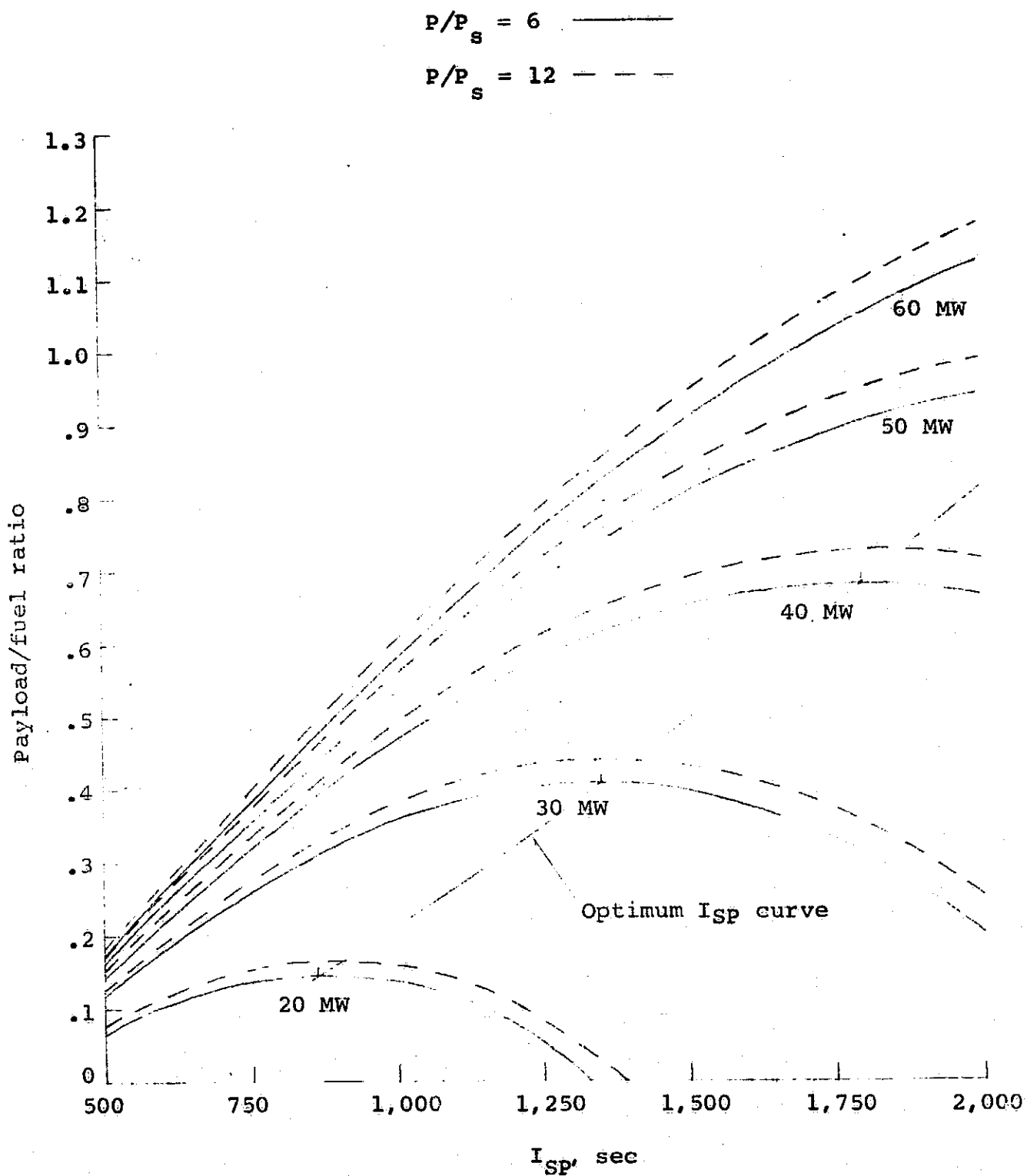


Figure 28. - Injection performance capabilities of laser propelled transfer vehicle ($C_3 = 120 \text{ km}^2/\text{sec}^2$; maximum laser transmission distance = 50,000 km).

vehicle would have to be brought up to the initial parking orbit in two or more shuttle vehicles. Figure 29 gives the propulsive powers and corresponding I_{SP} values that will produce an initial mass within the payload capabilities of one shuttle vehicle. The required I_{SP} 's corresponding to propulsive powers of 20 MW, 30 MW, 40 MW, 50 MW, and 60 MW which will give a total initial mass equal to the maximum payload capabilities of the shuttle are 713 sec, 888 sec, 1,038 sec, 1,180 sec, and 1,325 sec respectively. These parameters correspond to maximum injection mass, which can be determined from figures 25 and 27. The results are given in Table 22. As a comparison, the injection capabilities of the shuttle/chemical tug, shuttle/Centaur, shuttle/nuclear tug (Rover) and shuttle/nuclear tug (colloid core) are given in Table 23 for the same injection energy (refs. 37, 26). The table also includes the injection capabilities of Titan III E/Centaur and Saturn V/Centaur (ref. 38).

Tables 22 and 23 clearly show the truly outstanding injection capabilities of laser propelled transfer vehicles. The 60 MW configuration has a performance close to that of a nuclear powered colloid core shuttle orbiter. A 90 MW laser vehicle would outperform the colloid core shuttle and a Saturn V/Centaur. This figure is easily calculated because the ratio of propulsive power to total injected mass is a constant.

Of course, the preliminary boosting maneuvers required to reach the desired pre-injection orbit will take time to complete. But if the payload is radioactive waste material, this delay is not important. Even if the payload were a scientific satellite or planetary lander, the delay would be a relatively minor inconvenience; its operational effect would be equivalent to a shift in the

TABLE 22. - INJECTION CAPABILITIES OF GROUND-BASED LASER PROPELLED
 INTERORBITAL TRANSFER VEHICLE FOR $C_3 = 120 \text{ km}^2/\text{sec}^2$
 (maximum power transmission distance = 50,000 km)

P (MW)	I_{SP} (sec)	Total Injection Mass (kg)		Injection Payload (kg)	
		$P/P_s = 6$	$P/P_s = 12$	$P/P_s = 6$	$P/P_s = 12$
20	713	5,800	5,900	1,520	1,680
30	888	7,750	7,900	3,470	3,660
40	1,038	9,300	9,500	5,050	5,300
50	1,180	10,700	10,900	6,460	6,700
60	1,325	11,700	12,000	7,520	7,800

TABLE 23. - INJECTION CAPABILITIES OF HIGH PERFORMANCE
 ROCKET VEHICLES FOR $C_3 = 120 \text{ km}^2/\text{sec}^2$

Launch Vehicle	Injection Vehicle	I_{SP} sec	Payload kg
Shuttle	Centaur (with kick)	444	1,400
Shuttle	*CRP Tug (with kick)	470	3,200
Shuttle	*NRP (Rover)	875	3,800
Shuttle	NRP (Colloid Core)	1,100	10,000
Titan III E	Centaur	444	1,600
Saturn V	Centaur	444	13,500

* CRP = Chemical Rocket Propulsion
 NRP = Nuclear Rocket Propulsion

ORIGINAL PAGE IS
 OF POOR QUALITY

Initial orbital mass (478 km high, 31.8° inclination), kg

70,000

60,000

50,000

40,000

30,000

20,000

10,000

500

750

1,000

1,250

1,500

1,750

2,000

I_{SP} , sec

60,000 lbs payload limit of
ground-to-orbit shuttle for
478 km, 31.8° initial parking
orbit

60 MW

50 MW

40 MW

30 MW

20 MW

Figure 29. - Total initial mass of laser propelled transfer vehicle in 478 km, 31.8° parking orbit prior to boosting to pre-injection orbit and injection maneuver.

launch window. The time required for these preliminary maneuvers to the pre-injection orbit can be estimated to be a few days longer than the times T_1 required for the primary boosting maneuvers to synchronous orbit given in Tables 11 to 16. The guidance and attitude control required during the interplanetary journey will be supplied by the injected vehicle. Hence, the payload is not separated from the vehicle after the injection maneuver is accomplished.

CONCLUSIONS

The results of this study indicate that a laser propelled reusable transfer vehicle with a propulsive power of 50 to 70 MW will be capable of transferring high mass payloads on round-trip trajectories to synchronous orbit. Such vehicles will also have the capability of injecting high-mass payloads onto escape trajectories with $C_3 = 120 \text{ km}^2/\text{sec}^2$. Table 24 is a summary of the performance characteristics of several possible vehicle configurations. These configurations, defined as:

GB-1 = ground based laser transfer vehicle brought up to initial parking orbit with payload inside cargo bay of one shuttle.

GB-3 = ground based laser transfer vehicle brought up to initial parking orbit inside one shuttle with enough fuel so that the combined orbiter-fuel mass is equal to the maximum shuttle payload limit; payload brought up in two other shuttles

SB-1 = space based laser transfer vehicle; payload and fuel brought up by one shuttle.

SB-N = space based laser transfer vehicle; payload and fuel brought up by N shuttle deliveries where $N > 3$ is an integer (payload assembled in parking orbit).

The missions are defined as:

Mission 1 = one-way transfer to synchronous orbit; orbiter expended.

Mission 2 = one-way transfer to synchronous orbit; orbiter returned to initial parking orbit empty.

Mission 3 = round-trip transfer to synchronous orbit (equal mass payloads up and down).

Mission 4 = boost payload to pre-injection orbit with $P/P_s = 6$ and injected onto an escape trajectory with $C_3 = 120 \text{ km}^2/\text{sec}^2$.

The beamed power interorbital transfer vehicle concept described herein does not have to use a high power laser beam as the energy carrier. Previous studies (refs. 39 and 40) indicate that a system based on microwaves could also be constructed. Unlike a laser system, the earth's atmosphere will have little if any effect on a microwave beam (with a wavelength of 3 cm) and power could even be transmitted through a rainstorm. Moreover, the technology needed for the development of high-power microwave generators and phased-array transmitting apertures is already here. Microwave generators with power levels in the one MW range with efficiencies approaching 90% are readily available as "off-the-shelf" items (ref. 41). Large microwave phased array transmitting antennas with electronic beam steering have been operational since the early 1960s. In 1965, Bendix Corporation developed for the U.S. Air Force, the AN/FPS-85 microwave

TABLE 24. - PERFORMANCE CAPABILITIES OF LASER PROPELLED
INTERORBITAL TRANSFER VEHICLES WITH
DESIGN PARAMETERS:

I_{SP}	= 2,000 sec
Propulsive power	= 65.4 MW
Thrust	= 1,500 lbs.
Dry Mass	= 3,700 kg + 5% fuel mass
Initial orbital altitude	= 478 km
Latitude of laser transmitter	= 31.8° N
Maximum power transmission distance	= 50,000 km
Minimum beam elevation angle	= 15°

Configuration	Mission No.	Payload kg	Flight Time Up days
GB-1	1	16,400	≈35
GB-3	1	54,400	≈70
SB-1	1	20,500	≈40
SB-N	1	20,400 N	≈50 N ²
GB-1	2	14,700	≈30
GB-3	2	54,400	≈75
SB-1	2	18,400	≈45
SB-N	2	20,400 N -1,500	≈50 N ²
GB-1	3	11,030	≈30
SB-1	3	13,400	≈35
GB-1	4	5,280	≈30

phased array radar antenna which has a radiated power exceeding 50 MW (ref. 42). It is used for tracking small earth satellites. Microwave rocket engines with I_{SP} approaching 1,000 sec were tested over ten years ago (ref. 9). Unfortunately, the large beam spread associated with microwave radiation puts an upper limit on its potential as a long range energy carrier. Extremely large transmitting and receiving antennas will be required for 50,000 km power transmission (e.g., on the order of 5,000 meters and 500 meters in diameter respectively). However, very large 500 meter diameter antennas could be designed for microwave powered interorbital transfer vehicles with a mass of only about 15,000 kg (ref. 28). The transmitter could be constructed on a remote island near the equator in the Pacific Ocean. Several possibilities are: Mussau Island, latitude $1^{\circ} 24'$ south, and Manus Island, latitude $1^{\circ} 40'$ south, located in the Bismark Archipelago, and Christmas Island, latitude $2^{\circ} 0'$ north (U.S. protectorate). Perhaps the best location is on one of the large islands in the Galapagos Archipelago. All of these islands are within 1° of the equator. The initial orbit of a microwave powered interorbital transfer vehicle could then have an inclination of 0° so that it would pass over (or nearly over) the transmitter to receive propulsive power on each and every orbit revolution during the primary boosting maneuvers.

When the technology of high power laser generators reaches the same level as microwave generators, the laser propelled interorbital transfer vehicles may prove to be far superior because of its much greater operational range. Although a laser beam will tend to wander around in an essentially random manner on a distant target due

to its passage through the atmosphere, this motion has been found to be extremely small (refs. 43, 44). It should also be noted that the large receiving antenna required on a microwave powered interorbital transfer vehicle may tend to burden the vehicle with excess inertial mass that would have to be overcome by higher propulsive forces. This excess mass would not be present with a laser powered vehicle. There are several extremely high mountains near the equator that might be suitable locations for the laser transmitter if an equatorial system is desired. For example, Mt. Kenya in Kenya, East Africa, with elevation 17,058 feet and latitude $0^{\circ} 8'$ south and Mt. Chimborazo in Ecuador with elevation 20,561 feet and latitude $1^{\circ} 15'$ south are two possibilities. However, it should be emphasized that the performance data given in this report is based on a non-equatorial transmitter located at 31.8° north latitude. (Chiricahua Peak, with an elevation of 9,796 feet in southern Arizona is at this latitude.)

One application of beamed vehicle propulsive power that will clearly favor laser rather than microwave radiation is the case where the transmitter is placed in orbit above the earth's atmosphere (ref. 45). This system would allow the power transmission range to be increased to nearly interplanetary distances. The resulting vehicle performance would be exceedingly high.

But whatever power transmission mode is used, the results of this study indicate that even a relatively low power system will be capable of extremely high performance, equal to or exceeding that of high power nuclear propelled transfer vehicles.

From an operational point of view, a laser propelled interorbital transfer vehicle system may be very economical.

One transmitter could power a fleet of perhaps ten or twenty such transfer vehicles at different times each day. Hence, one transmitter would enable ten or twenty different missions to be conducted simultaneously. There would be no atmospheric radioactivity contamination and no start up or shut down problems that are inherent with nuclear propelled vehicles. The laser propelled vehicles would be relatively inexpensive, and the power generator could never be lost due to vehicle malfunction. It would be easily accessible for routine maintenance.

Laser propelled vehicles could also be used to dispose of radioactive waste material from nuclear generating plants. For example, if the United States constructs 200 nuclear generating plants for the production of electric power with an average output of 500 MW each, these plants, operating continuously twenty-four hours a day, will generate radioactive waste at the rate of approximately 500,000 kg/year (based on a rate of 13.7 kg/GW-day calculated from data given in ref. 46). This material, accumulated over one year, could be disposed of by injecting it with the aid of 100 laser propelled 65 MW expendable rockets on gravity assist trajectories via Jupiter into the sun or out of the solar system. This would be carried out during the two-month Jupiter launch window. The vehicles would be boosted to the eccentric pre-injection orbits at a steady annual rate of about two vehicles per week.

If the transmitter were placed on the earth's equator, one 120 MW laser propelled transfer vehicle would be capable of transporting the enormous mass of an entire 10 GW Glaser type orbiting solar power station to synchronous orbit within approximately two to three years. Although this transfer time is relatively short considering the mass involved, it could be reduced considerably by constructing the station in ten detachable parts of approximately equal mass. After the station is constructed in the low initial orbit, it would be

disassembled into the 10 parts. Each part would be transported to synchronous orbit separately by its own transfer vehicle. The boosting maneuvers would be phased so that only one vehicle passes over the transmitter at any given time. As soon as one vehicle had finished its incremental boost, another would begin to make its pass to receive its incremental boost. In this way, power could be transmitted almost continuously, 24 hours a day. Hence, all of the parts could be boosted to synchronous orbit simultaneously. After reaching synchronous orbit, a rendezvous would be made at a convenient position and the station would be re-assembled. This transfer mode would cut the flight time to synchronous orbit to only a few weeks.

When the reusable ground-to-orbit shuttle vehicle becomes operational, flights to low orbits will be routine. Added improvements will reduce the transportation cost to these low orbits to only a few dollars per kilogram. But a high percentage of the payloads, such as communication satellites or manned orbiting laboratories, would require transportation to synchronous orbit. Other payloads, such as interplanetary vehicles, would require injection onto escape trajectories. Therefore, unless an economical, environmentally clean, reusable transfer vehicle is developed that will be capable of providing efficient inter-orbital transportation, the overall cost of space missions will continue to be high. The results of this study show that a laser propelled transfer vehicle drawing power from one ground based transmitter, will be capable of providing this service. Although the initial developmental costs will be high, the long-range economical benefits and performance may be very attractive.

SYMBOLS

a	semi-major axis
C_3	escape energy (square of vehicle's hyperbolic excess velocity)
D	distance between laser transmitter and vehicle
D_1	distance between laser transmitter and vehicle at beginning of power transmission
D_2	distance between laser transmitter and vehicle at end of power transmission
E	orbital energy
e	eccentricity
h	initial orbital altitude
I_{SP}	specific impulse
i	orbital inclination
$(k_{1,i}, k_{2,i})$	resonant integers defined in eq. (8)
M	total mass of vehicle and payload
Mass Ratio	vehicle's mass before propulsive maneuver divided by vehicle's mass after propulsive maneuver
m_o	vehicle's dry mass
m_f	vehicle's fuel mass
m_p	vehicle's payload mass
m_b	vehicle's fuel mass burned during injection maneuver
\dot{m}	exhaust mass flow rate
n	orbit's mean motion (average orbital angular velocity)
\bar{n}	orbit's anomalistic mean motion
P	orbital period
P_s	sidereal day (86,164.099 sec)
\bar{P}	orbital anomalistic period (time interval between two successive perifocal passages)

p	propulsive power
Q	apoapsis distance from earth's center
Q_h	apoapsis altitude above earth's surface
q	periapsis distance from earth's center
q_h	periapsis altitude above earth's surface
R	distance of vehicle from earth's center
s	beam diameter at vehicle
T	thrusting time of propulsive maneuver
t	time
U	gravitational potential function
u	exhaust velocity
V	vehicle velocity
V_∞	hyperbolic excess velocity
x	x axis of coordinate system
x_0	Constant equal to 1.593624
y	y axis of coordinate system
z	z axis of coordinate system
α	minimum allowed beam elevation angle
β	beam elevation angle
β_1	beam elevation angle at beginning of power transmission
β_2	beam elevation angle at end of power transmission
δn	change in orbit's mean motion due to propulsive maneuver
ΔV	change in vehicle's velocity due to propulsive maneuver
\cdot	earth's rotation rate ($7.292115144 \times 10^{-5}$ rad/sec)
λ	wavelength of electromagnetic radiation
μ	gravitational constant of earth ($398600.7 \text{ km}^3/\text{sec}^2$)
Π	orbital plane of vehicle

ρ_0	earth's mean radius (6371.3 km)
Σ	Cartesian inertial frame with origin at earth's center
ϕ_t	latitude of laser transmitter
ϕ_1	latitude of Cape Canaveral
Ω	longitude of orbit's ascending node (angle between + x - axis and orbit's ascending line of nodes) defined in fig. 9
$\dot{\Omega}$	rate of change of Ω
ω	orbit's argument of perigee (angle between orbit's line of apsides and ascending line of nodes) defined in fig. 9
$\dot{\omega}$	rate of change of ω

REFERENCES

1. Hunt, I. and Draper, W., Lightning in His Hand--The Life Story of Nikola Tesla, Sage Books, Denver, Colorado, 1964.
2. O'Neill, J. J. Prodigal Genius--The Life of Nikola Tesla, Ives Washburn Inc., New York.
3. New York Times, Jan. 8, 1943, p. 19, Col. 1; and pp. 231-241, Ref. 1.
4. p. 163 Ref. 1; and pp. 237-243 Ref. 2.
5. Skowron, J. F., MacMaster, G. H., and Brown, W. C., "The Super-Power CW Amplitron," Microwave Journal, Oct. 1964.
6. Luebke, W., and Caryotakis, G., "Development of a One Megawatt CW Klystron," Microwave Journal, Aug. 1966.
7. Brown, W. C. "Experiments in the Transportation of Energy by Microwave Beam," 1964 IEEE Int. Conv. Rec., Vol. 12, pt. 2, pp. 8-17.
8. Brown, W. C., Heenan, N. I. and Mims, J. R., "An Experimental Microwave-Powered Helicopter," IEEE Intern. Conv. Record, Vol. 13, pt. 5, pp. 225-235, 1965.
9. Schad, J. L. and Moriarty, J. J., "Microwave Rocket Concept," International Astronautical Federation, International Astronautical Congress, 16th, Athens, Greece, Sept. 13-18, 1965.
10. Hansen, R. C., "Minimum Spot Size of Focused Apertures," Electromagnetic Wave Theory, Part 2, Pergamon Press, Sept. 1965, pp. 661-667.

11. Hertzberg, A., Johnston, E., and Ahlstrom, H., "Photon Generators and Engines for Laser Power Transmission," AIAA 9th Aerospace Sciences Meeting, New York, New York, Jan. 25-27, 1971, AIAA Paper No. 71-106.
12. Kantrowitz, A. R., "The Relevance of Space," Astronautics and Aeronautics, Vol. 9, No. 3, March 1971, p. 35.
13. Kantrowitz, A. R., "Propulsion to Orbit by Ground-Based Lasers," Astronautics and Aeronautics, Vol. 10, No. 5, May 1972, pp. 74-76.
14. Minovitch, M. A., "The Laser Rocket--A Rocket Engine Design Concept for Achieving a High Exhaust Thrust with High I_{SP} ," Jet Propulsion Laboratory, TM 393-92, February 18, 1972.
15. Minovitch, M. A., "Laser Rocket," U.S. Patent No. 3,825,211, Filed June 19, 1972.
16. Rom, F. E., and Putre, H. A., "Laser Propulsion," Lewis Research Center, TM X-2510, April 1972.
17. Pirri, A. N. and Weiss, R. F., "Laser Propulsion," AIAA Paper No. 72-719, June 26, 1972.
18. Boom, R. W., et al., "Superconducting Energy Storage for Large Systems," IEEE Transactions on Magnetics Vol. MAG-11, No. 2, March 1975.
19. Laquer, H. L., "Superconducting Magnetic Energy Storage," Cryogenics, Vol. 16, No. 2, February 1975, pp. 73-78.
20. Minovitch, M. A., "Reactorless Nuclear Propulsion--The Laser Rocket," AIAA Paper No. 72-1095, November 29, 1972.

21. The NASA Program: A Forecast for the Future, NASA AAD-2, April 14, 1972, pp. 30-32.
22. Layton, P. J., "Our Next Steps in Space," Astronautics and Aeronautics, Vol. 10, No. 5, May 1972, pp. 56-65.
23. Harney, U. E., et al., "Geocentric Solar Electric Propulsion Vehicle Design," AIAA Paper No. 72-1126, Dec. 1972.
24. Godwin, R. C. and Rees, T., "Electric Propulsion for Orbital Transfer," XIXth International Astronautical Congress, Pergamon Press, 1970, pp. 265-279.
25. Friedlander, A. L., "Low Thrust Mission Applications," AIAA Paper No. 72-1125, November 29, 1972.
26. Meier, T. C., "Performance Potential of the Colloid Core Reactor Concept In Near-Earth Applications," AIAA Paper No. 72-1065, November 29, 1972.
27. Corcoran, V. J., and Crabbe, I. A., "Electronically Scanned Waveguide Laser Arrays," Applied Optics, Vol. 13, No. 8, August 1974, pp. 1755-1757.
28. Minovitch, M. A., "Long Range Telepropelled Vehicle Designs," Technical Report No. 101-7, July 10, 1973, Phaser Telepropulsion, Inc., Los Angeles, Calif.
29. Ehricke, K. A., "Perspective and Systems Engineering of Manned Planetary Flight," Space Shuttles and Interplanetary Missions, AAS Advances in the Astronautical Sciences, Vol. 28, 1970.
30. Melbourne, W. G., et al., Constants and Related Information for Astrodynamical Calculations, 1968, Jet Propulsion Laboratory Technical Report No. 32-1306, July 15, 1968.

31. Escobal, P. R., Methods of Orbit Determination, John Wiley & Sons, Inc., New York/London/Sydney, 1965, p. 49.
32. Kaula, W. M., Theory of Satellite Geodesy, Blaisdell Publishing Company, Waltham Massachusetts/Toronto/London, 1966, p. 39.
33. Escobal, P. R., Methods of Orbit Determination, John Wiley & Sons, Inc., New York/London/Sydney, 1965, p. 369.
34. Minovitch, M. A., The Determination and Characteristics of Ballistic Interplanetary Trajectories under the Influence of Multiple Planetary Attractions, Technical Report No. 32-464, October 31, 1963, Jet Propulsion Laboratory, California Institute of Technology.
35. Grucq, J., "The Reaction Wheels of the Netherlands Satellite ANS," Philips Technical Review, Vol. 34, No. 4, 1974, pp. 106-111.
36. Glaser, P. E., "Solar Power Via Satellite," Astronautics and Aeronautics, Vol. 11, No. 8, August 1973, pp. 60-68.
37. Niehoff, J. C. and Friedlander, A. L., "Comparison of Advanced Propulsion Capabilities for Future Planetary Missions," Journal of Spacecraft and Rockets, Vol. 11, No. 8, August 1974, pp. 566-573.
38. McGolrick, J. E. and Davis, B. W., "Launch Vehicles for Future Automated Space Missions," Journal of Spacecraft and Rockets, Vol. 6, No. 2, February 1969, pp. 129-135.

39. Minovitch, M. A., "Microwave Powered Reusable Orbiting Space Tug," U.S. Patent No. 3,891,160, Filed March 21, 1973.
40. Minovitch, M. A., "Microwave Powered Reusable Interorbital Transfer Vehicle," Technical Report 101-4, January 5, 1973, Phaser Telepropulsion, Inc., Los Angeles, California.
41. Brown, W. C., Final Report - Phase II, A Microwave Beam Power Transfer and Guidance System for Use In An Orbital Astronomy Support Facility, PT-3539, September 26, 1972, Raytheon Company - Microwave and Power Tube Division, Waltham, Massachusetts.
42. Amitay, N. et al., Theory and Analysis of Phased Array Antennas, John Wiley & Sons, Inc., 1972, p. 3.
43. Mason, J. B. and Lindberg, J. D., "Laser Beam Behavior on a Long High Path," Applied Optics, Vol. 12, No. 2, February 1973, pp. 187-190.
44. Ochs, G. R. and Lawrence, R. S., "Measurements of Laser Beam Spread and Curvature," Laser Journal, January/February 1971, pp. 14-27.
45. Hansen, C. F. and Lee, G. "Laser Power Stations in Orbit," Astronautics and Aeronautics, July 1972, pp. 42-55.
46. Snow, J. A., "Radioactive Waste from Reactors," Scientist and Citizen, May 1967, p. 95.